Correlation of the hidden-charm molecular tetraquarks and the charmoniumlike structures existing in the $B \to XYZ + K$ process

Fu-Lai Wang,[1,2,*] Xin-Dian Yang,[1,2,†] Rui Chen,[4,5,‡] and Xiang Liu[1,2,3,§]

[1]*School of Physical Science and Technology, Lanzhou University, Lanzhou 730000, China*
[2]*Research Center for Hadron and CSR Physics, Lanzhou University and Institute of Modern Physics of CAS, Lanzhou 730000, China*
[3]*Lanzhou Center for Theoretical Physics, Key Laboratory of Theoretical Physics of Gansu Province, and Frontiers Science Center for Rare Isotopes, Lanzhou University, Lanzhou 730000, China*
[4]*Key Laboratory of Low-Dimensional Quantum Structures and Quantum Control of Ministry of Education, Department of Physics and Synergetic Innovation Center for Quantum Effects and Applications, Hunan Normal University, Changsha 410081, China*
[5]*Center of High Energy Physics, Peking University, Beijing 100871, China*

(Received 6 August 2021; accepted 7 October 2021; published 8 November 2021)

The molecular assignments to the three P_c states and the similar production mechanism between the $\Lambda_b \to P_c + K$ and $B \to XYZ + K$ convince us the B decaying to a charmonium state plus light mesons could be the appropriate production process to search for the charmoniumlike molecular tetraquarks. In this work, we systematically study the interactions between a charmed (charmed-strange) meson and an anticharmed (anticharm-strange) meson, which include the $D^{(*)}\bar{D}^{(*)}$, $\bar{D}^{(*)}\bar{D}_1$, $D^{(*)}\bar{D}_2^*$, $D_s^{(*)}\bar{D}_s^{(*)}$, $D_s^{(*)}\bar{D}_{s0}^*$, $D_s^{(*)}\bar{D}_{s1}'$, $D_s^{(*)}\bar{D}_{s1}$, $D_s^{(*)}\bar{D}_{s2}^*$ systems. After adopting the one-boson-exchange effective potentials, our numerical results indicate that, on one hand, there can exist a serial of isoscalar charmoniumlike $\mathcal{D}\bar{\mathcal{D}}$ and $\mathcal{D}_s\bar{\mathcal{D}}_s$ molecular states, on the other hand, we can fully exclude the charged charmoniumlike states as the isovector charmoniumlike molecules. Meanwhile, we discuss the two-body hidden-charm decay channels for the obtained $\mathcal{D}\bar{\mathcal{D}}$ and $\mathcal{D}_s\bar{\mathcal{D}}_s$ molecules, especially the $D^*\bar{D}^*$ molecular tetraquarks. By analyzing the experimental data collected from the $B \to XYZ + K$ and the mass spectrum and two-body hidden-charm decay channels for the obtained $\mathcal{D}\bar{\mathcal{D}}$ and $\mathcal{D}_s\bar{\mathcal{D}}_s$ molecules, we find several possible hints of the existence of the charmoniumlike molecular tetraquarks, i.e., a peculiar characteristic mass spectrum of the isoscalar $D^*\bar{D}^*$ molecular systems can be applied to identify the charmoniumlike molecule. We look forward to the future experiments like the LHCb, Belle II, and BESIII Collaborations can test our results with more precise experimental data.

DOI: 10.1103/PhysRevD.104.094010

I. INTRODUCTION

In 2015, the LHCb Collaboration analyzed the $\Lambda_b \to J/\psi p K$ decay and reported two P_c structures ($P_c(4380)$ and $P_c(4450)$) existing in the $J/\psi p$ invariant mass spectrum [1]. After four years, the LHCb revised $\Lambda_b \to J/\psi p K$ process with higher precision data and found that former $P_c(4450)$ contains two substructures $P_c(4440)$ and $P_c(4457)$ [2]. Besides, a new enhancement structure $P_c(4312)$ was announced [2]. In fact, this updated result of P_c states provides a direct evidence to support the existence of the hidden-charm molecular pentaquark states [3–9].

In Fig. 1, we present the quark level description of the $\Lambda_b \to P_c K$, which is a typical hadronic weak decay. If replacing ud quarks of the Λ_b by an antiquark $\bar{q}$, we may get the $B \to XYZ + K$ process, where XYZ denote the charmoniumlike structures. Obviously, due to the similar production mechanism between the $\Lambda_b \to P_c K$ and $B \to XYZ + K$ (see Fig. 1), we naturally conjecture that the $B \to XYZ + K$ should be the ideal processes to produce the hidden-charm molecular tetraquark states, especially with establishing the hidden-charm molecular tetraquark states. As is well known, the $X(3872)$ is a typical example of hidden-charm molecular tetraquark state, which was found

*wangfl2016@lzu.edu.cn
†yangxd20@lzu.edu.cn
‡chen_rui@pku.edu.cn
§Corresponding author.
xiangliu@lzu.edu.cn

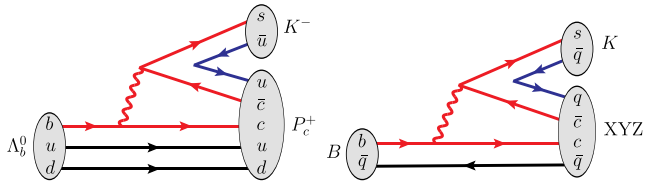

FIG. 1. The production mechanisms of the P_c states from the Λ_b baryon decays and the XYZ states from the B meson decays.

in the $B^{\pm} \to J/\psi\pi^+\pi^- K^{\pm}$ process by the Belle collaboration in 2003 [10]. The $X(3872)$ was suggested to be an isoscalar $D\bar{D}^*$ molecular state with $J^{PC} = 1^{++}$ [11–17].

In fact, the road of identifying the hidden-charm molecular tetraquark states is getting confusing [18–24]. In 2004, the Belle Collaboration reported the observation of the charmoniumlike state $Y(3940)$ in the $J/\psi\omega$ invariant mass spectrum of the $B \to J/\psi\omega K$ [25]. In 2009, the CDF Collaboration observed another charmoniumlike state $Y(4140)$ in the $J/\psi\phi$ invariant mass spectrum of the $B \to J/\psi\phi K$ [26]. In Ref. [27], Liu and Zhu noticed the similarity between the $Y(3940)$ and $Y(4140)$, and proposed $S-$wave $D^*\bar{D}^*$ and $D_s^*\bar{D}_s^*$ molecular states assignment to the $Y(3940)$ and $Y(4140)$, respectively, where the J^{PC} quantum numbers for the $Y(3940)$ and $Y(4140)$ should be either 0^{++} or 2^{++} due to a simple selection rules from the parity and angular momentum conservation [27]. In the subsequent experiments, the LHCb analyzed the $B \to J/\psi\phi K$ process, where the $Y(4140)$ was confirmed and other three new structures $X(4274)$, $X(4500)$ and $X(4700)$ were discovered in the $J/\psi\phi$ invariant mass spectrum [28]. However, the LHCb announced that the preferred J^{PC} quantum number of the $Y(4140)$ is 1^{++} [29], which obviously cannot support the molecular assignment to the $Y(4140)$ suggested in Ref. [27]. If checking the experimental and theoretical research status of the $Z(4430)$, which was reported by the Belle in the $B \to \psi(3686)\pi K$ [30], the same situation again happens. Since the $Z(4430)$ is near the threshold of $D^*\bar{D}_1^{(\prime)}$ channel, the authors of Refs. [31,32] suggested that the $Z(4430)$ can be the good candidate of the $S-$wave $D_1\bar{D}^*$ molecular state[1] with $J^P = 0^-, 1^-, 2^-$ by the one-boson-exchange (OBE) model calculation. However, the Belle [33] and LHCb [34] reanalyzed the $B \to \psi(3686)\pi K$ and indicated that the $Z(4430)$ has quantum number $J^P = 1^+$, which is contradict with the $S-$wave $D_1\bar{D}^*$ molecular state assignment [31,32].

Although there were a dozen of charmoniumlike structures reported by experiments in the B meson decays [22], unfortunately we have not definitely identify one hidden-charm molecular tetraquark state until now [18–24]. It is big challenge to assign the molecular state explanations to the charmoniumlike structures from the $B \to XYZ + K$ processes.

If we still believe the similar production mechanism between the $\Lambda_b \to P_c K$ and $B \to XYZ + K$ (see Fig. 1), we have reason to believe the existence of the hidden-charm molecular tetraquark state in the $B \to XYZ + K$ processes. Facing this situation mentioned above, we should try to find possible solutions existing in the reported experimental data of the $B \to XYZ + K$. In fact, the lesson of observation of the P_c states in 2015 [1] and 2019 [2] may inspire us. In 2015, the LHCb measured the J^P quantum numbers of the $P_c(4380)$ and $P_c(4450)$, gave that their preferred J^P quantum numbers are of opposite parity [1], which is a challenge to the hadronic molecular assignment [9]. This situation was dramatically changed with further LHCb experiment in 2019, where the $P_c(4450)$ is composed of two substructures $P_c(4440)$ and $P_c(4457)$ [2], which means that the measurement of spin-parity quantum number of the observed $P_c(4450)$ can be ignored [1]. To some extent, this fact reflects the importance of higher precision to the study of hadron spectroscopy.

With the running of the Belle II [35] and the accumulation of Run II and Run III data at the LHCb [36], obviously investigation of the charmoniumlike XYZ states must enter a new era. Thus, we should systematically reexamine the correlation of the hidden-charm molecular states and the charmoniumlike structures existing in the $B \to XYZ + K$ processes [18–24], where the constraint from J^{PC} quantum numbers and so-called resonance parameters of depicting these observed charmoniumlike XYZ structures should be more cautious in the interpretation of these resonances as the molecular states.

Along this line, we systematically restudy the $S-$wave interactions between a charmed (charmed-strange) meson and an anticharmed (anticharmed-strange) meson in the framework of the OBE model in this work [18,21]. In concrete calculations, both the $S-D$ wave mixing effect and the coupled channel effect are taken into account. Additionally, we discuss the two-body hidden-charm decay channels for the obtained $\mathcal{D}\bar{\mathcal{D}}$ and $\mathcal{D}_s\bar{\mathcal{D}}_s$ molecules, especially the $D^*\bar{D}^*$ molecular tetraquarks. Based on above discussion, we find a series of possible hints of the hidden-charm molecular tetraquarks existing in the released experimental data of the B meson decays, which will be a main task of the present work.

The remainder of this paper is organized as follows. In Sec. II, a comparison of the relevant experimental data and the corresponding thresholds will be given. In Sec. III, the mass spectrum and the two-body hidden-charm decay channels of these discussed hidden-charm molecular tetraquark systems will be given, and a series of possible hints of the hidden-charm molecular tetraquarks existing in the reported experimental data of the B meson decays will be presented. Finally, a brief summary will be given in Sec. IV.

[1]To be convenient, we use the shorthand notation $\mathcal{A}\bar{\mathcal{B}}$ to denote the $\mathcal{A}\bar{\mathcal{B}} + c.c.$ system in the following parts, where the notations $\mathcal{A}$ and $\mathcal{B}$ represent two different charmed (charmed-strange) mesons, respectively.

II. A COMPARISON OF THE EXPERIMENTAL DATA AND THE CORRESPONDING THRESHOLDS

In this work, the main task is to find possible hints of the hidden-charm molecular tetraquarks existing in the reported experimental data of the $B \to XYZ + K$ [22], and the hidden-charm molecular tetraquarks are composed of a charmed (charmed-strange) meson and an anticharmed (anticharmed-strange) meson. Thus, we need to make comparison of the involved experimental data and the corresponding thresholds of charmed meson pairs or charmed-strange meson pairs.

Usually, the S-wave and P-wave charmed mesons can be grouped into three doublets $H = [D(0^-), D^*(1^-)]$, $S = [D_0^*(0^+), D_1'(1^+)]$, and $T = [D_1(1^+), D_2^*(2^+)]$ according to the heavy quark spin symmetry [37]. Similarly, there also exist three doublets for the $S-$wave and P-wave charmed-strange mesons, i.e., $H = [D_s, D_s^*]$, $S = [D_{s0}^*, D_{s1}']$, and $T = [D_{s1}, D_{s2}^*]$ [37]. In Table I, we list these thresholds of charmed meson pairs or charmed-strange meson pairs [38], which are distributed over a very wide energy range 3.7–5.2 GeV. However, if only considering the kinetics of the $B \to XYZ + K$ decays, the maximum mass of the involved XYZ structures should be $M(XYZ)_{\max} = M(B) - M(K) = 4783$ MeV, which makes us select these thresholds with mass lower than 4783 MeV when making further analysis. Additionally, the charmed mesons in $S-$ doublet have broad widths around several hundred MeV [38], which may be a obstacle for the formation of the hadronic molecular states [39,40]. Different from the charmed mesons in $S-$ doublet, these charmed mesons in the H-doublet and T-doublet have narrow widths [38], which can be regarded as the suitable components to form the hadronic molecular states [32,39,40]. Just considering the above fact, we consider the cases of $H\bar{H}$ and $H\bar{T}$ for charmed meson pairs and the cases of $H\bar{H}$, $H\bar{S}$, and $H\bar{T}$ for charmed-strange meson pairs when performing a comparison of these thresholds with the released experimental data.

At present, the experimental information of the $B \to XYZ + K$ are very abundant [18–24]. Here, the XYZ data are from the $J/\psi\pi\pi$ invariant mass spectrum of the $B \to J/\psi\pi\pi K$ [10], the $J/\psi\omega$ invariant mass spectrum of the $B \to J/\psi\omega K$ [25,41,42], the $J/\psi\eta$ invariant mass spectrum of the $B \to J/\psi\eta K$ [43], the $J/\psi\phi$ invariant mass spectrum of the $B \to J/\psi\phi K$ [26,28,29,44–49], the $\eta_c\pi$ invariant mass spectrum of the $B \to \eta_c\pi K$ [50], the $J/\psi\pi$ invariant mass spectrum of the $B \to J/\psi\pi K$ [51–53], the $\psi(3686)\pi$ invariant mass spectrum of the $B \to \psi(3686)\pi K$ [30,33,34,54], the $\chi_{c1}\pi$ invariant mass spectrum of the $B \to \chi_{c1}\pi K$ [55–58], and the $\chi_{c2}\pi$ invariant mass spectrum of the $B \to \chi_{c2}\pi K$ [57]. For clearly discussing the present issue, we categorized these XYZ data into three groups:

(i) Isoscalar XYZ data without hidden-strange quantum number are involved in the $B \to J/\psi\omega K$ and $B \to J/\psi\eta K$;
(ii) Isoscalar XYZ data with hidden-strange quantum number are relevant to the $B \to J/\psi\phi K$;
(iii) Isovector XYZ data without hidden-strange quantum number have relation to five decay processes, i.e., the $B \to \eta_c\pi K$, $B \to J/\psi\pi K$, $B \to \psi(3686)\pi K$, $B \to \chi_{c1}\pi K$, and $B \to \chi_{c2}\pi K$.

In the following, we adopt this line to make comparison of the released experimental data and the corresponding thresholds.

A. Isoscalar XYZ data without hidden-strange quantum number

In 2005, the Belle Collaboration analyzed the $J/\psi\omega$ invariant mass spectrum of the $B \to J/\psi\omega K$ decay, where the charmoniumlike structure $Y(3940)$ was reported, which can be depicted by resonance parameters $M = (3943 \pm 11 \pm 13)$ MeV and $\Gamma = (87 \pm 22 \pm 26)$ MeV [25]. In 2008, the *BABAR* Collaboration confirmed this observation

TABLE I. The thresholds of charmed (charmed-strange) meson pairs (in unit of MeV).

Without hidden-strange quantum number						
DD	DD^*	D^*D^*	DD_0^*	DD_1	DD_1'	DD_2^*
3734.48	3875.80	4017.12	4191.74	4289.24	4294.24	4330.29
$D^*D_0^*$	D^*D_1	D^*D_1'	$D^*D_2^*$	$D_0^*D_0^*$	$D_0^*D_1$	$D_0^*D_1'$
4333.06	4430.56	4435.56	4471.61	4649.00	4746.50	4751.50
$D_0^*D_2^*$	D_1D_1	$D_1'D_1$	$D_1'D_1'$	$D_1D_2^*$	$D_1'D_2^*$	$D_2^*D_2^*$
4787.55	4844.00	4849.00	4854.00	4885.05	4890.05	4926.10
With hidden-strange quantum number						
D_sD_s	$D_sD_s^*$	$D_s^*D_s^*$	$D_sD_{s0}^*$	D_sD_{s1}'	$D_s^*D_{s0}^*$	D_sD_{s1}
3936.68	4080.54	4224.40	4286.14	4427.84	4430	4503.45
$D_sD_{s2}^*$	$D_s^*D_{s1}'$	$D_{s0}^*D_{s0}^*$	$D_s^*D_{s1}$	$D_s^*D_{s2}^*$	$D_{s0}^*D_{s1}'$	$D_{s0}^*D_{s1}$
4537.44	4571.70	4635.60	4647.31	4681.30	4777.30	4852.91
$D_{s0}^*D_{s2}^*$	$D_{s1}'D_{s1}'$	$D_{s1}'D_{s1}$	$D_{s1}D_{s1}$	$D_{s1}'D_{s2}^*$	$D_{s1}D_{s2}^*$	$D_{s2}^*D_{s2}^*$
4886.90	4919.00	4994.61	5028.60	5070.22	5104.20	5138.20

in the same process with a lower mass, named as the $Y(3915)$, and its mass and width were measured to be $(M,\Gamma) = (3914.6^{+3.8}_{-3.4} \pm 2.0\ \text{MeV}, 34^{+12}_{-8} \pm 5\ \text{MeV})$ [41]. In the subsequent *BABAR* experiment in 2010 [42], the mass and width of the $Y(3915)$ were measured to be $M = (3919.1^{+3.8}_{-3.5} \pm 2.0)$ MeV and $\Gamma = (31^{+10}_{-8} \pm 5)$ MeV, respectively.

If checking these data of the $J/\psi\omega$ invariant mass spectrum of the $B \to J/\psi\omega K$ from the Belle and *BABAR* [25,41,42], we may find the impact of experimental precision on reflecting the details. In the Belle data [25], there are only four experimental points sandwiched by the $D\bar{D}^*$ and $D^*\bar{D}^*$ thresholds. After several years, the number of experimental points in this energy range reach up to 12 and 14, which correspond to the *BABAR* data measured in 2008 [41] and 2010 [42], respectively. In Fig. 2, we collect all reported data of the $J/\psi\omega$ invariant mass spectrum from the $B \to J/\psi\omega K$ [25,41,42]. In fact, the *BABAR* data released in 2008 [41] show the possibility of existing two structures around 3.9 GeV below the $D^*\bar{D}^*$ threshold in the $J/\psi\omega$ invariant mass spectrum. Especially, the *BABAR* measurement in 2010 further enforce this possibility [42].

If D^* and $\bar{D}^*$ can be bound together to form the hidden-charm molecular tetraquarks, the J^{PC} quantum numbers of the $S-$wave isoscalar $D^*\bar{D}^*$ molecular system must be 0^{++}, 1^{+-}, and 2^{++} [27]. Under this assumption, the behavior of mass spectrum of the $S-$wave isoscalar $D^*\bar{D}^*$ molecular states can explain why two substructures around 3.9 GeV exist in the $J/\psi\omega$ invariant mass spectrum of the $B \to J/\psi\omega K$ [25,41,42]. Thus, we strongly encourage our experimental colleagues to focus on the detail of the structures around 3.9 GeV with more precise data. If these substructures can be confirmed in future experiments discussed above, it will provide strong evidence of existing the hidden-charm molecular tetraquark. Later, we will revisit a dynamics study of the $S-$wave isoscalar $D^*\bar{D}^*$ system, and come back to address this point.

Besides the enhancement structures around 3.9 GeV exist in the $J/\psi\omega$ invariant mass spectrum, we may find a very broad structure around 4.3 GeV exists in the $J/\psi\omega$ invariant mass spectrum of the $B \to J/\psi\omega K$ [25,41,42], where there exist four thresholds ($D\bar{D}_1$, $D\bar{D}_2^*$, $D^*\bar{D}_1$, and $D^*\bar{D}_2^*$) in this energy range, which inspire our interest in exploring whether the isoscalar $D\bar{D}_1$, $D\bar{D}_2^*$, $D^*\bar{D}_1$, and $D^*\bar{D}_2^*$ molecular tetraquarks exist in nature, which will be one of tasks in this work. Obviously, the details of such broad structure around 4.3 GeV should be given in future experiments with more precise data accumulation.

For the isoscalar XYZ data without hidden-strange quantum number, we should mention the measurement of the $J/\psi\eta$ invariant mass spectrum in the $B \to J/\psi\eta K$ decay. In 2004, the *BABAR* released the result of the $J/\psi\eta$ invariant mass spectrum in the $B \to J/\psi\eta K$ [43]. In Fig. 2, we compare the *BABAR* data with the several thresholds of charmed meson pairs, and may find the evidence of one

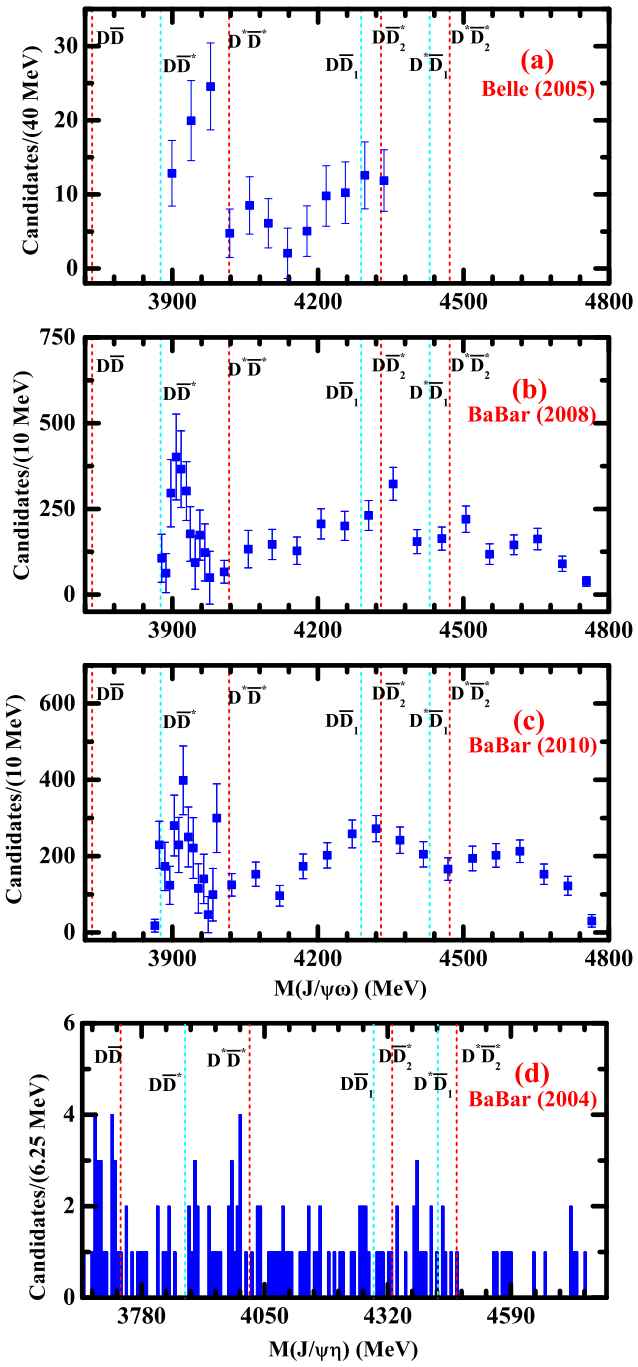

FIG. 2. The $J/\psi\omega$ and $J/\psi\eta$ invariant mass distributions in the $B \to J/\psi\omega K$ and $B \to J/\psi\eta K$, respectively, and the comparison with the thresholds of charmed meson pairs. Here, the experimental data of the $J/\psi\omega$ invariant mass spectrum are taken from the Belle [25], *BABAR* [41], and *BABAR* [42], which correspond to diagrams (a)–(c), and the experimental data of the $J/\psi\eta$ invariant mass spectrum is from the *BABAR* measurement [43] (see diagram (d)).

structure below $D^*\bar{D}^*$ threshold and possible enhancement structure around 4.3 GeV which overlaps with the $D\bar{D}_1$, $D\bar{D}_2^*$, $D^*\bar{D}_1$, and $D^*\bar{D}_2^*$ thresholds. In fact, this phenomenon again shows studying the isoscalar $D^*\bar{D}^*$, $D\bar{D}_1$, $D\bar{D}_2^*$,

$D^*\bar{D}_1$, and $D^*\bar{D}_2^*$ hadronic molecular states is an urgent research issue, which may provide crucial information to find the evidence of the existence of the hidden-charm molecular tetraquark.

B. Isoscalar *XYZ* data with hidden-strange quantum number

Up to now, the $B \to J/\psi\phi K$ decay have been analyzed by the different experiment collaborations [26,28,29,44–49], where we are mainly interested in the experimental data of the $J/\psi\phi$ invariant mass spectrum from the CDF [26], CMS [44], and LHCb [28] in the following discussion. Since the quark components of the ϕ and J/ψ are the $s\bar{s}$ and $c\bar{c}$, respectively, we present the thresholds of charmed-strange meson pairs in Fig. 3 when making comparison with these released experimental data.

First, we should brief introduce the experimental status of the obtained $J/\psi\phi$ invariant mass spectrum in the $B \to J/\psi\phi K$ decay [26,28,44]. As shown in Fig. 3(a), the CDF Collaboration reported the charmoniumlike structure $Y(4140)$ in the $J/\psi\phi$ mass spectrum of the $B \to J/\psi\phi K$ decay in 2009 [26]. When depicting this enhancement structure, the resonance parameters can be obtained, i.e., the mass and width of the $Y(4140)$ were measured to be $M = (4143.0 \pm 2.9 \pm 1.2)$ MeV and $\Gamma = (11.7^{+8.3}_{-5.0} \pm 3.7)$ MeV [26], respectively. Besides the $Y(4140)$ structure, the CDF also reported another enhancement structure, named as the $Y(4274)$, in the $J/\psi\phi$ invariant mass spectrum, where its mass and width are $(M,\Gamma) = (4274.4^{+8.4}_{-6.7} \pm 1.9\ \text{MeV}, 32.3^{+21.9}_{-15.3} \pm 7.6\ \text{MeV})$ [26], respectively. Later, the CMS confirmed these two structures $Y(4140)$ and $Y(4274)$ in the same decay process in 2014, where the resonance parameters of the $Y(4140)$ and $Y(4274)$ were measured to be $(M,\Gamma)_{Y(4140)} = (4148.0 \pm 2.4 \pm 6.3\ \text{MeV}, 28^{+15}_{-11} \pm 19\ \text{MeV})$ and $(M,\Gamma)_{Y(4274)} = (4313.8 \pm 5.3 \pm 7.3\ \text{MeV}, 38^{+30}_{-15} \pm 16\ \text{MeV})$ [44], respectively. Surprisingly, the LHCb Collaboration announced four charmoniumlike resonances in the $J/\psi\phi$ mass spectrum of the $B \to J/\psi\phi K$ decay in 2017 [28]. Here, we collect their resonance parameters, i.e., $(M,\Gamma)_{Y(4140)} = (4146.5 \pm 4.5^{+4.6}_{-2.8}\ \text{MeV}, 83 \pm 21^{+21}_{-14}\ \text{MeV})$, $(M,\Gamma)_{Y(4274)} = (4273.3 \pm 8.3^{+17.2}_{-3.6}\ \text{MeV}, 56.2 \pm 10.9^{+8.4}_{-11.1}\ \text{MeV})$, $(M,\Gamma)_{X(4500)} = (4506 \pm 11^{+12}_{-15}\ \text{MeV}, 92 \pm 21^{+21}_{-20}\ \text{MeV})$, and $(M,\Gamma)_{X(4700)} = (4704 \pm 10^{+14}_{-24}\ \text{MeV}, 120 \pm 31^{+42}_{-33}\ \text{MeV})$ [28].

If comparing three experimental data listed in Fig. 3, we find that the precision of the LHCb data [28] is higher than the CDF and CMS data [26,44], where there are 12 experimental points in the energy range sandwiched by the $D_s\bar{D}_s^*$ and $D_s^*\bar{D}_s^*$ thresholds for the LHCb data [28], which reflect some abundant details difference from former CDF and CMS [26,44]. When only adopting a Breit-Wigner formula to describe this resonance structure around 4140 MeV, the width given by the LHCb [28] becomes wider than that from the CDF and CMS [26,44]. This phenomenon is puzzling for us since the LHCb released this result [28], especially the recent LHCb result of the $Y(4140)$ [49].

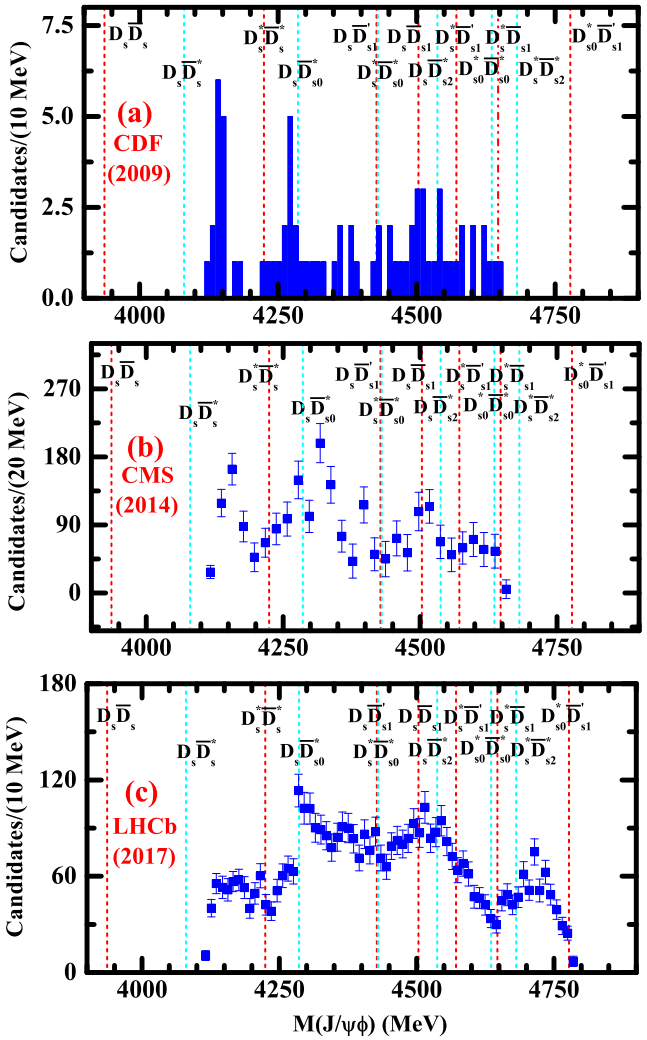

FIG. 3. The measured $J/\psi\phi$ invariant mass distribution of the $B \to J/\psi\phi K$ and the thresholds of charmed-strange meson pairs. Here, the experimental data are taken from the CDF [26], CMS [44], and LHCb [28], which correspond to diagrams (a)–(c).

We notice an interesting fact that this structure around 4140 MeV reported by the CDF is below the $D_s^*\bar{D}_s^*$ threshold [26], and Liu and Zhu proposed that the $Y(4140)$ observed by the CDF can be regarded as partner of the $Y(3940)$ due to the similarity between the $Y(3940)$ and $Y(4140)$ in 2009 [27]. Thus, the $D_s^*\bar{D}_s^*$ hadronic molecular state explanation to the $Y(4140)$ was given [27]. Along this line, there may exist $S-$wave $D_s^*\bar{D}_s^*$ molecular states, which is similar to the situation of the $S-$wave isoscalar $D^*\bar{D}^*$ molecular system discussed in Sec. II A. Facing such abundant details given by the LHCb in 2017 [28], we may conjecture that the $Y(4140)$ structure may be contain at least two substructures, which can be

tested by future experiments based on more precise data. If introducing this proposal, the conclusion of the spin-parity quantum number $J^{PC} = 1^{++}$ for the $Y(4140)$ given by the LHCb seems unreliable[2] [28]. Here, we need to mention that the recent LHCb Collaboration updated the amplitude analysis of the $B^+ \to J/\psi\phi K^+$ decay with higher precision data and reported the $X(4140)$ with $J^{PC} = 1^{++}$ and $X(4150)$ with $J^{PC} = 2^{-+}$ [49], which imply the very complicated structures around the $D_s^*\bar{D}_s^*$ threshold. In the following, the investigation of the $S-$wave $D_s^*\bar{D}_s^*$ hadronic molecular system will become a main point of this work, which will be further discussed in the next section.

Besides the structure around 4140 MeV existing in the $J/\psi\phi$ invariant mass spectrum, we should focus on the $Y(4274)$ [26,28,44], which is just near the $D_s\bar{D}_{s0}^*$ threshold. Thus, the study of the $D_s\bar{D}_{s0}^*$ molecular system will be paid attention in this work. Although the LHCb reported $X(4500)$ and $X(4700)$ in 2017 [28], we can find more abundant structures above 4250 MeV existing in the $J/\psi\phi$ invariant mass spectrum if carefully checking the LHCb data [28]. Indeed, the recent LHCb Collaboration announced the observation of other new resonance structures existing in this energy range with more precise data, i.e., the $X(4630)$ with $J^{PC} = 1^{-+}$ and $X(4685)$ with $J^{PC} = 1^{++}$ [49]. We also notice that there are abundant thresholds of charmed-strange meson pairs in this interesting energy range. Thus, we will investigate the hidden-charm and hidden-strange molecular tetraquarks involved these thresholds in this work.

C. Isovector *XYZ* data without hidden-strange quantum number

In the past 18 years, the isovector XYZ data from the $B \to XYZ + K$ were accumulated [18–24]. In Figs. 4 and 5, we collected all relevant experimental data and make a comparison with several typical thresholds of charmed meson pairs. For different decay processes listed in Figs. 4 and 5, we briefly review the experimental information:

(1) The $B \to \psi(2S)\pi K$ decay: As a super star among these reported charged charmoniumlike structures, the $Z^+(4430)$ structure was first observed by the Belle Collaboration in the $\psi(2S)\pi$ invariant mass distribution of the $B \to \psi(2S)\pi K$ decay in 2008 [30]. Here, its mass and width were measured to be $M = (4433 \pm 4 \pm 2)$ MeV and $\Gamma = (45^{+18+30}_{-13-13})$ MeV, respectively [30]. In the following years, the Belle Collaboration continued their studies on the $Z^+(4430)$, and the measured mass of the $Z^+(4430)$ structure are $M = (4443^{+15\ +19}_{-12\ -13})$ MeV [54] and $M = (4485^{+22\ +28}_{-22\ -11})$ MeV [33], respectively. After ten years, the LHCb Collaboration confirmed the existence of the $Z^+(4430)$ structure [34], and the resonance parameters are $M = (4475 \pm 7^{+15}_{-25})$ MeV and $\Gamma = (172 \pm 13^{+37}_{-34})$ MeV, respectively. But, the width from the LHCb [34] is more broad than that from the Belle [30,33,54]. Additionally, the LHCb found a new structure $Z^+(4240)$ in the $\psi(2S)\pi$ invariant mass distribution of the $B \to \psi(2S)\pi K$, which can be depicted by resonance parameters $M = (4239 \pm 18^{+45}_{-10})$ MeV and $\Gamma = (220 \pm 47^{+108}_{-74})$ MeV, respectively [34]. Comparing with the Belle data [30,33,54], the LHCb data have smaller error bars [34]. Since the $Z^+(4430)$ structure is near several thresholds of charmed meson pair, there were extensive discussion of the hidden-charm molecular tetraquark explanation to the $Z^+(4430)$ [31,32,59]. In this work, we will still dedicate this topic, which is the study of the isovector hidden-charm molecular tetraquark involved in this energy range.

(2) The $B \to \eta_c\pi K$ decay: In 2018, the LHCb found the evidence of a broad charmoniumlike structure in the $\eta_c\pi$ invariant mass spectrum of the $B \to \eta_c\pi K$ decay, which was named as the $X(4100)$ with the mass $M = (4096 \pm 20^{+18}_{-22})$ MeV and the width $\Gamma = (152 \pm 58^{+60}_{-35})$ MeV [50]. In fact, there exists event accumulation around 4.5 GeV, where several thresholds of charmed meson pairs can be found [see Fig. 4(e)].

(3) The $B \to \chi_{c1}\pi K$ decay: For the $\chi_{c1}\pi$ invariant mass distribution in the $B \to \chi_{c1}\pi K$ decay, two charged charmoniumlike structures $Z^+(4051)$ and $Z^+(4248)$ were announced by the Belle Collaboration in the exclusive $B \to \chi_{c1}\pi K$ decay [55], where their resonance parameters were measured to be $(M,\Gamma)_{Z^+(4051)} = (4051 \pm 14^{+20}_{-41}$ MeV$, 82^{+21\ +47}_{-17\ -22}$ MeV$)$ and $(M,\Gamma)_{Z^+(4248)} = (4248^{+44\ +180}_{-29\ -35}$ MeV$, 177^{+54\ +316}_{-39\ -61}$ MeV$)$ [55], respectively. However, these two charged charmoniumlike structures were not seen in the following *BABAR* experiment [56]. In 2016, the Belle Collaboration carried out a new measurement of the $B \to \chi_{c1}\pi K$, where the distribution of the $\chi_{c1}\pi$ invariant mass spectrum was given [57]. In fact, the line shape of the $\chi_{c1}\pi$ invariant mass spectrum is complicated. Additionally, for searching for the $X(3872)$ and $X(3915)$ decaying to the final state $\chi_{c1}\pi$ in the B meson decay, the Belle measured the $\chi_{c1}\pi$ invariant mass spectrum from the B meson decay, by which they did not find the significant signals of the $X(3872)$ and $X(3915)$ [58].

(4) The $B \to \chi_{c2}\pi K$ decay: In 2016, the Belle Collaboration provided the measured $\chi_{c2}\pi$ invariant mass

[2]For the $S-$wave $D_s^*\bar{D}_s^*$ molecular system, its J^{PC} quantum numbers are either 0^{++} or 2^{++}, which is due to a selection rule for the quantum numbers [27]. However, the LHCb measurement suggested $J^{PC} = 1^{++}$ for the $Y(4140)$ [28], which results in the difficulty to understand the $Y(4140)$ under the hadronic molecular state assignment.

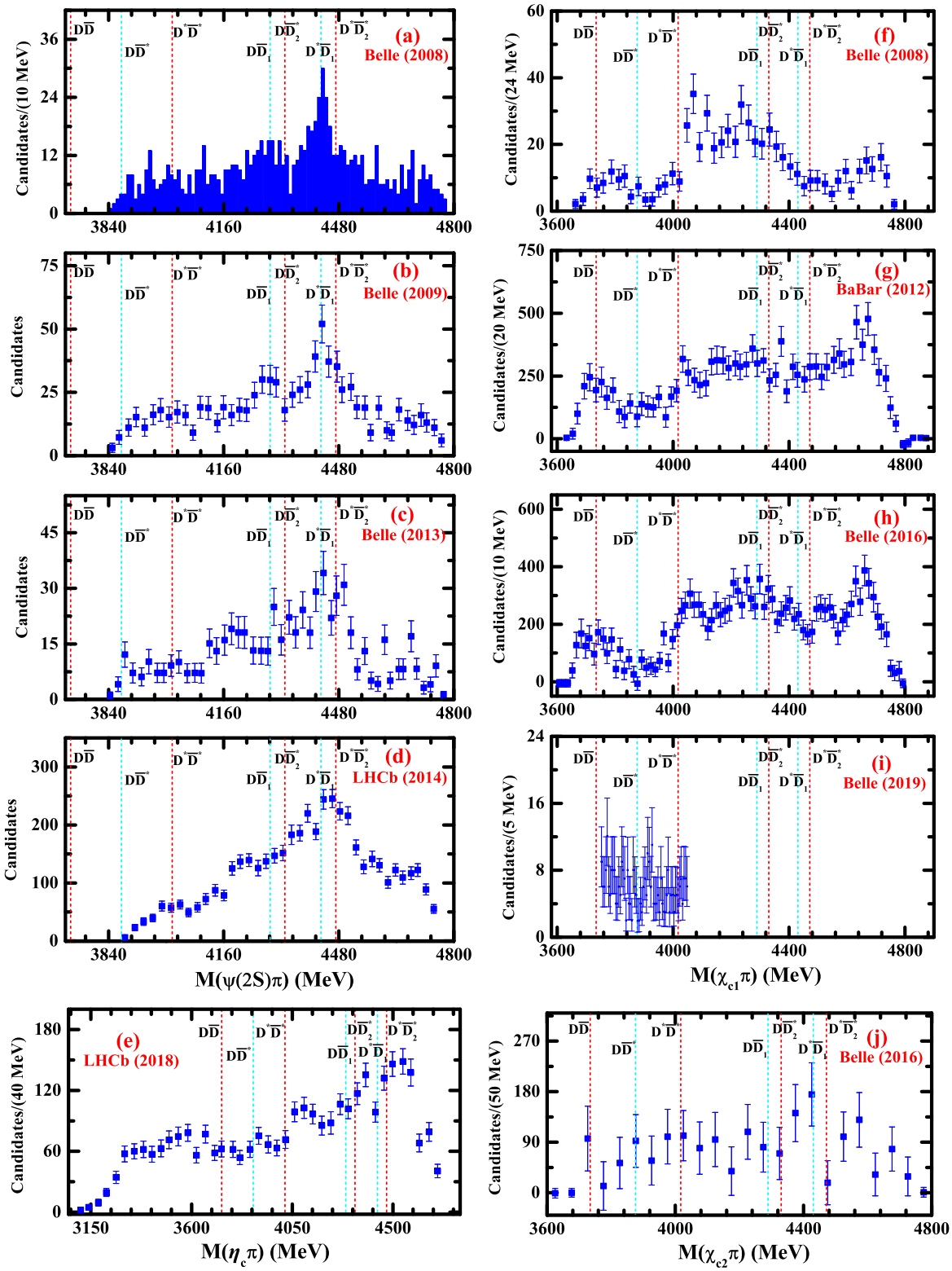

FIG. 4. The measured $\psi(2S)\pi$, $\eta_c\pi$, $\chi_{c1}\pi$, and $\chi_{c2}\pi$ invariant mass distributions in the $B \to XYZ + K$ decays, and the comparison with the thresholds of charmed meson pairs. Here, the experimental data of the $\psi(2S)\pi$ are taken from (a) the Belle [30], (b) the Belle [54], (c) the Belle [33], and (d) the LHCb [34], while the experimental data of $\eta_c\pi$ is taken from the LHCb [50] [see diagram (e)]. In addition, the experimental data of $\chi_{c1}\pi$ are taken from (f) the Belle [55], (g) the *BABAR* [56], (h) the Belle [57], and (i) the Belle [58], while the experimental result of the $\chi_{c2}\pi$ invariant mass spectrum is given by the Belle [57] [see diagram (j)].

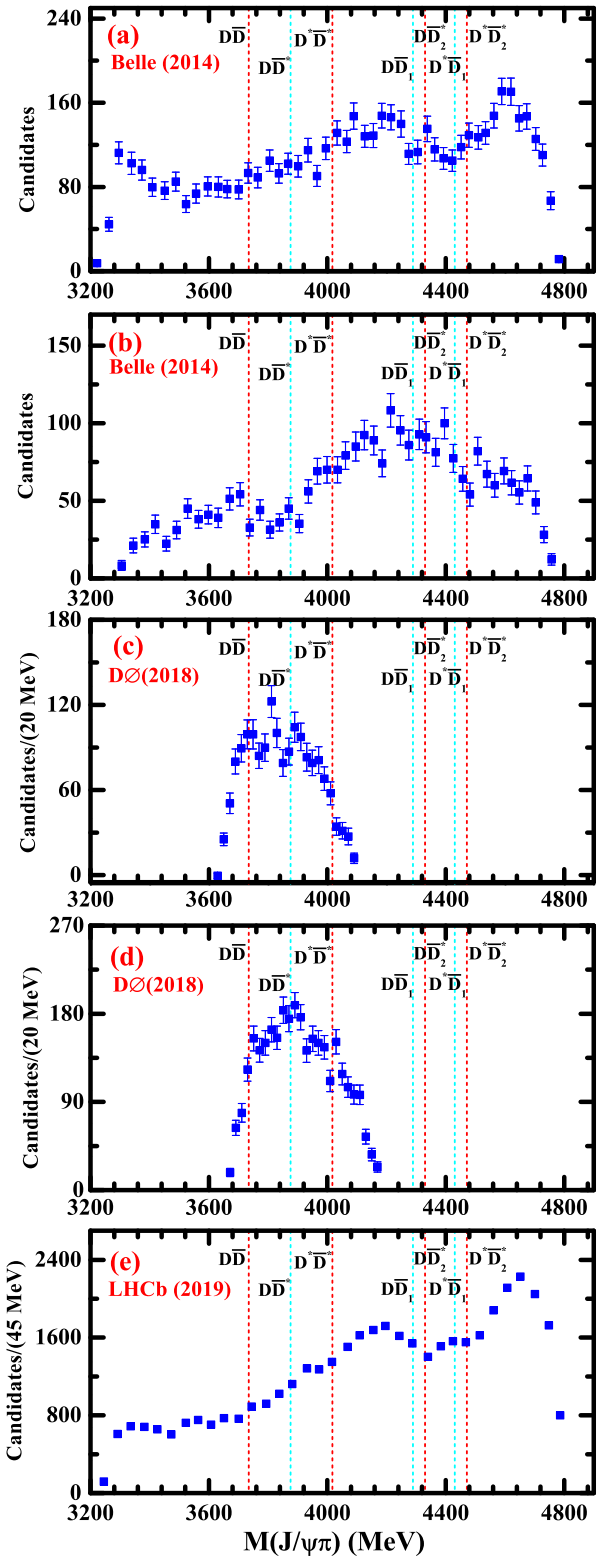

FIG. 5. The $J/\psi\pi$ invariant mass distribution in the $B \to J/\psi\pi K$ and the relevant thresholds of charmed meson pairs. Here, the experimental datas are taken from the Belle [51] [(a) for 1.20 GeV$^2 < m^2(K\pi) <$ 2.05 GeV^2 and (b) for 2.05 GeV$^2 < m^2(K\pi) <$ 3.20 GeV^2], the DØ [52] [(c) for 4.25 GeV $< m(J/\psi\pi^+\pi^-) <$ 4.30 GeV and (d) for 4.30 GeV $< m(J/\psi\pi^+\pi^-) <$ 4.40 GeV], and (e) the LHCb [53], respectively.

spectrum with low precision [57]. Here, the comparison of data and thresholds is shown.

(5) The $B \to J/\psi\pi K$ decay: As shown in Fig. 5(a) and 5(b), the Belle[3] Collaboration presented the results of an amplitude analysis of the $B \to J/\psi\pi K$ decay in 2014, and reported a very broad charged charmoniumlike structure $Z_c(4200)^+$, where its mass and width were measured to be $(M,\Gamma) = (4196^{+31}_{-29}{}^{+17}_{-13}$ MeV, $370^{+70}_{-70}{}^{+70}_{-132}$ MeV) [51], respectively. We may find such broad structure overlaps with many thresholds (see Fig. 5(a) and 5(b) for more details). The correlation of this broad structure with the corresponding isovector hidden-charm molecular tetraquarks should be investigated, which will become an important issue in this work. In 2018, the DØ Collaboration analyzed the data of the $J/\psi\pi$ invariant mass spectrum from the $B \to J/\psi\pi K$ [52], where they only focused on $3600 < m_{J/\psi\pi} < 4200$ MeV range inspired by the observed $Z_c(3900)^\pm$ from the BESIIII [60] and Belle [61]. And the DØ data show the evidence of charged charmoniumlike structure similar to the $Z_c(3900)^\pm$, where the measured mass of the $Z_c(3900)^\pm$ is $3895.0 \pm 5.2^{+4.0}_{-2.7}$ MeV. Since the width information of such structure is still absent in the DØ measurement, it is hard to conclude that the DØ evidence truly corresponds to the $Z_c(3900)^\pm$ [60,61]. Additionally, the $J/\psi\pi$ invariant mass spectrum of the $B \to J/\psi\pi K$ decay has been studied by the LHCb Collaboration in 2019 [53], and two enhancement structures are visible at 4200 and 4600 MeV.

As introduced above, the isovector XYZ data of the $B \to XYZ + K$ decays stimulate our interest in exploring the isovector hidden-charm molecular systems, which will be illustrated in Sec. III. By this study, we want to answer whether these isovector XYZ structures have close relation to the isovector hidden-charm molecular tetraquarks.

III. MASS SPECTRUM OF THE CHARMONIUMLIKE MOLECULAR TETRAQUARK SYSTEMS

In this section, we restudy the mass spectrum behaviors from a pair of charmed (charm-strange) meson and anticharmed (anticharm-strange) meson interactions, these charmed or anticharmed mesons are in the H, S, and T doublets. Here, we still adopt the OBE model and consider the $S-D$ wave mixing effect and the coupled channel effect. As is well known, since Yukawa firstly proposed the nucleon-nucleon interaction is mediated through the pion-exchange in 1935 [62], the OBE model obtains great promotion. On one hand, theorists consider the scalar

[3]Besides announcing the $Z_c(4200)^+$ structure, the Belle also gave the evidence for the $Z(4430)^+$ structure [51].

meson (σ) and vector meson (ρ/ω) exchanges interactions to depict the intermediate and short range interactions, respectively. On the other hand, several various corrections are introduced to discuss the fine properties of the hadron-hadron interactions, like the isospin breaking effects, the coupled-channel effects, the spin-orbit force, and the recoil corrections. Up to now, the OBE model have been frequently adopted to study the hadron-hadron interactions in the heavy flavor sector [18,21].

A. OBE effective potentials

For deducing the OBE effective potentials for the hadron-hadron interactions at the hadronic level quantitatively, we usually adopt the effective Lagrangian approach. The general procedures include three typical steps [63–69]. First, we can write out the scattering amplitude $\mathcal{M}(h_1h_2 \to h_3h_4)$ for the relevant scattering process $h_1h_2 \to h_3h_4$ according to the effective Lagrangians. And then, the effective potentials in the momentum space $\mathcal{V}_E^{h_1h_2\to h_3h_4}(\boldsymbol{q})$ can be related to the corresponding scattering amplitudes $\mathcal{M}(h_1h_2 \to h_3h_4)$ by using the Breit approximation [70,71], i.e.,

$$\mathcal{V}_E^{h_1h_2\to h_3h_4}(\boldsymbol{q}) = -\frac{\mathcal{M}(h_1h_2 \to h_3h_4)}{\sqrt{\prod_i 2m_i \prod_f 2m_f}}, \tag{3.1}$$

where $m_i (i = h_1, h_2)$ and $m_f (f = h_3, h_4)$ denote the masses of the initial and final states, respectively. Finally, the effective potentials in the coordinate space $\mathcal{V}_E^{h_1h_2\to h_3h_4}(\boldsymbol{r})$ can be obtained by performing the Fourier transformation, i.e.,

$$\mathcal{V}_E^{h_1h_2\to h_3h_4}(\boldsymbol{r}) = \int \frac{d^3\boldsymbol{q}}{(2\pi)^3} e^{i\boldsymbol{q}\cdot\boldsymbol{r}} \mathcal{V}_E^{h_1h_2\to h_3h_4}(\boldsymbol{q}) \mathcal{F}^2(q^2, m_E^2), \tag{3.2}$$

which will be applied to search for the bound state solutions by solving the coupled channel Schrödinger equation, and we can further extract the bound state properties from the obtained bound state solutions. Because the discussed hadrons are not pointlike particles, we introduce the monopole type form factor in each interaction vertex [72,73], i.e.,

$$\mathcal{F}(q^2, m_E^2) = \frac{\Lambda^2 - m_E^2}{\Lambda^2 - q^2}, \tag{3.3}$$

which reflects the finite size effect of the discussed hadrons and compensate the off-shell effect of the exchanged light mesons [67]. Here, Λ, m_E, and q are the cutoff parameter, the mass, and the four momentum of the exchanged light mesons, respectively.

Subsequently, let us construct the relevant effective Lagrangians. According to the heavy quark limit [37], the relevant super-fields $H_a^{(Q)}$, $H_a^{(\bar{Q})}$, $S_a^{(Q)}$, $S_a^{(\bar{Q})}$, $T_a^{(Q)\mu}$, and $T_a^{(\bar{Q})\mu}$ can be defined as [74]

$$\begin{aligned}
H_a^{(Q)} &= \mathcal{P}_+(D_a^{*(Q)\mu}\gamma_\mu - D_a^{(Q)}\gamma_5), \\
H_a^{(\bar{Q})} &= (\bar{D}_a^{*(\bar{Q})\mu}\gamma_\mu - \bar{D}_a^{(\bar{Q})}\gamma_5)\mathcal{P}_-, \\
S_a^{(Q)} &= \mathcal{P}_+(D_{1a}^{\prime(Q)\mu}\gamma_\mu\gamma_5 - D_{0a}^{*(Q)}), \\
S_a^{(\bar{Q})} &= (D_{1a}^{\prime(\bar{Q})\mu}\gamma_\mu\gamma_5 - D_{0a}^{*(\bar{Q})})\mathcal{P}_-, \\
T_a^{(Q)\mu} &= \mathcal{P}_+\left[D_{2a}^{*(Q)\mu\nu}\gamma_\nu - \sqrt{\frac{3}{2}}D_{1a\nu}^{(Q)}\gamma_5\left(g^{\mu\nu} - \frac{1}{3}\gamma^\nu(\gamma^\mu - v^\mu)\right)\right], \\
T_a^{(\bar{Q})\mu} &= \left[\bar{D}_{2a}^{*(\bar{Q})\mu\nu}\gamma_\nu - \sqrt{\frac{3}{2}}\bar{D}_{1a\nu}^{(\bar{Q})}\gamma_5\left(g^{\mu\nu} - \frac{1}{3}\gamma^\nu(\gamma^\mu - v^\mu)\right)\right]\mathcal{P}_-,
\end{aligned} \tag{3.4}$$

respectively. Here, $\mathcal{P}_\pm = (1 \pm \not{v})/2$ are the projection operators, and $v^\mu = (1, \mathbf{0})$ denotes the four velocity in the nonrelativistic approximation. Their conjugate fields read as $\bar{X} = \gamma_0 X^\dagger \gamma_0$ with $X = H_a^{(Q)}, H_a^{(\bar{Q})}, S_a^{(Q)}, S_a^{(\bar{Q})}, T_a^{(Q)\mu}$, and $T_a^{(\bar{Q})\mu}$.

According to the heavy quark symmetry, the chiral symmetry, and the hidden local symmetry [75–79], one can construct the effective Lagrangians describing the interactions between the (anti)charmed mesons in the $H/S/T$-doublet and the light scalar, pseudoscalar, and vector mesons [74],

$$\begin{aligned}
\mathcal{L} &= g_\sigma\langle H_a^{(Q)}\sigma\bar{H}_a^{(Q)}\rangle + g_\sigma\langle\bar{H}_a^{(\bar{Q})}\sigma H_a^{(\bar{Q})}\rangle + g'_\sigma\langle S_a^{(Q)}\sigma\bar{S}_a^{(Q)}\rangle + g'_\sigma\langle\bar{S}_a^{(\bar{Q})}\sigma S_a^{(\bar{Q})}\rangle + g''_\sigma\langle T_a^{(Q)\mu}\sigma\bar{T}_{a\mu}^{(Q)}\rangle + g''_\sigma\langle\bar{T}_a^{(\bar{Q})\mu}\sigma T_{a\mu}^{(\bar{Q})}\rangle \\
&+ \frac{h_\sigma}{f_\pi}[\langle S_a^{(Q)}\gamma^\mu\partial_\mu\sigma\bar{H}_a^{(Q)}\rangle - \langle\bar{H}_a^{(\bar{Q})}\gamma^\mu\partial_\mu\sigma S_a^{(\bar{Q})}\rangle + \text{H.c.}] + \frac{h'_\sigma}{f_\pi}[\langle T_a^{(Q)\mu}\partial_\mu\sigma\bar{H}_b^{(Q)}\rangle + \langle\bar{H}_a^{(\bar{Q})}\partial_\mu\sigma T_b^{(\bar{Q})\mu}\rangle + \text{H.c.}] \\
&+ ig\langle H_b^{(Q)}\mathcal{A}_{ba}\gamma_5\bar{H}_a^{(Q)}\rangle + ig\langle\bar{H}_a^{(\bar{Q})}\mathcal{A}_{ab}\gamma_5 H_b^{(\bar{Q})}\rangle + i\tilde{k}\langle S_b^{(Q)}\mathcal{A}_{ba}\gamma_5\bar{S}_a^{(Q)}\rangle + i\tilde{k}\langle\bar{S}_a^{(\bar{Q})}\mathcal{A}_{ab}\gamma_5 S_b^{(\bar{Q})}\rangle \\
&+ ik\langle T_b^{(Q)\mu}\mathcal{A}_{ba}\gamma_5\bar{T}_{a\mu}^{(Q)}\rangle + ik\langle\bar{T}_a^{(\bar{Q})\mu}\mathcal{A}_{ab}\gamma_5 T_{b\mu}^{(\bar{Q})}\rangle + [ih\langle S_b^{(Q)}\mathcal{A}_{ba}\gamma_5\bar{H}_a^{(Q)}\rangle + ih\langle\bar{H}_a^{(\bar{Q})}\mathcal{A}_{ab}\gamma_5 S_b^{(\bar{Q})}\rangle + \text{H.c.}]
\end{aligned}$$

$$+\left[i\left\langle T_b^{(Q)\mu}\left(\frac{h_1}{\Lambda_\chi}D_\mu\mathcal{A}+\frac{h_2}{\Lambda_\chi}\not{D}\mathcal{A}_\mu\right)_{ba}\gamma_5\bar{H}_a^{(Q)}\right\rangle+\text{H.c.}\right]+\left[i\left\langle \bar{H}_a^{(\bar{Q})}\left(\frac{h_1}{\Lambda_\chi}\mathcal{A}\overleftarrow{D}'_\mu+\frac{h_2}{\Lambda_\chi}\mathcal{A}_\mu\overleftarrow{\not{D}'}\right)_{ab}\gamma_5 T_b^{(\bar{Q})\mu}\right\rangle+\text{H.c.}\right]$$
$$+\langle iH_b^{(Q)}(\beta v^\mu(\mathcal{V}_\mu-\rho_\mu)+\lambda\sigma^{\mu\nu}F_{\mu\nu}(\rho))_{ba}\bar{H}_a^{(Q)}\rangle-\langle i\bar{H}_a^{(\bar{Q})}(\beta v^\mu(\mathcal{V}_\mu-\rho_\mu)-\lambda\sigma^{\mu\nu}F_{\mu\nu}(\rho))_{ab}H_b^{(\bar{Q})}\rangle$$
$$+\langle iS_b^{(Q)}(\beta' v^\mu(\mathcal{V}_\mu-\rho_\mu)+\lambda'\sigma^{\mu\nu}F_{\mu\nu}(\rho))_{ba}\bar{S}_a^{(Q)}\rangle-\langle i\bar{S}_a^{(\bar{Q})}(\beta' v^\mu(\mathcal{V}_\mu-\rho_\mu)-\lambda'\sigma^{\mu\nu}F_{\mu\nu}(\rho))_{ab}S_b^{(\bar{Q})}\rangle$$
$$+\langle iT_{b\lambda}^{(Q)}(\beta'' v^\mu(\mathcal{V}_\mu-\rho_\mu)+\lambda''\sigma^{\mu\nu}F_{\mu\nu}(\rho))_{ba}\bar{T}_a^{(Q)\lambda}\rangle-\langle i\bar{T}_{a\lambda}^{(\bar{Q})}(\beta'' v^\mu(\mathcal{V}_\mu-\rho_\mu)-\lambda''\sigma^{\mu\nu}F_{\mu\nu}(\rho))_{ab}T_b^{(\bar{Q})\lambda}\rangle$$
$$+[\langle H_b^{(Q)}(i\zeta\gamma^\mu(\mathcal{V}_\mu-\rho_\mu)+i\mu\sigma^{\lambda\nu}F_{\lambda\nu}(\rho))_{ba}\bar{S}_a^{(Q)}\rangle+\text{H.c.}]+[\langle\bar{S}_a^{(\bar{Q})}(i\zeta\gamma^\mu(\mathcal{V}_\mu-\rho_\mu)+i\mu\sigma^{\lambda\nu}F_{\lambda\nu}(\rho))_{ab}H_b^{(\bar{Q})}\rangle+\text{H.c.}]$$
$$+[\langle T_b^{(Q)\mu}(i\zeta_1(\mathcal{V}_\mu-\rho_\mu)+\mu_1\gamma^\nu F_{\mu\nu}(\rho))_{ba}\bar{H}_a^{(Q)}\rangle+\text{H.c.}]-[\langle\bar{H}_a^{(\bar{Q})}(i\zeta_1(\mathcal{V}_\mu-\rho_\mu)-\mu_1\gamma^\nu F_{\mu\nu}(\rho))_{ab}T_b^{(\bar{Q})\mu}\rangle+\text{H.c.}],\tag{3.5}$$

Here, the covariant derivatives are written as $D_\mu=\partial_\mu+\mathcal{V}_\mu$ and $D'_\mu=\partial_\mu-\mathcal{V}_\mu$. And the axial current $\mathcal{A}_\mu$, the vector current $\mathcal{V}_\mu$, the vector meson field ρ_μ, and the vector meson strength tensor $F_{\mu\nu}(\rho)$ are defined as

$$\mathcal{A}_\mu=\frac{1}{2}(\xi^\dagger\partial_\mu\xi-\xi\partial_\mu\xi^\dagger)_\mu,$$
$$\mathcal{V}_\mu=\frac{1}{2}(\xi^\dagger\partial_\mu\xi+\xi\partial_\mu\xi^\dagger)_\mu,$$
$$\xi=\exp(i\mathbb{P}/f_\pi),\qquad \rho_\mu=\frac{ig_V}{\sqrt{2}}\mathbb{V}_\mu,$$
$$F_{\mu\nu}(\rho)=\partial_\mu\rho_\nu-\partial_\nu\rho_\mu+[\rho_\mu,\rho_\nu].\tag{3.6}$$

respectively. The light pseudoscalar meson matrix $\mathbb{P}$ and the light vector meson matrix $\mathbb{V}_\mu$ have the conventional form [63,68,69], which can be expressed as

$$\mathbb{P}=\begin{pmatrix}\frac{\pi^0}{\sqrt{2}}+\frac{\eta}{\sqrt{6}} & \pi^+ & K^+\\ \pi^- & -\frac{\pi^0}{\sqrt{2}}+\frac{\eta}{\sqrt{6}} & K^0\\ K^- & \bar{K}^0 & -\sqrt{\frac{2}{3}}\eta\end{pmatrix},$$
$$\mathbb{V}_\mu=\begin{pmatrix}\frac{\rho^0}{\sqrt{2}}+\frac{\omega}{\sqrt{2}} & \rho^+ & K^{*+}\\ \rho^- & -\frac{\rho^0}{\sqrt{2}}+\frac{\omega}{\sqrt{2}} & K^{*0}\\ K^{*-} & \bar{K}^{*0} & \phi\end{pmatrix}_\mu,\tag{3.7}$$

respectively. After expanding the compact effective Lagrangians in Eq. (3.5) to the leading order of the pseudo-Goldstone field ξ, we can further obtain the concrete effective Lagrangians (see Refs. [65–67,80,81] for more information). The normalized relations for these discussed charmed mesons are written as

$$\langle 0|D|c\bar{q}(0^-)\rangle=\sqrt{m_D},\quad \langle 0|D^{*\mu}|c\bar{q}(1^-)\rangle=\epsilon^\mu\sqrt{m_{D^*}},$$
$$\langle 0|D_0^*|c\bar{q}(0^+)\rangle=\sqrt{m_{D_0^*}},\quad \langle 0|D_1'^\mu|c\bar{q}(1^+)\rangle=\epsilon^\mu\sqrt{m_{D_1'}},$$
$$\langle 0|D_1^\mu|c\bar{q}(1^+)\rangle=\epsilon^\mu\sqrt{m_{D_1}},\quad \langle 0|D_2^{*\mu\nu}|c\bar{q}(2^+)\rangle=\zeta^{\mu\nu}\sqrt{m_{D_2^*}},\tag{3.8}$$

respectively. Here, $\epsilon_m^\mu(m=0,\pm1)$ and $\zeta_m^{\mu\nu}(m=0,\pm1,\pm2)$ correspond to the polarization vector and tensor, respectively. In the static limit, they have the form of $\epsilon_0^\mu=(0,0,0,-1)$, $\epsilon_\pm^\mu=(0,\pm1,i,0)/\sqrt{2}$, and $\zeta_m^{\mu\nu}=\sum_{m1,m2}\langle 1,m_1;1,m_2|2,m\rangle\epsilon_{m_1}^\mu\epsilon_{m_2}^\nu$ [82].

In order to obtain the concrete effective potentials, one need to further construct the wave functions for the investigated systems. They include the color part, the flavor part, the spin-orbit part, and the spatial wave functions. For the systems composed by colorless hadrons, the color wave functions are simply **1**. In Table II, we summarize the flavor wave functions $|I,I_3\rangle$ for the S-wave $\mathcal{A}\bar{\mathcal{A}}$ and $\mathcal{A}\bar{\mathcal{B}}$ systems, here, notations $\mathcal{A}$ and $\mathcal{B}$ stand for the different charmed mesons, and J, J_1, and J_2 correspond to the total angular momentum quantum numbers of the discussed charmoniumlike systems $\mathcal{A}\bar{\mathcal{B}}$, the charmed (charmed-strange) mesons $\mathcal{A}$, and the charmed (charmed-strange) mesons $\mathcal{B}$, respectively. In particular, we need to emphasize the C parity for the discussed systems is determined by $C=cx_1x_2(-1)^{J-J_1-J_2}$ with $c=\pm1$, where the charge conjugate transformation conventions satisfy $\mathcal{A}\leftrightarrow x_1\bar{\mathcal{A}}$ and $\mathcal{B}\leftrightarrow x_2\bar{\mathcal{B}}$ [14,16,31,32,67,80,81,83–88].

TABLE II. Flavor wave functions $|I,I_3\rangle$ for these discussed S-wave $\mathcal{A}\bar{\mathcal{A}}$ and $\mathcal{A}\bar{\mathcal{B}}$ systems. Here, the notations $\mathcal{A}$ and $\mathcal{B}$ stand for different charmed mesons, and I and I_3 represent their isospin and the third component of these discussed charmoniumlike systems, respectively.

Systems	$\lvert I,I_3\rangle$	Flavor wave functions
$\mathcal{A}\bar{\mathcal{A}}$	$\lvert 1,1\rangle$	$\mathcal{A}^+\bar{\mathcal{A}}^0$
	$\lvert 1,0\rangle$	$\frac{1}{\sqrt{2}}(\mathcal{A}^0\bar{\mathcal{A}}^0-\mathcal{A}^+\mathcal{A}^-)$
	$\lvert 1,-1\rangle$	$\mathcal{A}^0\mathcal{A}^-$
	$\lvert 0,0\rangle$	$\frac{1}{\sqrt{2}}(\mathcal{A}^0\bar{\mathcal{A}}^0+\mathcal{A}^+\mathcal{A}^-)$
$\mathcal{A}\bar{\mathcal{B}}$	$\lvert 1,1\rangle$	$\frac{1}{\sqrt{2}}(\mathcal{A}^+\bar{\mathcal{B}}^0+c\mathcal{B}^+\bar{\mathcal{A}}^0)$
	$\lvert 1,0\rangle$	$\frac{1}{2}[(\mathcal{A}^0\bar{\mathcal{B}}^0-\mathcal{A}^+\mathcal{B}^-)+c(\mathcal{B}^0\bar{\mathcal{A}}^0-\mathcal{B}^+\mathcal{A}^-)]$
	$\lvert 1,-1\rangle$	$\frac{1}{\sqrt{2}}(\mathcal{A}^0\mathcal{B}^-+c\mathcal{B}^0\mathcal{A}^-)$
	$\lvert 0,0\rangle$	$\frac{1}{2}[(\mathcal{A}^0\bar{\mathcal{B}}^0+\mathcal{A}^+\mathcal{B}^-)+c(\mathcal{B}^0\bar{\mathcal{A}}^0+\mathcal{B}^+\mathcal{A}^-)]$

TABLE III. The relevant quantum numbers J^P and possible channels $|^{2S+1}L_J\rangle$ involved in this work. Here, ... means that the $S-$wave components for the corresponding channels do not exist.

J^P	$\mathcal{D}_0\bar{\mathcal{D}}_0$	$\mathcal{D}_0\bar{\mathcal{D}}_1$	$\mathcal{D}_0\bar{\mathcal{D}}_2$	$\mathcal{D}_1\bar{\mathcal{D}}_1$	$\mathcal{D}_1\bar{\mathcal{D}}_2$
$0^\pm$	$\|^1\mathbb{S}_0\rangle$	...	...	$\|^1\mathbb{S}_0\rangle/\|^5\mathbb{D}_0\rangle$	...
$1^\pm$	...	$\|^3\mathbb{S}_1\rangle/\|^3\mathbb{D}_1\rangle$	...	$\|^3\mathbb{S}_1\rangle/\|^{3,5}\mathbb{D}_1\rangle$	$\|^3\mathbb{S}_1\rangle/\|^{3,5,7}\mathbb{D}_1\rangle$
$2^\pm$	...	...	$\|^5\mathbb{S}_2\rangle/\|^5\mathbb{D}_2\rangle$	$\|^5\mathbb{S}_2\rangle/\|^{1,3,5}\mathbb{D}_2\rangle$	$\|^5\mathbb{S}_2\rangle/\|^{3,5,7}\mathbb{D}_2\rangle$
$3^\pm$	...	...	...	...	$\|^7\mathbb{S}_3\rangle/\|^{3,5,7}\mathbb{D}_3\rangle$

The spin-orbit wave functions $|^{2S+1}L_J\rangle$ for the $|\mathcal{D}_{J_1}\bar{\mathcal{D}}_{J_2}\rangle$ systems can be constructed as

$$|\mathcal{D}_0\bar{\mathcal{D}}_1\rangle = \sum_{m,m_L} C^{J,M}_{1m,Lm_L}\epsilon^{\mu}_{m}|Y_{L,m_L}\rangle, \tag{3.9}$$

$$|\mathcal{D}_0\bar{\mathcal{D}}_2\rangle = \sum_{m,m_L} C^{J,M}_{2m,Lm_L}\zeta^{\mu\nu}_{m}|Y_{L,m_L}\rangle, \tag{3.10}$$

$$|\mathcal{D}_1\bar{\mathcal{D}}_1\rangle = \sum_{m,m',m_S,m_L} C^{S,m_S}_{1m,1m'}C^{J,M}_{Sm_S,Lm_L}\epsilon^{\mu}_{m}\epsilon^{\nu}_{m'}|Y_{L,m_L}\rangle, \tag{3.11}$$

$$|\mathcal{D}_1\bar{\mathcal{D}}_2\rangle = \sum_{m,m',m_S,m_L} C^{S,m_S}_{1m,2m'}C^{J,M}_{Sm_S,Lm_L}\epsilon^{\lambda}_{m}\zeta^{\mu\nu}_{m'}|Y_{L,m_L}\rangle. \tag{3.12}$$

In the above expressions, the notations $\mathcal{D}_0$, $\mathcal{D}_1$, and $\mathcal{D}_2$ denote the charmed (charm-strange) mesons with the total angular momentum quantum numbers $J=0$, 1, and 2, respectively. $C^{e,f}_{ab,cd}$ is the Clebsch-Gordan coefficient, and $|Y_{L,m_L}\rangle$ is the spherical harmonics function. In Table III, we summary the relevant spin-orbit wave functions $|^{2S+1}L_J\rangle$ and the discussed channels under considering the coupled channel effect.

For the $\mathcal{A}\bar{\mathcal{B}}\to\mathcal{A}\bar{\mathcal{B}}$ processes, there exist the direct channel and cross channel Feynman diagrams [31,67], where $\mathcal{A}$ and $\mathcal{B}$ stand for two different charmed (charm-strange) mesons. The total effective potentials can be written as [14,16,67,84]

$$\mathcal{V}_{\rm Total}(\boldsymbol{r}) = \mathcal{V}_D(\boldsymbol{r}) + c\mathcal{V}_C(\boldsymbol{r}). \tag{3.13}$$

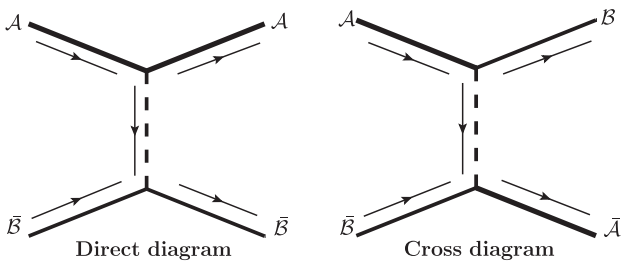

FIG. 6. The direct channel and cross channel Feynman diagrams for the $\mathcal{A}\bar{\mathcal{B}}\to\mathcal{A}\bar{\mathcal{B}}$ processes. Here, the notations $\mathcal{A}$ and $\mathcal{B}$ represent two different charmed (charmed-strange) mesons.

In Fig. 6, we present the direct channel and cross channel Feynman diagrams. For the $\mathcal{A}\bar{\mathcal{A}}$ systems, there exist the direct channel contribution.

With the standard procedures of the OBE model [63,65–69], we can finally obtain the effective potentials in the coordinate space. In the Appendix, we collect the concrete expressions for all the OBE effective potentials. We estimate the coupling constants by fitting the reported experimental data and using several theoretical models [32,65–67,76,80,89–101]. In particular, we fix the phases between these coupling constants by the quark model [94]. In Table IV, we collect their values. In addition, we need to introduce the following parameters of the hadron masses, $m_\sigma=600.00$ MeV, $m_\pi=137.27$ MeV, $m_\eta=547.86$ MeV, $m_\rho=775.49$ MeV, $m_\omega=782.65$ MeV, $m_\phi=1019.46$ MeV, $m_D=1867.24$ MeV, $m_{D^*}=2008.56$ MeV, $m_{D_0^*}=2324.50$ MeV, $m_{D_1'}=2427.00$ MeV, $m_{D_1}=2422.00$ MeV, $m_{D_2^*}=2463.05$ MeV, $m_{D_s}=1968.34$ MeV, $m_{D_s^*}=2112.20$ MeV, $m_{D_{s0}^*}=2317.80$ MeV, $m_{D_{s1}'}=2459.50$ MeV, $m_{D_{s1}}=2535.11$ MeV, and $m_{D_{s2}^*}=2569.10$ MeV [38].

B. Numerical results and discussions

In this section, we attempt to find the loosely bound state solutions for the charmed (charm-strange) meson and anticharmed (anticharm-strange) meson systems by solving the coupled channel Schrödinger equation. As the only one free parameter here, we vary the cutoff parameters in the range of 0.8–3.0 GeV. The loosely bound state with cutoff value around 1.0 GeV can be the prime hadronic molecular candidate, since this value range is widely accepted as a reasonable input parameter based on the experience of studying the deuteron [65,72,73]. As is well known, a reasonable loosely bound hadronic molecule should satisfy its binding energy is around several to several tens MeV, and its typical size should be larger than the size of all the component hadrons [18,102].

Here, we need to emphasis that we mainly focus on the mass spectrum for the hidden-charm molecular tetraquark systems in this work, which is inspired by the abundant experimental data. In addition, we also give rough estimations of the branching ratios of the two-body hidden-charm decay behaviors for the $D^*\bar{D}^*$ molecular tetraquarks within

TABLE IV. A summary of the coupling constants adopted in our calculations. Units of the coupling constants $h' = (h_1 + h_2)/\Lambda_\chi$, λ, λ', λ'', μ, and μ_1 are GeV^{-1}, and the coupling constant f_π is given in unit of GeV.

g_σ	g'_σ	g''_σ	$\lvert h_\sigma\rvert$	$\lvert h'_\sigma\rvert$	g
−0.76	0.76	0.76	0.32	0.35	0.59
$\tilde{k}$	k	$\lvert h\rvert$	$\lvert h'\rvert$	f_π	β
0.59	0.59	0.56	0.55	0.132	−0.90
β'	β''	λ	λ'	λ''	$\lvert\zeta\rvert$
0.90	0.90	−0.56	0.56	0.56	0.727
$\lvert\mu\rvert$	$\lvert\zeta_1\rvert$	μ_1	g_V		
0.364	0.20	0	5.83		

the heavy quark symmetry analysis, which is due to possible peculiar characteristic mass spectrum of the isoscalar $D^*\bar{D}^*$ molecular systems existing in the reported experimental data of the B meson decays (see Fig. 2). For other obtained $\mathcal{D}\bar{\mathcal{D}}$ and $\mathcal{D}_s\bar{\mathcal{D}}_s$ molecules, we only simply list the two-body hidden-charm decay channels. Their decay behaviors will be further discussed in the future work. Our results will be categorized into three corresponding cases:

(1) The isoscalar charmoniumlike molecular systems without hidden-strange quantum number,
(2) The charmoniumlike molecular systems with hidden-strange quantum number,
(3) The isovector hidden-charm molecular tetraquark systems.

1. Isoscalar charmoniumlike molecular systems without hidden-strange quantum number

The isoscalar $D^*\bar{D}^*$ system.—In Table V, we present the corresponding bound state properties for the $S-$wave isoscalar $D^*\bar{D}^*$ system. When cutoff values vary from 0.8 to 3.0 GeV, we can obtain bound state solutions for the $S-$wave isoscalar $D^*\bar{D}^*$ states with $J^{PC} = 0^{++}$, 1^{+-}, and 2^{++}. And we can obtain the relation of $\Lambda[0(0^{++})] < \Lambda[0(1^{+-})] < \Lambda[0(2^{++})]$. Suppose bound states with a smaller cutoff binds deeper when we set the same binding energy. We can find the isoscalar $D^*\bar{D}^*$ interaction with $I(J^{PC}) = 0(0^{++})$ is strongest attractive, followed by the states with $I(J^{PC}) = 0(1^{+-})$ and $0(2^{++})$. Thus, we can conclude these three states are possible isoscalar hidden-charm molecular tetraquark candidates, and their masses satisfy $M[0(0^{++})] < M[0(1^{+-})] < M[0(2^{++})]$. Here, our results are also consistent with the conclusions in Refs. [16,27,72,87,103–113].

After that, we give rough estimations of the branching ratios of the two-body hidden-charm decay behaviors for these possible $S-$wave isoscalar $D^*\bar{D}^*$ molecular candidates by using the heavy quark symmetry. As an approximate symmetry, the heavy quark symmetry is often applied to study the structures of the hadrons which contain the heavy quarks. In order to perform the heavy quark symmetry analysis for the two-body hidden-charm decay behaviors, we should first expand the spin wave functions of the heavy hadrons systems $|\ell_1 s_1 j_1, \ell_2 s_2 j_2, JM\rangle$ in terms of the heavy quark basis $|\ell_1\ell_2 L, s_1 s_2 S, JM\rangle$, i.e.,

$$|\ell_1 s_1 j_1, \ell_2 s_2 j_2, JM\rangle = \sum_{S,L} \hat{S}\hat{L}\hat{j}_1\hat{j}_2 \begin{Bmatrix} \ell_1 & \ell_2 & L \\ s_1 & s_2 & S \\ j_1 & j_2 & J \end{Bmatrix} |\ell_1\ell_2 L, s_1 s_2 S, JM\rangle \tag{3.14}$$

with $\hat{A} = \sqrt{2A+1}$. Here, the $9-j$ symbol is used to relate two bases $|\ell_1 s_1 j_1, \ell_2 s_2 j_2, JM\rangle$ and $|\ell_1\ell_2 L, s_1 s_2 S, JM\rangle$ with the investigated system coupled in a different way [114].

For these possible $S-$wave isoscalar $D^*\bar{D}^*$ molecular candidates, the two-body hidden-charm decay channels include the $\eta_c\eta$, $\eta_c\eta'$, $\eta_c\omega$, $J/\psi\eta$, and $J/\psi\omega$ channels. We can expand their spin wave functions in the heavy quark spin symmetry basis, i.e.,

TABLE V. Bound state properties for the $S-$wave isoscalar $D^*\bar{D}^*$ system. Cutoff Λ, binding energy E, and root-mean-square (rms) radius r_{rms} are in units of GeV, MeV, and fm, respectively. Here, we label the major probability for the corresponding channels in a bold manner.

Effect	Single channel			$S-D$ wave mixing effect			
J^{PC}	Λ	E	r_{rms}	Λ	E	r_{rms}	$P(^1\mathbb{S}_0/^5\mathbb{D}_0)$
0^{++}	0.92	−0.56	3.98	0.91	−0.61	3.89	**99.56**/0.44
	0.99	−11.81	1.09	0.98	−10.80	1.15	**99.42**/0.58
J^{PC}	Λ	E	r_{rms}	Λ	E	r_{rms}	$P(^3\mathbb{S}_1/^3\mathbb{D}_1)$
1^{+-}	1.07	−0.38	4.54	1.05	−0.35	4.67	**99.49**/0.51
	1.16	−12.01	1.09	1.15	−12.35	1.10	**99.13**/0.87
J^{PC}	Λ	E	r_{rms}	Λ	E	r_{rms}	$P(^5\mathbb{S}_2/^1\mathbb{D}_2/^5\mathbb{D}_2)$
2^{++}	2.06	−0.28	5.18	1.82	−0.33	5.05	**99.03**/0.07/0.90
	3.00	−12.35	1.26	2.81	−12.45	1.28	**98.00**/0.15/1.85

$$|0^{++}\rangle = \frac{\sqrt{3}}{2}|0^{-+}_{q\bar{q}}, 0^{-+}_{c\bar{c}}, 0^{++}\rangle - \frac{1}{2}|1^{--}_{q\bar{q}}, 1^{--}_{c\bar{c}}, 0^{++}\rangle, \quad (3.15)$$

$$|1^{+-}\rangle = \frac{1}{\sqrt{2}}|1^{--}_{q\bar{q}}, 0^{-+}_{c\bar{c}}, 1^{+-}\rangle + \frac{1}{\sqrt{2}}|0^{-+}_{q\bar{q}}, 1^{--}_{c\bar{c}}, 1^{+-}\rangle, \quad (3.16)$$

$$|2^{++}\rangle = |1^{--}_{q\bar{q}}, 1^{--}_{c\bar{c}}, 2^{++}\rangle, \quad (3.17)$$

where $L^{P_q,C_q}_{q\bar{q}}$ and $S^{P_Q,C_Q}_{c\bar{c}}$ stand for the spin parities for the light-flavor meson and charmonium state, respectively. In the heavy quark symmetry, we can estimate that

(i) The isoscalar $D^*\bar{D}^*$ molecular state with $J^{PC} = 0^{++}$ can decay into the $\eta_c\eta^{(\prime)}$ and $J/\psi\omega$ channels through the $S-$wave interaction, the relative decay ratio $\mathcal{B}_0 = \Gamma_0[J/\psi\omega]/\Gamma_0[\eta_c\eta^{(\prime)}]$ is roughly 1:3.

(ii) For the isoscalar $D^*\bar{D}^*$ molecular state with $J^{PC} = 1^{+-}$, it can decay into the $J/\psi\eta^{(\prime)}$ and $\eta_c\omega$ via the $S-$wave coupling. The relative decay branching ratio for the $J/\psi\eta^{(\prime)}$ and $\eta_c\omega$ channels is $\mathcal{B}_1 = \Gamma_1[J/\psi\eta]/\Gamma_1[\eta_c\omega] = 1:1$. Since the phase space for the $D^*\bar{D}^* \to J/\psi\eta$ is larger than that in the $\eta_c\omega$ final state around 100 MeV, the partial decay widths for these two hidden-charm decay processes satisfy $\Gamma_1[J/\psi\eta] > \Gamma_1[\eta_c\omega]$, it leads to the $J/\psi\eta$ channel is the prime decay channel to search for the isoscalar $D^*\bar{D}^*$ molecular state with $J^{PC} = 1^{+-}$.

(iii) For the isoscalar $D^*\bar{D}^*$ molecular state with $J^{PC} = 2^{++}$, the $J/\psi\omega$ is the only one two-body hidden-charm decay mode by the $S-$wave interaction.

In addition, the isoscalar $D^*\bar{D}^*$ molecular state with $J^{PC} = 0^{++}$ can strongly couple to the $D\bar{D}$ channel via the $S-$wave coupling, and the $D^*\bar{D}^*[0(2^{++})]$ can decay into the $D\bar{D}^*$ and $D\bar{D}$ channels through the D-wave interactions, which indicate that the two-body open-charm decay widths satisfy $\Gamma_{\rm Open}[0(0^{++})] > \Gamma_{\rm Open}[0(2^{++})]$. Thus, we can estimate that the strong decay width for the $D^*\bar{D}^*$ molecule with $I(J^{PC}) = 0(0^{++})$ is larger than that for the $D^*\bar{D}^*$ molecule with $I(J^{PC}) = 0(2^{++})$.[4] To summarize, if both the $D^*\bar{D}^*$ states with $I(J^{PC}) = 0(0^{++})$ and $0(2^{++})$ are the possible charmoniumlike molecular candidates, their mass and decay width should satisfy $M[0(0^{++})] < M[0(2^{++})]$ and $\Gamma[0(0^{++})] > \Gamma[0(2^{++})]$, respectively. These important characters on their mass spectrum and two-body strong decay behaviors provided here can help us to search and further identify the $D^*\bar{D}^*$ charmoniumlike molecules.

According to the above analysis, the $J/\psi\omega$ final state has the potential to observe the possible $D^*\bar{D}^*$ charmoniumlike molecules with $I(J^{PC}) = 0(0^{++})$ and $0(2^{++})$. Recalling the *BABAR* data presented in Fig. 2, we can find possible evidence of the existence of two enhancement structures below the $D^*\bar{D}^*$ threshold by analyzing the $J/\psi\omega$ invariant mass spectrum of the $B \to J/\psi\omega K$ [41,42]. In Fig. 7(a), we label the possible positions of the $D^*\bar{D}^*$ charmoniumlike molecules with $I(J^{PC}) = 0(0^{++})$ and $0(2^{++})$ in the $J/\psi\omega$ invariant mass spectrum in the $B \to J/\psi\omega K$ [41,42]. We look forward the future experiments with higher precision data can test our theoretical predictions.

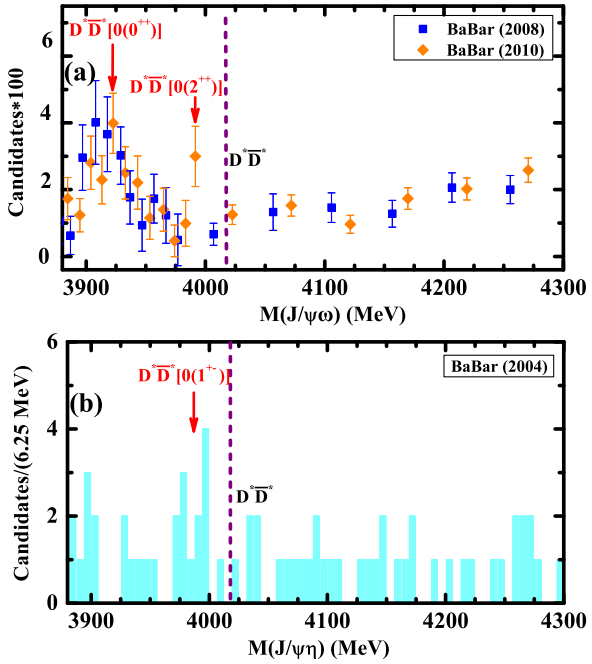

FIG. 7. The $J/\psi\omega$ and $J/\psi\eta$ invariant mass spectrum around the $D^*\bar{D}^*$ threshold in the $B \to J/\psi\omega K$ [41,42] and $B \to J/\psi\eta K$ [43], respectively.

Meanwhile, it is interesting to note that the $S-$wave $D^*\bar{D}^*$ state with $I(J^{PC}) = 0(1^{+-})$ is favored to be the possible charmoniumlike molecular candidate, and the $J/\psi\eta$ channel is the important two-body hidden-charm decay mode. Experimental, we may find an enhancement structure around 3.9 GeV in the $J/\psi\eta$ invariant mass spectrum of the $B \to J/\psi\eta K$ [43], which may correspond to the $S-$wave isoscalar $D^*\bar{D}^*$ molecular state with $J^{PC} = 1^{+-}$ (see Fig. 7(b)). In addition, we notice that the BESIII Collaboration [115] and the Belle Collaboration [116] respectively analyzed the $J/\psi\eta$ invariant mass spectrum in the e^+e^- annihilation process and the $B \to J/\psi\eta K$ process, unfortunately, no significant signal around 3.9 GeV was found. This could be because there are only several dozen events or less in the $J/\psi\eta$ invariant mass spectrum [43,115,116], in comparison with the observations of the $J/\psi\omega$ invariant mass spectrum [25,41,42], we expect more precision experimental data to further check the structure around 3.9 GeV in the $J/\psi\eta$ invariant mass spectrum.

[4]Here, we neglect the other decay modes with very small contribution, like the three-body decay modes, the two-body decay modes via the D-wave interaction.

In short, due to the lack of the sufficiently accurate experimental results, the present data sample from the B meson decays was not large enough to analyze these possible charmoniumlike molecular tetraquark structures in the $J/\psi\omega$ and $J/\psi\eta$ invariant mass spectrum [25,41–43,116], and the study of these possible charmoniumlike molecular tetraquark candidates will become an important research field at the precision frontier in future experiments. Thus, we strongly expect experimental colleagues to focus on the detailed structures around 3.9 GeV in the $J/\psi\omega$ and $J/\psi\eta$ invariant mass spectrum with more precise experimental data, like the LHCb, Belle II, and BESIII, it will provide strong evidence of existing charmoniumlike molecular tetraquark states if these possible enhancement structures can be confirmed in future experiments.

The others isoscalar $\mathcal{D}\bar{\mathcal{D}}$ systems.—In this section, we mainly try to understand very broad structure around 4.3 GeV in the $J/\psi\omega$ invariant mass spectrum of the $B \to J/\psi\omega K$ process [25,41,42]. The mass thresholds of the $D^*\bar{D}_1$, $D^*\bar{D}_2^*$, $D\bar{D}_2^*$, and $D\bar{D}_1$ systems locate around this energy region. In general, the pion exchange interaction usually plays a crucial role in forming the hadronic molecular states [18]. In the following, we discuss these $S-$wave isoscalar charmoniumlike molecular tetraquark systems with three different groups, i.e., the $S-$wave isoscalar charmoniumlike molecular tetraquark systems with the pion exchange contribution occurring in the direct channel effective potentials, the $S-$wave isoscalar charmoniumlike molecular tetraquark systems with the pion exchange contribution occurring in the cross channel effective potentials, and the $S-$wave isoscalar charmoniumlike molecular tetraquark systems without the pion exchange process. For the sake of completeness, we also discuss the mass spectrum and the two-body hidden-charm decay channels for the $S-$wave isoscalar $D\bar{D}$ and $D\bar{D}^*$ systems.

(i) The $S-$wave isoscalar $D^*\bar{D}_1$ and $D^*\bar{D}_2^*$ systems.

By performing numerical calculations, we can obtain the loosely bound state solutions for the $S-$wave isoscalar $D^*\bar{D}_1$ and $D^*\bar{D}_2^*$ systems when the cutoff values are tuned from 0.8 to 3.0 GeV. In Table VI, we present the corresponding bound state solutions. Compared to the high spin states, we find that the low spin states can be easier to bind as charmoniumlike molecular candidates for the $S-$wave isoscalar $D^*\bar{D}_1$ and $D^*\bar{D}_2^*$ systems. Here, we also consider the coupled channel effect, and find the coupled channel effect plays a minor role in the above discussed systems. In fact, there are several papers on the predictions of the possible $S-$wave isoscalar $D^*\bar{D}_1$ and $D^*\bar{D}_2^*$ charmoniumlike molecular tetraquark states [59,85,86,117–119].

In Fig. 8, we present the cutoff parameter Λ dependence of the binding energy E for the S-wave $D^*\bar{D}_1$ state with $I(J^{PC}) = 0(0^{--})$, and there exist the loosely bound state solutions when the cutoff parameter is larger than 0.96 GeV, where the binding energy increases with the cutoff value monotonically. For simplicity, we only take $\Lambda = 0.96$ and 1.03 GeV to present the loosely bound state solutions for the S-wave $D^*\bar{D}_1$ state with $I(J^{PC}) = 0(0^{--})$ in Table VI.

(ii) The $S-$wave isoscalar $D\bar{D}_2^*$ and $D\bar{D}^*$ systems.

For the $D\bar{D}_2^*$ and $D\bar{D}^*$ systems, the π exchange occurs in the $D\bar{D}_2^* \to D_2^*\bar{D}$ and $D\bar{D}^* \to D^*\bar{D}$ processes, and the interaction Feynman diagram corresponds to the Cross diagram in Fig. 6. In Table VII, we collect the bound state solutions for the $S-$wave isoscalar $D\bar{D}_2^*$ and $D\bar{D}^*$ systems. It is obvious that these $S-$wave isoscalar $D\bar{D}_2^*$ and $D\bar{D}^*$ states can be possible charmoniumlike molecular candidates as their bound state solutions satisfy the typical characters for a loosely bound hadronic molecule.[5] In fact, the $S-$wave isoscalar $D\bar{D}^*$ molecular states have been extensively studied in Refs. [11–17,72,107–113,120–128]. However, our knowledge of the S-wave isoscalar $D\bar{D}_2^*$ molecular states is still not enough up to now [85,86].

(iii) The $S-$wave isoscalar $D\bar{D}_1$ and $D\bar{D}$ systems.

Despite the π exchange does not contribute to the effective potentials for the $S-$wave $D\bar{D}_1$ system as the parity forbidden, the scalar and vector mesons exchange interactions may be strong enough to generate an bound state [65,129]. As shown in Table VIII, our numerical results suggest the isoscalar $D\bar{D}_1$ states with $I(J^{PC}) = 0[(1^{--}), (1^{-+})]$ and the $S-$wave $D\bar{D}$ state with $I(J^{PC}) = 0(0^{++})$ can be possible charmoniumlike molecular candidates. In fact, the $S-$wave isoscalar $D\bar{D}_1$ molecular states were intensively discussed in Refs. [59,74,85,86,93,101,117], which may be related to the $Y(4260)$[6] [131]. In Refs. [16,104,108,110–113], the $S-$wave $D\bar{D}$ bound state with $I(J^{PC}) = 0(0^{++})$ was estimated.

Let's give a short summary, we can predict a serial of possible charmoniumlike molecules composed by the $S-$wave isoscalar $D^*\bar{D}_1$, $D^*\bar{D}_2^*$, $D\bar{D}_2^*$, $D\bar{D}^*$, $D\bar{D}_1$, and $D\bar{D}$ systems. In Table IX, we summary their two-body hidden-charm decay information for all the possible $S-$wave isoscalar $D^*\bar{D}_1$, $D^*\bar{D}_2^*$, $D\bar{D}_2^*$, $D\bar{D}^*$, $D\bar{D}_1$, and $D\bar{D}$ charmoniumlike molecules. For example, the $J/\psi\omega$ channel is the two-body hidden-charm decay mode for the isoscalar $D^*\bar{D}_1[(0,1,2)^{-+}]$, $D^*\bar{D}_2^*[3^{-+}]$, and $D\bar{D}_1[1^{-+}]$ bound states, perhaps, it is possible to observe the experimental signal of these possible charmoniumlike molecules in the $J/\psi\omega$ final state. When we recall the experimental data of the $B \to J/\psi\omega K$ [25,41,42], our predictions of these

[5]When the cutoff Λ is taken around 1 GeV, the binding energy is around several to several tens MeV, and the size of bound state is larger than the size of its component.

[6]In 2017, the BESIII gave more precise data of the $e^+e^- \to J/\psi\pi^+\pi^-$ [130], which shows that the $Y(4260)$ [131] is split into two resonances $Y(4220)$ and $Y(4320)$.

TABLE VI. Bound state solutions for the $S-$wave isoscalar $D^*\bar{D}_1$ and $D^*\bar{D}_2^*$ systems. Conventions are the same as Table V.

Effect	Single channel			$S-D$ wave mixing effect			
				$D^*\bar{D}_1$			
J^{PC}	Λ	E	$r_{\rm rms}$	Λ	E	$r_{\rm rms}$	$P(^1\mathbb{S}_0/^5\mathbb{D}_0)$
0^{--}	0.96	−0.59	3.73	0.95	−0.52	3.92	**99.70**/0.30
	1.03	−11.12	1.07	1.03	−12.40	1.03	**99.59**/0.41
0^{-+}	0.92	−0.56	3.91	0.91	−0.55	3.96	**99.53**/0.47
	0.99	−11.42	1.08	0.99	−12.82	1.05	**99.41**/0.59
J^{PC}	Λ	E	$r_{\rm rms}$	Λ	E	$r_{\rm rms}$	$P(^3\mathbb{S}_1/^3\mathbb{D}_1/^5\mathbb{D}_1)$
1^{--}	1.10	−0.48	4.11	1.08	−0.33	4.61	**99.64**/0.35/0.01
	1.20	−12.57	1.03	1.19	−12.74	1.03	**99.38**/0.61/0.01
1^{-+}	1.06	−0.45	4.25	1.04	−0.34	4.68	**99.47**/0.52/0.01
	1.15	−11.80	1.07	1.14	−11.75	1.09	**99.13**/0.86/0.01
J^{PC}	Λ	E	$r_{\rm rms}$	Λ	E	$r_{\rm rms}$	$P(^5\mathbb{S}_2/^1\mathbb{D}_2/^3\mathbb{D}_2/^5\mathbb{D}_2)$
2^{--}	2.56	−0.32	4.89	2.60	−0.33	4.90	**98.90**/0.05/$o(0)$/1.05
	2.58	−9.86	1.16	2.74	−8.65	1.33	**93.06**/4.18/$o(0)$/2.75
2^{-+}	1.73	−0.81	3.68	1.59	−0.34	4.90	**99.30**/0.08/$o(0)$/0.62
	2.14	−12.16	1.24	2.07	−12.74	1.24	**98.77**/0.27/$o(0)$/0.93
				$D^*\bar{D}_2^*$			
J^{PC}	Λ	E	$r_{\rm rms}$	Λ	E	$r_{\rm rms}$	$P(^3\mathbb{S}_1/^3\mathbb{D}_1/^5\mathbb{D}_1/^7\mathbb{D}_1)$
1^{--}	0.94	−0.28	4.78	0.94	−0.56	3.90	**99.77**/0.07/$o(0)$/0.16
	1.02	−12.82	1.01	1.02	−13.86	0.99	**99.69**/0.05/$o(0)$/0.26
1^{-+}	0.97	−0.27	4.80	0.97	−0.51	4.00	**99.81**/0.09/$o(0)$/0.10
	1.05	−10.92	1.09	1.05	−11.81	1.06	**99.71**/0.19/$o(0)$/0.09
J^{PC}	Λ	E	$r_{\rm rms}$	Λ	E	$r_{\rm rms}$	$P(^5\mathbb{S}_2/^3\mathbb{D}_2/^5\mathbb{D}_2/^7\mathbb{D}_2)$
2^{--}	1.21	−0.67	3.68	1.19	−0.28	4.84	**99.67**/$o(0)$/0.33/$o(0)$
	1.36	−12.76	1.04	1.35	−12.82	1.05	**99.38**/0.01/0.60/0.01
2^{-+}	1.11	−0.31	4.77	1.10	−0.28	4.84	**99.78**/$o(0)$/0.22/$o(0)$
	1.21	−11.55	1.08	1.21	−12.66	1.04	**99.59**/0.01/0.40/$o(0)$
J^{PC}	Λ	E	$r_{\rm rms}$	Λ	E	$r_{\rm rms}$	$P(^7\mathbb{S}_3/^3\mathbb{D}_3/^5\mathbb{D}_3/^7\mathbb{D}_3)$
3^{--}	1.90	−0.32	4.94	1.73	−0.31	4.98	**99.21**/0.07/$o(0)$/0.72
	2.87	−12.26	1.23	2.64	−12.24	1.25	**98.36**/0.39/0.03/1.22
3^{-+}	1.97	−0.32	4.94	1.77	−0.33	4.91	**99.03**/0.04/$o(0)$/0.93
	2.74	−12.49	1.21	2.51	−12.41	1.24	**97.70**/0.19/0.03/2.07

possible charmoniumlike molecules also reflect the complexity of the structures in the $J/\psi\omega$ invariant mass spectrum around 4.3 GeV. At present, it is a little difficult to definitely identify these possible charmoniumlike molecules, we hope further experiments can provide more precise measurement of the B meson decay into a charmonium state plus a light-flavor meson. In addition, the $\chi_{cJ}(1P)\omega$ with $J=0,1,2$ are the two-body hidden-charm decay channels for the possible $S-$wave isoscalar $D^*\bar{D}_1$, $D^*\bar{D}_2^*$, $D\bar{D}_2^*$, and $D\bar{D}_1$ systems of negative C-parity in our calculations.

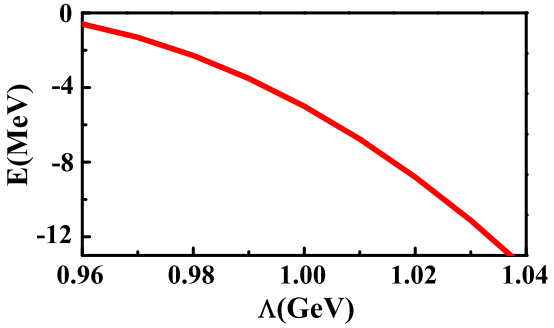

FIG. 8. The cutoff parameter Λ dependence of the binding energy E for the S-wave $D^*\bar{D}_1$ state with $I(J^{PC})=0(0^{--})$.

2. Charmoniumlike molecular tetraquark systems with hidden-strange quantum number

With the help of the SU(3) flavor symmetry, we can further study the interactions between the charm-strange meson and anticharm-strange meson, in this section, we analyze the existence probability of the charmoniumlike molecules with hidden-strange quantum number and give their two-body hidden-charm decay channels.

The $D_s^*\bar{D}_s^*$ system.—For the $D_s^*\bar{D}_s^*$ system, the η and ϕ exchanges contribute to the effective potentials in the OBE

TABLE VII. Bound state solutions for the $S-$ wave isoscalar $D\bar{D}_2^*$ and $D\bar{D}^*$ systems. Conventions are the same as Table V.

Effect	Single channel			$S-D$ wave mixing effect			
$D\bar{D}_2^*[J^{PC}]$	Λ	E	$r_{\rm rms}$	Λ	E	$r_{\rm rms}$	$P(^5\mathbb{S}_2/^5\mathbb{D}_2)$
2^{--}	1.46	−0.25	5.08	1.46	−0.34	4.74	**99.99**/0.01
	1.85	−12.22	1.11	1.82	−12.40	1.11	**99.91**/0.09
2^{-+}	1.30	−0.36	4.69	1.29	−0.24	5.17	**99.99**/0.01
	1.47	−12.03	1.11	1.47	−12.89	1.08	**99.93**/0.07
$D\bar{D}^*[J^{PC}]$	Λ	E	$r_{\rm rms}$	Λ	E	$r_{\rm rms}$	$P(^3\mathbb{S}_1/^3\mathbb{D}_1)$
1^{+-}	1.62	−0.36	4.70	1.36	−0.39	4.71	**97.38**/2.62
	1.77	−12.51	1.07	1.49	−12.32	1.19	**92.15**/7.85
1^{++}	1.18	−0.27	5.15	1.08	−0.27	5.22	**99.05**/0.95
	1.53	−12.39	1.19	1.30	−12.09	1.23	**96.99**/3.01

TABLE VIII. Bound state solutions for the $S-$ wave isoscalar $D\bar{D}_1$ system. Conventions are the same as Table V.

Effect	Single channel			$S-D$ wave mixing effect			
$D\bar{D}[J^{PC}]$	Λ	E	$r_{\rm rms}$				
0^{++}	1.46	−0.29	5.08				
	1.76	−12.55	1.15				
$D\bar{D}_1[J^{PC}]$	Λ	E	$r_{\rm rms}$	Λ	E	$r_{\rm rms}$	$P(^3\mathbb{S}_1/^3\mathbb{D}_1)$
1^{--}	1.39	−0.36	4.72	1.39	−0.39	4.60	**99.98**/0.02
	1.67	−12.13	1.14	1.67	−12.42	1.13	**99.92**/0.08
1^{-+}	1.38	−0.29	4.92	1.38	−0.32	4.80	**99.98**/0.02
	1.63	−12.63	1.09	1.63	−12.89	1.08	**99.93**/0.07

TABLE IX. A summary of the two-body hidden-charm decay channels for all the possible $S-$ wave isoscalar $D^*\bar{D}_1$, $D^*\bar{D}_2^*$, $D\bar{D}_2^*$, $D\bar{D}^*$, $D\bar{D}_1$, and $D\bar{D}$ charmoniumlike molecules.

States	Two-body hidden-charm decay channels
$D^*\bar{D}_1[0^{-+}]$	$J/\psi\omega$, $\chi_{c0}(1P)\eta$, $\chi_{c0}(1P)\eta'$
$D^*\bar{D}_1[0^{--}]$	$\chi_{c1}(1P)\omega$, $\eta_c\omega$, $J/\psi\eta$, $J/\psi\eta'$
$D^*\bar{D}_1[1^{-+}]$	$J/\psi\omega$, $\chi_{c1}(1P)\eta$, $\eta_c\eta$, $\eta_c\eta'$,
$D^*\bar{D}_1[1^{--}]$	$\chi_{c2}(1P)\omega$, $\chi_{c1}(1P)\omega$, $\chi_{c0}(1P)\omega$, $\eta_c\omega$, $J/\psi\eta$, $J/\psi\eta'$
$D^*\bar{D}_1[2^{-+}]$	$J/\psi\omega$, $\chi_{c2}(1P)\eta$
$D^*\bar{D}_1[2^{--}]$	$\chi_{c2}(1P)\omega$, $\chi_{c1}(1P)\omega$, $\eta_c\omega$, $J/\psi\eta$, $J/\psi\eta'$
$D^*\bar{D}_2^*[1^{-+}]$	$\chi_{c1}(1P)\eta$, $\eta_c\eta$, $\eta_c\eta'$, $J/\psi\omega$, $\chi_{c1}(1P)\eta'$
$D^*\bar{D}_2^*[1^{--}]$	$\chi_{c2}(1P)\omega$, $\eta_c\omega$, $J/\psi\eta$, $J/\psi\eta'$, $\chi_{c0}(1P)\omega$, $\chi_{c1}(1P)\omega$
$D^*\bar{D}_2^*[2^{-+}]$	$\chi_{c2}(1P)\eta$, $J/\psi\omega$
$D^*\bar{D}_2^*[2^{--}]$	$\chi_{c2}(1P)\omega$, $\eta_c\omega$, $J/\psi\eta$, $J/\psi\eta'$, $\chi_{c1}(1P)\omega$
$D^*\bar{D}_2^*[3^{-+}]$	$J/\psi\omega$
$D^*\bar{D}_2^*[3^{--}]$	$\chi_{c2}(1P)\omega$
$D\bar{D}_2^*[2^{-+}]$	$\chi_{c2}(1P)\eta$, $J/\psi\omega$
$D\bar{D}_2^*[2^{--}]$	$\chi_{c1}(1P)\omega$, $\eta_c\omega$, $J/\psi\eta$, $J/\psi\eta'$
$D\bar{D}^*[1^{++}]$	$J/\psi\omega$
$D\bar{D}^*[1^{+-}]$	$\eta_c\omega$, $J/\psi\eta$
$D\bar{D}_1[1^{-+}]$	$J/\psi\omega$, $\eta_c\eta'$, $\eta_c\eta$, $\chi_{c1}(1P)\eta$
$D\bar{D}_1[1^{--}]$	$\chi_{c0}(1P)\omega$, $\eta_c\omega$, $J/\psi\eta$, $J/\psi\eta'$
$D\bar{D}[0^{++}]$	$\eta_c\eta$

model. The relevant numerical results for the $S-$ wave $D_s^*\bar{D}_s^*$ system are given in Table X, and the cutoff parameters are taken in the range from 1.0 to 3.0 GeV.

For the $S-$ wave $D_s^*\bar{D}_s^*$ states with $J^{PC}=0^{++}$ and 1^{+-}, we can obtain the loosely bound state solutions for these states when the cutoff values are taken to be around 1.6 and 1.9 GeV, respectively. Thus, the $S-$ wave $D_s^*\bar{D}_s^*$ states with $J^{PC}=0^{++}$ and 1^{+-} can be the possible hidden-charm and hidden-strange molecular tetraquark candidates, especially the $D_s^*\bar{D}_s^*$ molecular state with $J^{PC}=0^{++}$ [132,133]. If taking a large cutoff $\Lambda>3.0$ GeV, there exist the loosely bound state solutions for the $D_s^*\bar{D}_s^*$ state with $J^{PC}=2^{++}$ in Ref. [27]. However, such cutoff parameter is far from the usual value around 1.0 GeV [65,72,73], which is consistent with our numerical results.

The $D_s\bar{D}_s$, $D_s\bar{D}_s^*$, $D_s\bar{D}_{s0}^*$, $D_s\bar{D}_{s1}'$, $D_s^*\bar{D}_{s0}^*$, $D_s^*\bar{D}_{s1}'$, $D_s^{(*)}\bar{D}_{s1}$, and $D_s^{(*)}\bar{D}_{s2}^*$ systems.—Besides the $S-$ wave $D_s^*\bar{D}_s^*$ system, we also investigate the bound state properties of the $S-$ wave $D_s\bar{D}_s$, $D_s\bar{D}_s^*$, $D_s\bar{D}_{s0}^*$, $D_s\bar{D}_{s1}'$, $D_s^*\bar{D}_{s0}^*$, and $D_s^*\bar{D}_{s1}'$ systems by tuning the cutoff values Λ from 1.0 to 3.0 GeV, and the corresponding numerical results are listed in Table XI. If we still adopt the general criterion of the loosely hadron-hadron molecule [65,67,72,73], we can find

(i) There may exist several possible charmoniumlike molecular tetraquark candidates with hidden-strange

TABLE X. Bound state solutions for the $S-$wave $D_s^*\bar{D}_s^*$ system. Conventions are the same as Table V.

Effect	Single channel			$S-D$ wave mixing effect			
J^{PC}	Λ	E	$r_{\rm rms}$	Λ	E	$r_{\rm rms}$	$P(^1\mathbb{S}_0/^5\mathbb{D}_0)$
0^{++}	1.59	−0.72	3.49	1.58	−0.23	4.98	**99.98**/0.02
	1.65	−11.09	0.98	1.65	−11.34	0.97	**99.95**/0.05
J^{PC}	Λ	E	$r_{\rm rms}$	Λ	E	$r_{\rm rms}$	$P(^3\mathbb{S}_1/^3\mathbb{D}_1)$
1^{+-}	1.89	−0.52	4.00	1.88	−0.26	4.89	**99.98**/0.02
	2.00	−12.37	0.95	2.00	−12.52	0.94	**99.96**/0.04

quantum number, such as the $D_s\bar{D}_s^*$ state with $J^{PC}=1^{+-}$ [108,133], the $D_s\bar{D}_{s0}^*$ state with $J^{PC}=0^{-\mp}$ [81,97–99], the $D_s\bar{D}_{s1}'$ state with $J^{PC}=1^{--}$, the $D_s^*\bar{D}_{s1}'$ states with $J^{PC}=0^{-\mp}$ and 1^{-+}. In particular, the coupled channel effect plays an important role in generating these loosely bound states, i.e., the $D_s\bar{D}_s^*$ state with $J^{PC}=1^{+-}$, the $D_s\bar{D}_{s0}^*$ state with $J^{PC}=0^{-\mp}$, and the $D_s\bar{D}_{s1}'$ state with $J^{PC}=1^{--}$.

(ii) If we increase the cutoff value around 2.0 GeV, we can obtain loosely bound state solutions for the $D_s\bar{D}_s^*$ state with $J^{PC}=1^{++}$, the $D_s^*\bar{D}_{s0}^*$ state with $J^{PC}=1^{--}$, and the $D_s^*\bar{D}_{s1}'$ state with $J^{PC}=1^{--}$. They may be the possible charmoniumlike molecular candidates with hidden-strange quantum number.

(iii) In addition, we do not obtain bound state solutions for the $D_s\bar{D}_s$ state with $J^{PC}=0^{++}$, the $D_s\bar{D}_{s1}'$ state with $J^{PC}=1^{-+}$, and the $D_s^*\bar{D}_{s1}'$ state with $J^{PC}=2^{-\mp}$ by tuning cutoff values from 1.0 to 3.0 GeV.

In our previous work [67], we systematic study the interactions between a pair of charm-strange meson and anticharm-strange meson in the H-doublet or T-doublet by using the OBE model and considering the $S-D$ wave mixing and the coupled channel effect, and we can predict

TABLE XI. Bound state solutions for the $S-$wave $D_s\bar{D}_s^*$, $D_s\bar{D}_{s0}^*$, $D_s\bar{D}_{s1}'$, $D_s^*\bar{D}_{s0}^*$, and $D_s^*\bar{D}_{s1}'$ systems. Conventions are the same as Table V.

Effect	Single channel			$S-D$ wave mixing effect				Coupled channel effect			
States$[J^{PC}]$	Λ	E	$r_{\rm rms}$	Λ	E	$r_{\rm rms}$	$P(^3\mathbb{S}_1/^3\mathbb{D}_1)$	Λ	E	$r_{\rm rms}$	$P(D_s\bar{D}_s^*/D_s^*\bar{D}_s^*)$
$D_s\bar{D}_s^*[1^{+-}]$	2.65	−0.26	4.96	2.27	−0.43	4.39	**99.25**/0.75	1.63	−0.13	5.41	**96.64**/3.36
	2.85	−11.95	0.98	2.43	−11.85	1.03	**96.56**/3.44	1.66	−8.92	0.99	**78.85**/21.15
$D_s\bar{D}_s^*[1^{++}]$	×	×	×	2.71	−0.27	4.99	**99.46**/0.54				
	×	×	×	3.00	−5.69	1.49	**97.69**/2.31				
States$[J^{PC}]$	Λ	E	$r_{\rm rms}$					Λ	E	$r_{\rm rms}$	$P(D_s\bar{D}_{s0}^*/D_s^*\bar{D}_{s1}')$
$D_s\bar{D}_{s0}^*[0^{--}]$	×	×	×					1.87	−2.52	1.77	**85.11**/14.89
	×	×	×					1.88	−8.21	0.94	**75.72**/24.48
$D_s\bar{D}_{s0}^*[0^{-+}]$	2.83	−0.28	4.93					1.49	−0.43	4.27	**96.97**/3.03
	3.00	−0.92	3.32					1.52	−10.05	1.00	**81.81**/18.19
State$[J^{PC}]$	Λ	E	$r_{\rm rms}$	Λ	E	$r_{\rm rms}$	$P(^3\mathbb{S}_1/^3\mathbb{D}_1)$	Λ	E	$r_{\rm rms}$	$P(D_s\bar{D}_{s1}'/D_s^*\bar{D}_{s0}^*/D_s^*\bar{D}_{s1}')$
$D_s\bar{D}_{s1}'[1^{--}]$	2.17	−0.33	4.65	2.15	−0.29	4.79	**99.98**/0.02	1.87	−0.31	4.69	**98.76**/1.24/$o(0)$
	2.55	−12.60	1.00	2.51	−12.35	1.00	**99.82**/0.18	1.99	−12.64	0.92	**87.08**/12.92/$o(0)$
State$[J^{PC}]$	Λ	E	$r_{\rm rms}$	Λ	E	$r_{\rm rms}$	$P(^3\mathbb{S}_1/^3\mathbb{D}_1)$	Λ	E	$r_{\rm rms}$	$P(D_s^*\bar{D}_{s0}^*/D_s^*\bar{D}_{s1}')$
$D_s^*\bar{D}_{s0}^*[1^{--}]$	2.17	−0.31	4.73	2.17	−0.31	4.72	**100.00**/$o(0)$	2.17	−0.31	4.72	**100.00**/$o(0)$
	2.53	−12.42	1.00	2.53	−12.42	1.00	**100.00**/$o(0)$	2.53	−12.42	1.00	**100.00**/$o(0)$
States$[J^{PC}]$	Λ	E	$r_{\rm rms}$	Λ	E	$r_{\rm rms}$	$P(^1\mathbb{S}_0/^5\mathbb{D}_0)$				
$D_s^*\bar{D}_{s1}'[0^{--}]$	1.37	−0.41	4.33	1.37	−0.52	3.99	**99.96**/0.04				
	1.45	−12.34	0.98	1.45	−12.82	0.97	**99.90**/0.10				
$D_s^*\bar{D}_{s1}'[0^{-+}]$	1.87	−0.33	4.24	1.87	−0.36	4.13	**99.99**/0.01				
	1.91	−10.27	0.85	1.91	−10.40	0.85	**99.99**/0.01				
States$[J^{PC}]$	Λ	E	$r_{\rm rms}$	Λ	E	$r_{\rm rms}$	$P(^3\mathbb{S}_1/^3\mathbb{D}_1/^5\mathbb{D}_1)$				
$D_s^*\bar{D}_{s1}'[1^{--}]$	2.29	−0.59	3.53	2.28	−0.47	3.87	**99.97**/0.03/$o(0)$				
	2.37	−13.38	0.78	2.36	−13.47	0.79	**99.88**/0.12/$o(0)$				
$D_s^*\bar{D}_{s1}'[1^{-+}]$	1.55	−0.22	5.10	1.55	−0.36	4.52	**99.95**/0.05/$o(0)$				
	1.68	−11.38	1.02	1.68	−12.17	1.00	**99.84**/0.16/$o(0)$				

TABLE XII. A summary of the bound state properties and two-body hidden-charm decay channels for all the investigated possible $S-$ wave charmoniumlike molecules with hidden-strange quantum number. Here, notations $\surd$ and ✗ are marked the charmoniumlike molecular candidates with their bound state solutions with the cutoff Λ around 1 to 2 GeV and around 2 to 3 GeV, respectively.

States	Bound state properties	Two-body hidden-charm decay channels
$D_s^*\bar{D}_s^*[0^{++}]$	$\surd$	$\eta_c\eta'$, $J/\psi\phi$, $\eta_c\eta$, $\chi_{c1}(1P)\eta$
$D_s^*\bar{D}_s^*[1^{+-}]$	$\surd$	$J/\psi\eta'$, $\eta_c\phi$, $J/\psi\eta$
$D_s\bar{D}_s^*[1^{++}]$	✗	$\chi_{c0}(1P)\eta$, $\chi_{c1}(1P)\eta$
$D_s\bar{D}_s^*[1^{+-}]$	$\surd$	$\eta_c\phi$, $J/\psi\eta$, $J/\psi\eta'$
$D_s\bar{D}_{s0}^*[0^{-+}]$	$\surd$	$J/\psi\phi$, $\chi_{c0}(1P)\eta$
$D_s\bar{D}_{s0}^*[0^{--}]$	$\surd$	$\eta_c\phi$, $J/\psi\eta'$, $J/\psi\eta$
$D_s\bar{D}_{s1}'[1^{--}]$	$\surd$	$J/\psi\eta'$, $J/\psi\eta$, $\eta_c\phi$
$D_s^*\bar{D}_{s0}^*[1^{--}]$	✗	$\eta_c\phi$, $J/\psi\eta'$, $J/\psi\eta$
$D_s^*\bar{D}_{s1}'[0^{-+}]$	$\surd$	$J/\psi\phi$, $\chi_{c0}(1P)\eta'$, $\chi_{c0}(1P)\eta$
$D_s^*\bar{D}_{s1}'[0^{--}]$	$\surd$	$\chi_{c1}(1P)\phi$, $J/\psi\eta'$, $J/\psi\eta$, $\eta_c\phi$
$D_s^*\bar{D}_{s1}'[1^{-+}]$	$\surd$	$\chi_{c1}(1P)\eta'$, $J/\psi\phi$, $\chi_{c1}(1P)\eta$, $\eta_c\eta$, $\eta_c\eta'$
$D_s^*\bar{D}_{s1}'[1^{--}]$	✗	$\chi_{c0}(1P)\phi$, $\chi_{c1}(1P)\phi$, $J/\psi\eta'$, $J/\psi\eta$, $\eta_c\phi$
$D_s^*\bar{D}_{s1}[0^{-+}]$	$\surd$	$\chi_{c0}(1P)\eta'$, $\chi_{c0}(1P)\eta$, $J/\psi\phi$
$D_s^*\bar{D}_{s1}[0^{--}]$	$\surd$	$\chi_{c1}(1P)\phi$, $J/\psi\eta'$, $J/\psi\eta$, $\eta_c\phi$
$D_s^*\bar{D}_{s1}[1^{-+}]$	$\surd$	$J/\psi\phi$, $\chi_{c1}(1P)\eta'$, $\chi_{c1}(1P)\eta$, $\eta_c\eta$, $\eta_c\eta'$
$D_s^*\bar{D}_{s1}[1^{--}]$	$\surd$	$\chi_{c0}(1P)\phi$, $\chi_{c2}(1P)\phi$, $\chi_{c1}(1P)\phi$, $J/\psi\eta'$, $J/\psi\eta$, $\eta_c\phi$
$D_s^*\bar{D}_{s2}^*[1^{-+}]$	$\surd$	$\chi_{c1}(1P)\eta'$, $J/\psi\phi$, $\chi_{c1}(1P)\eta$, $\eta_c\eta$, $\eta_c\eta'$
$D_s^*\bar{D}_{s2}^*[1^{--}]$	$\surd$	$\chi_{c2}(1P)\phi$, $\chi_{c1}(1P)\phi$, $\chi_{c0}(1P)\phi$, $J/\psi\eta'$, $J/\psi\eta$, $\eta_c\phi$
$D_s^*\bar{D}_{s2}^*[2^{-+}]$	$\surd$	$\chi_{c2}(1P)\eta'$, $\chi_{c2}(1P)\eta$, $J/\psi\phi$
$D_s^*\bar{D}_{s2}^*[2^{--}]$	✗	$\chi_{c2}(1P)\phi$, $\chi_{c1}(1P)\phi$, $J/\psi\eta'$, $J/\psi\eta$, $\eta_c\phi$

several possible $H\bar{T}$-type charmoniumlike molecular states, i.e., the $D_s^*\bar{D}_{s1}$ molecular states with $J^{PC}=0^{-\pm}/1^{-\pm}$ and the $D_s^*\bar{D}_{s2}^*$ molecular states with $J^{PC}=1^{-\pm}/2^{-\pm}$.

In Table XII, we summary their bound properties and two-body hidden-charm decay channels for all the investigated possible $S-$ wave charmoniumlike molecules with hidden-strange quantum number.

The obtained results are theoretic reference to search for possible charmoniumlike molecular tetraquark with hidden-strange quantum number. So far, many charmoniumlike structures have been observed in the $J/\psi\phi$ invariant mass spectrum. In particular, the recent LHCb Collaboration updated the amplitude analysis of the $B^+\to J/\psi\phi K^+$ decay with the combined dataset collected in Run I plus Run II [49], and they reported several enhancement structures, some of them locate close to the mass thresholds of our investigated charmoniumlike molecular tetraquark systems with hidden-strange quantum number, our study for these charmoniumlike molecules with hidden-strange quantum number may provide hints to understand the nature of the reported charmoniumlike states, i.e.,

(1) The masses of the $X(4140)$ with $J^{PC}=1^{++}$ and the $X(4150)$ with $J^{PC}=2^{-+}$ [49] are close to the $D_s^*\bar{D}_s^*$ threshold. It is obvious that their quantum configurations do not fit into the $S-$ wave $D_s^*\bar{D}_s^*$ molecules. If their resonance parameters and quantum numbers can be further confirmed in the future, the assignment of these complicated structures as the $S-$ wave $D_s^*\bar{D}_s^*$ molecular states will be facing great challenge.

(2) When we recall the other charmoniumlike structure $Y(4274)$ [26,28,44] (see Fig. 3 for more details), its mass are close to the $D_s\bar{D}_{s0}^*$ threshold, its spin-parity is favored as $J^{PC}=1^{++}$ by the LHCb Collaboration [28,49], the similar situation happens, our results do not support the $Y(4274)$ with $J^{PC}=1^{++}$ as the $S-$ wave $D_s\bar{D}_{s0}^*$ molecular state.

(3) In the mass region from 4.5 to 4.7 GeV, the recent LHCb Collaboration reported the four enhancement structures $X(4500)$, $X(4630)$, $X(4685)$, and $X(4700)$ in the $J/\psi\phi$ mass spectrum from the $B\to J/\psi\phi K$ decay [49]. Our results indicate there can exist six possible charmoniumlike molecular tetraquark candidates with hidden-strange quantum number with positive C-parity. Some of them can decay to the $J/\psi\phi$ final state. In our former work [64], the $X(4630)$ can be assigned as the $D_s^*\bar{D}_{s1}$ charmoniumlike molecule with $J^{PC}=1^{-+}$. If these six predicted charomoniumlike molecules really exist, it is a big challenge to search and further identify separately by using the data from the $B\to J/\psi\phi K$ process.

(4) In addition, our calculations can predict several possible charmoniumlike molecular candidates

with negative C-parity, which deserve to attract the experiment's attentions. Because their two-body hidden-charm decay channels include the $\chi_{c0,1,2}(1P)\phi$, the $B \to \chi_{c0,1,2}(1P)\phi + K \to J/\psi\gamma\phi + K$ may be the prime decay process to search for these possible charmoniumlike molecules.

In fact, the phenomena in high mass region are very complicated, beside these possible charmoniumlike molecular structures, there can exist several traditional charmonium states with their masses around these discussed thresholds. For example, the Lanzhou group indicated that the masses for the $\chi_{c0}(3^3P_0)$, $\chi_{c1}(3^3P_1)$, and $\chi_{c2}(3^3P_2)$ states are around 4177, 4197, and 4213 MeV [134,135], which is close to the $D_s^*\bar{D}_s^*$ thresholds. Both the theoretical side and the experimental side will make many efforts to clarify this puzzling phenomenon in the future.

By this study, we find a series of possible isoscalar $\mathcal{D}\bar{\mathcal{D}}$-type hidden-charm molecular tetraquarks. Some of the isoscalar charmoniumlike XYZ states can be explained as the isoscalar hidden-charm molecules as their masses and quantum number configurations match the calculations of the isoscalar $\mathcal{D}\bar{\mathcal{D}}$-type loosely bound states. Even so, it is difficult to make a definitely decision if they are pure hidden-charm molecular tetraquarks or not. They are possible to be mixtures of the conventional charmonium states and the isoscalar hidden-charm molecular tetraquarks. However, the charged charmoniumlike states are genuine tetraquark states, if they are the real particles. In the following, we will search for possible isovector hidden-charm molecular tetraquarks, and check if the charged Z isovector states have a close relation to these isovector hidden-charm molecular tetraquarks.

3. Isovector charmoniumlike molecular tetraquark systems

In this section, let us discuss the final proposal whether there exist isovector charmoniumlike molecules from a charmed meson and an anticharmed meson interactions, where the charmed (anticharmed) mesons are in the H/T doublets. In comparison with the isoscalar $\mathcal{D}\bar{\mathcal{D}}$ systems, the OBE effective potentials for the $S-$wave isovector $\mathcal{D}\bar{\mathcal{D}}$ systems are very different. Since the π and ρ exchanges couple to the isospin charge, their properties in the isovector $\mathcal{D}\bar{\mathcal{D}}$ systems are contrary to those in the isoscalar $\mathcal{D}\bar{\mathcal{D}}$ systems, and the corresponding effective potentials are three times weaker (see Eqs. (A3)–(A6) for details). Therefore, the OBE effective potentials for the $S-$wave isovector $\mathcal{D}\bar{\mathcal{D}}$ systems may be not strong enough to bind isovector charmoniumlike molecular states.

When we input the corresponding OBE effective potentials, only the $S-$wave isovector $D^*\bar{D}_1$ state with $J^{PC} = 2^{-+}$ can generate the loosely bound state with the cutoff parameter Λ around 3.0 GeV. Even though we consider the $S-D$ wave mixing and the coupled channel effect, the cutoff Λ is still much larger than 1.0 GeV [72,73]. If we take the cutoff value from the deuteron as the reasonable input, the interactions from a pair of charmed meson and anticharmed meson are not strong enough to bind $S-$wave isovector charmoniumlike molecular tetraquark states.

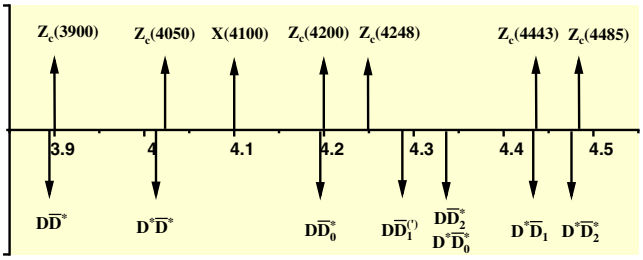

FIG. 9. The masses comparison between the charged charmoniumlike states [18–24] and the $\mathcal{D}\bar{\mathcal{D}}$ thresholds.

Experimentally, there have accumulated abundant experimental observations of the charged charmoniumlike states from the B meson decays as introduced in the Sec. II C. If they are real particles, they cannot be traditional mesons but the multiquark matters. As shown in Fig. 9, their masses are all above the mass thresholds of the corresponding $\mathcal{D}\bar{\mathcal{D}}$ systems. Obviously, they cannot be assigned as the isovector charmoniumlike molecular states. In short, our results exclude the charged charmoniumlike states as the isovector meson-meson molecular states, which perfectly match the experimental observations. In fact, the other groups also support our conclusions [16,21,31,74,88,104,108,109,120,125,136–141].

Before closing our discussion on the isovector charmoniumlike systems, we would like to emphasize that we only analyze whether the charged charmoniumlike states can be the isovector charmoniumlike molecular states composed of a pair of charmed meson and anticharmed meson. Furthermore, the interaction of the off-diagonal couplings may be important to reproduce these charged charmoniumlike states by the threshold cusp [142–146], such as the $\pi J/\psi - DD$ and $\rho\eta_c - DD$ couplings, it is an interesting topic to consider the more complex coupled channels calculation to deal with these charged charmoniumlike states. In Ref. [147], Lanzhou group once reproduced the $Z_c(3900)$ structure through the initial-single-pion-emission mechanism. In fact, many theoretical groups propose other different explanations on the nature of the charged charmoniumlike states, like the compact tetraquark configurations, the meson-meson scattering states, and the kinematical effect (including the coupled channel cusp effect, the reflection mechanism, the interference effect, the initial single pion emission mechanism, the triangle singularities, the rescattering effect, and so on), people can refer articles [18,21,24,147–161] for more details.

IV. SUMMARY

Exploration of the hadronic molecular states is an interesting and important research topics in the hadron

physics. Since 2003, serials of charmoniumlike structures have been reported by different experiments in different beams, different reactions, and different energy regions, some of them are very close to a pair of charmed meson and anticharmed meson thresholds, which inspired theorists to explain them in the hadronic molecular scenario. Although the charmoniumlike hadronic molecular states are not forbidden by the quantum chromodynamics (QCD), one cannot give a precisely conclusion whether the charmoniumlike hadronic molecular states exist or not up to now.

The perfect match between experimental observations and the theoretical predictions on the three P_c states provides a strong evidence of the existence of hidden-charm meson-baryon molecular pentaquark states. If replacing ud quarks of Λ_b by an antiquark $\bar{q}$, the production mechanisms of the P_c states from Λ_b baryon decays and the XYZ states from B meson decays are very similar. The $B \to XYZ + K$ decay should be the ideal process to produce charmoniumlike molecular states.

In such a situation, we firstly focus on the isoscalar $D^*\bar{D}^*$ systems with $J^{PC} = 0^{++}$, 1^{+-}, and 2^{++}. And we find their interactions are attractive enough to generate bound charmoniumlike molecular states. After analyzing their two-body hidden-charm decay behaviors, we find that the $J/\psi\omega$ and $J/\psi\eta$ channels are the essential decay modes for the isoscalar $D^*\bar{D}^*$ molecular states with $J^{PC} = 0^{++}/2^{++}$ and 1^{+-}, respectively. If checking the data from the $J/\psi\omega$ invariant mass distribution in the $B \to J/\psi\omega K$ and the $J/\psi\eta$ invariant mass distribution in the $B \to J/\psi\eta K$, one can roughly find double enhancement structures in $J/\psi\omega$ invariant mass distribution and single structure in $J/\psi\eta$ invariant mass distribution, their masses are just below the $D^*\bar{D}^*$ threshold, which may correspond to the isoscalar $D^*\bar{D}^*$ charmoniumlike molecules with $J^P = 0^{++}/2^{++}$ and 1^{+-}, respectively. The behavior of the double enhancement structures around 3.9 GeV below the $D^*\bar{D}^*$ threshold from the $B \to J/\psi\omega K$ and the single structure in the same energy region from the $B \to J/\psi\eta K$ can provide crucial information to identify the charmoniumlike molecule. Thus, we suggest to systematically check the correlation of charmoniumlike molecular states and charmoniumlike structures existing in the XYZ data of the $B \to XYZ + K$ decay.

After that, we promote our study to the interactions between a charmed (charm-strange) meson and an anticharmed (anticharm-strange) meson, including the $D^{(*)}\bar{D}^{(*)}$, $\bar{D}^{(*)}\bar{D}_1$, $D^{(*)}\bar{D}_2^*$, $D_s^{(*)}\bar{D}_s^{(*)}$, $D_s^{(*)}\bar{D}_{s0}^*$, $D_s^{(*)}\bar{D}_{s1}'$, $D_s^{(*)}\bar{D}_{s1}$, $D_s^{(*)}\bar{D}_{s2}^*$ systems. After input the OBE effective potentials, we can find a series of promising isoscalar charmoniumlike molecular tetraquark candidates as summarized in Tables IX. Our results exclude these discussed $S-$ wave isovector charmoniumlike tetraquark states as the hadronic molecular candidates in the OBE model. Besides analyzing the mass spectrum, we also give their two-body hidden-charm decay channels of these possible molecular tetraquark candidates. In Table IX, we collect the two-body hidden-charm decay channels for these promising charmoniumlike molecular candidates. These obtained results can be very helpful to search and identify these discussed molecular tetraquark candidates.

In this work, our results indicate that the underlying phenomena behind the wide structure around 4.3 GeV in the $B \to J/\psi\omega K$ is very complicated. There can exist several possible isoscalar charmoniumlike molecular candidates, and the $J/\psi\omega$ channel is their two-body hidden-charm decay channel. In addition, we can predict many isoscalar charmoniumlike molecular states with negative C-parity in the same mass region, and their two-body hidden-charm decay modes are the $\chi_{cJ}(1P)\omega$ with $J = 0, 1, 2$. The $B \to \chi_{cJ}(1P)\omega + K \to J/\psi\gamma\omega + K$ may be the good production process to search for these predicted isoscalar charmoniumlike molecular states with $C = -$.

Meanwhile, we also study the mass spectrum and give two-body hidden-charm decay channels for the possible charmoniumlike $\mathcal{D}_s\bar{\mathcal{D}}_s$ molecular states with hidden-strange quantum number summarized in Table XII, where $\mathcal{D}_s$ stands for the charm-strange meson. The $J/\psi\phi$ channel is the two-body hidden-charm decay channel for most of the possible $\mathcal{D}_s\bar{\mathcal{D}}_s$ molecular states. In order to further distinguish these structures, one need more precision experimental data, and more analysis on the other decay channel could be also useful.

Finding the charmoniumlike states has been going on for around 20 years. With the running of Belle II [35] and the accumulation of Run II and Run III data at LHCb [36], the study of the charmoniumlike states will step into a new area, here, we suggest to systematically check the correlation of charmoniumlike molecular states and charmoniumlike structures existing in the XYZ data of the $B \to XYZ + K$ decay. The present work provides a good start point and new insight for identifying charmoniumlike molecule. We expect more theoretical and experimental efforts in exploring this important and intriguing research topic in the coming golden decade.

ACKNOWLEDGMENTS

F.-L. Wang would like to thank J. Z. Wang and M. X. Duan for very helpful discussions. This work is supported by the China National Funds for Distinguished Young Scientists under Grant No. 11825503, National Key Research and Development Program of China under Contract No. 2020YFA0406400, the 111 Project under Grant No. B20063, and the National Natural Science Foundation of China under Grant No. 12047501. R. C. is supported by the National Postdoctoral Program for Innovative Talent.

APPENDIX: RELEVANT SUBPOTENTIALS

Before presenting the effective potentials for these investigated tetraquark systems, we first define several operators $\mathcal{O}_k^{(\prime)}$ involved in this work, which include

$$
\begin{aligned}
&\mathcal{O}_1=\boldsymbol{\epsilon}_4^\dagger\cdot\boldsymbol{\epsilon}_2,\qquad \mathcal{O}_2=\boldsymbol{\epsilon}_3^\dagger\cdot\boldsymbol{\epsilon}_2,\qquad \mathcal{O}_3=T(\boldsymbol{\epsilon}_3^\dagger,\boldsymbol{\epsilon}_2),\\
&\mathcal{O}_4=(\boldsymbol{\epsilon}_3^\dagger\cdot\boldsymbol{\epsilon}_1)(\boldsymbol{\epsilon}_4^\dagger\cdot\boldsymbol{\epsilon}_2),\qquad \mathcal{O}_5=(\boldsymbol{\epsilon}_3^\dagger\times\boldsymbol{\epsilon}_1)\cdot(\boldsymbol{\epsilon}_4^\dagger\times\boldsymbol{\epsilon}_2),\\
&\mathcal{O}_6=T(\boldsymbol{\epsilon}_3^\dagger\times\boldsymbol{\epsilon}_1,\boldsymbol{\epsilon}_4^\dagger\times\boldsymbol{\epsilon}_2),\\
&\mathcal{O}_7=\sum(\boldsymbol{\epsilon}_{4m}^\dagger\cdot\boldsymbol{\epsilon}_{2a})(\boldsymbol{\epsilon}_{4n}^\dagger\cdot\boldsymbol{\epsilon}_{2b}),\\
&\mathcal{O}_8=\frac{2}{27}\sum(\boldsymbol{\epsilon}_{3m}^\dagger\cdot\boldsymbol{\epsilon}_{2a})(\boldsymbol{\epsilon}_{3n}^\dagger\cdot\boldsymbol{\epsilon}_{2b}),\\
&\mathcal{O}_9=\frac{1}{27}\sum T(\boldsymbol{\epsilon}_{3m}^\dagger,\boldsymbol{\epsilon}_{3n}^\dagger)T(\boldsymbol{\epsilon}_{2a},\boldsymbol{\epsilon}_{2b})\\
&\qquad+\frac{2}{27}\sum T(\boldsymbol{\epsilon}_{3m}^\dagger,\boldsymbol{\epsilon}_{2a})T(\boldsymbol{\epsilon}_{3n}^\dagger,\boldsymbol{\epsilon}_{2b}),\\
&\mathcal{O}_{10}=\frac{2}{27}\sum(\boldsymbol{\epsilon}_{3m}^\dagger\cdot\boldsymbol{\epsilon}_{2a})T(\boldsymbol{\epsilon}_{3n}^\dagger,\boldsymbol{\epsilon}_{2b}),\\
&\mathcal{O}_{11}=-\frac{1}{3}(\boldsymbol{\epsilon}_3^\dagger\cdot\boldsymbol{\epsilon}_1)(\boldsymbol{\epsilon}_4^\dagger\cdot\boldsymbol{\epsilon}_2)+\frac{1}{3}(\boldsymbol{\epsilon}_3^\dagger\cdot\boldsymbol{\epsilon}_4^\dagger)(\boldsymbol{\epsilon}_1\cdot\boldsymbol{\epsilon}_2),\\
&\mathcal{O}_{12}=\frac{2}{3}T(\boldsymbol{\epsilon}_3^\dagger,\boldsymbol{\epsilon}_1)T(\boldsymbol{\epsilon}_4^\dagger,\boldsymbol{\epsilon}_2)+\frac{1}{3}T(\boldsymbol{\epsilon}_3^\dagger,\boldsymbol{\epsilon}_4^\dagger)T(\boldsymbol{\epsilon}_1,\boldsymbol{\epsilon}_2),\\
&\mathcal{O}_{13}=\frac{1}{6}(\boldsymbol{\epsilon}_3^\dagger\cdot\boldsymbol{\epsilon}_4^\dagger)T(\boldsymbol{\epsilon}_1,\boldsymbol{\epsilon}_2)+\frac{1}{6}(\boldsymbol{\epsilon}_1\cdot\boldsymbol{\epsilon}_2)T(\boldsymbol{\epsilon}_3^\dagger,\boldsymbol{\epsilon}_4^\dagger)\\
&\qquad-\frac{1}{3}(\boldsymbol{\epsilon}_3^\dagger\cdot\boldsymbol{\epsilon}_1)T(\boldsymbol{\epsilon}_4^\dagger,\boldsymbol{\epsilon}_2),\\
&\mathcal{O}_{14}=\sum(\boldsymbol{\epsilon}_3^\dagger\cdot\boldsymbol{\epsilon}_1)(\boldsymbol{\epsilon}_{4m}^\dagger\cdot\boldsymbol{\epsilon}_{2a})(\boldsymbol{\epsilon}_{4n}^\dagger\cdot\boldsymbol{\epsilon}_{2b}),\\
&\mathcal{O}'_{14}=\sum(\boldsymbol{\epsilon}_4^\dagger\cdot\boldsymbol{\epsilon}_2)(\boldsymbol{\epsilon}_{3m}^\dagger\cdot\boldsymbol{\epsilon}_{1a})(\boldsymbol{\epsilon}_{3n}^\dagger\cdot\boldsymbol{\epsilon}_{1b}),\\
&\mathcal{O}_{15}=\sum(\boldsymbol{\epsilon}_{4m}^\dagger\cdot\boldsymbol{\epsilon}_{2a})[(\boldsymbol{\epsilon}_3^\dagger\times\boldsymbol{\epsilon}_1)\cdot(\boldsymbol{\epsilon}_{4n}^\dagger\times\boldsymbol{\epsilon}_{2b})],\\
&\mathcal{O}'_{15}=\sum(\boldsymbol{\epsilon}_{3m}^\dagger\cdot\boldsymbol{\epsilon}_{1a})[(\boldsymbol{\epsilon}_4^\dagger\times\boldsymbol{\epsilon}_2)\cdot(\boldsymbol{\epsilon}_{3n}^\dagger\times\boldsymbol{\epsilon}_{1b})],\\
&\mathcal{O}_{16}=\sum(\boldsymbol{\epsilon}_{4m}^\dagger\cdot\boldsymbol{\epsilon}_{2a})T(\boldsymbol{\epsilon}_3^\dagger\times\boldsymbol{\epsilon}_1,\boldsymbol{\epsilon}_{4n}^\dagger\times\boldsymbol{\epsilon}_{2b}),\\
&\mathcal{O}'_{16}=\sum(\boldsymbol{\epsilon}_{3m}^\dagger\cdot\boldsymbol{\epsilon}_{1a})T(\boldsymbol{\epsilon}_4^\dagger\times\boldsymbol{\epsilon}_2,\boldsymbol{\epsilon}_{3n}^\dagger\times\boldsymbol{\epsilon}_{1b}),\\
&\mathcal{O}_{17}=\sum(\boldsymbol{\epsilon}_{3m}^\dagger\cdot\boldsymbol{\epsilon}_1)(\boldsymbol{\epsilon}_4^\dagger\cdot\boldsymbol{\epsilon}_{2a})(\boldsymbol{\epsilon}_{3n}^\dagger\cdot\boldsymbol{\epsilon}_{2b}),\\
&\mathcal{O}'_{17}=\sum(\boldsymbol{\epsilon}_{4m}^\dagger\cdot\boldsymbol{\epsilon}_2)(\boldsymbol{\epsilon}_3^\dagger\cdot\boldsymbol{\epsilon}_{1a})(\boldsymbol{\epsilon}_{4n}^\dagger\cdot\boldsymbol{\epsilon}_{1b}),\\
&\mathcal{O}_{18}=\sum(\boldsymbol{\epsilon}_{3m}^\dagger\cdot\boldsymbol{\epsilon}_1)(\boldsymbol{\epsilon}_4^\dagger\cdot\boldsymbol{\epsilon}_{2a})T(\boldsymbol{\epsilon}_{3n}^\dagger,\boldsymbol{\epsilon}_{2b}),\\
&\mathcal{O}'_{18}=\sum(\boldsymbol{\epsilon}_{4m}^\dagger\cdot\boldsymbol{\epsilon}_2)(\boldsymbol{\epsilon}_3^\dagger\cdot\boldsymbol{\epsilon}_{1a})T(\boldsymbol{\epsilon}_{4n}^\dagger,\boldsymbol{\epsilon}_{1b}),\\
&\mathcal{O}_{19}=\frac{1}{27}\sum[(\boldsymbol{\epsilon}_{3m}^\dagger\times\boldsymbol{\epsilon}_1)\cdot(\boldsymbol{\epsilon}_4^\dagger\times\boldsymbol{\epsilon}_{2a})](\boldsymbol{\epsilon}_{3n}^\dagger\cdot\boldsymbol{\epsilon}_{2b})\\
&\qquad+\frac{1}{27}\sum[(\boldsymbol{\epsilon}_{3m}^\dagger\times\boldsymbol{\epsilon}_1)\cdot\boldsymbol{\epsilon}_{2b}][\boldsymbol{\epsilon}_{3n}^\dagger\cdot(\boldsymbol{\epsilon}_4^\dagger\times\boldsymbol{\epsilon}_{2a})],\\
&\mathcal{O}'_{19}=\frac{1}{27}\sum[(\boldsymbol{\epsilon}_{4m}^\dagger\times\boldsymbol{\epsilon}_2)\cdot(\boldsymbol{\epsilon}_3^\dagger\times\boldsymbol{\epsilon}_{1a})](\boldsymbol{\epsilon}_{4n}^\dagger\cdot\boldsymbol{\epsilon}_{1b})\\
&\qquad+\frac{1}{27}\sum[(\boldsymbol{\epsilon}_{4m}^\dagger\times\boldsymbol{\epsilon}_2)\cdot\boldsymbol{\epsilon}_{1b}][\boldsymbol{\epsilon}_{4n}^\dagger\cdot(\boldsymbol{\epsilon}_3^\dagger\times\boldsymbol{\epsilon}_{1a})],\\
&\mathcal{O}_{20}=\frac{1}{27}\sum T(\boldsymbol{\epsilon}_{3m}^\dagger\times\boldsymbol{\epsilon}_1,\boldsymbol{\epsilon}_{3n}^\dagger)T(\boldsymbol{\epsilon}_4^\dagger\times\boldsymbol{\epsilon}_{2a},\boldsymbol{\epsilon}_{2b})\\
&\qquad+\frac{1}{27}\sum T(\boldsymbol{\epsilon}_{3m}^\dagger\times\boldsymbol{\epsilon}_1,\boldsymbol{\epsilon}_4^\dagger\times\boldsymbol{\epsilon}_{2a})T(\boldsymbol{\epsilon}_{3n}^\dagger,\boldsymbol{\epsilon}_{2b})\\
&\qquad+\frac{1}{27}\sum T(\boldsymbol{\epsilon}_{3m}^\dagger\times\boldsymbol{\epsilon}_1,\boldsymbol{\epsilon}_{2b})T(\boldsymbol{\epsilon}_{3n}^\dagger,\boldsymbol{\epsilon}_4^\dagger\times\boldsymbol{\epsilon}_{2a}),\\
&\mathcal{O}'_{20}=\frac{1}{27}\sum T(\boldsymbol{\epsilon}_{4m}^\dagger\times\boldsymbol{\epsilon}_2,\boldsymbol{\epsilon}_{4n}^\dagger)T(\boldsymbol{\epsilon}_3^\dagger\times\boldsymbol{\epsilon}_{1a},\boldsymbol{\epsilon}_{1b})\\
&\qquad+\frac{1}{27}\sum T(\boldsymbol{\epsilon}_{4m}^\dagger\times\boldsymbol{\epsilon}_2,\boldsymbol{\epsilon}_3^\dagger\times\boldsymbol{\epsilon}_{1a})T(\boldsymbol{\epsilon}_{4n}^\dagger,\boldsymbol{\epsilon}_{1b})\\
&\qquad+\frac{1}{27}\sum T(\boldsymbol{\epsilon}_{4m}^\dagger\times\boldsymbol{\epsilon}_2,\boldsymbol{\epsilon}_{1b})T(\boldsymbol{\epsilon}_{4n}^\dagger,\boldsymbol{\epsilon}_3^\dagger\times\boldsymbol{\epsilon}_{1a}),\\
&\mathcal{O}_{21}=\frac{1}{54}\sum[(\boldsymbol{\epsilon}_{3m}^\dagger\times\boldsymbol{\epsilon}_1)\cdot(\boldsymbol{\epsilon}_4^\dagger\times\boldsymbol{\epsilon}_{2a})]T(\boldsymbol{\epsilon}_{3n}^\dagger,\boldsymbol{\epsilon}_{2b})\\
&\qquad+\frac{1}{54}\sum[(\boldsymbol{\epsilon}_{3m}^\dagger\times\boldsymbol{\epsilon}_1)\cdot\boldsymbol{\epsilon}_{2b}]T(\boldsymbol{\epsilon}_{3n}^\dagger,\boldsymbol{\epsilon}_4^\dagger\times\boldsymbol{\epsilon}_{2a})\\
&\qquad+\frac{1}{54}\sum(\boldsymbol{\epsilon}_{3n}^\dagger\cdot\boldsymbol{\epsilon}_{2b})T(\boldsymbol{\epsilon}_{3m}^\dagger\times\boldsymbol{\epsilon}_1,\boldsymbol{\epsilon}_4^\dagger\times\boldsymbol{\epsilon}_{2a})\\
&\qquad+\frac{1}{54}\sum[\boldsymbol{\epsilon}_{3n}^\dagger\cdot(\boldsymbol{\epsilon}_4^\dagger\times\boldsymbol{\epsilon}_{2a})]T(\boldsymbol{\epsilon}_{3m}^\dagger\times\boldsymbol{\epsilon}_1,\boldsymbol{\epsilon}_{2b}),\\
&\mathcal{O}'_{21}=\frac{1}{54}\sum[(\boldsymbol{\epsilon}_{4m}^\dagger\times\boldsymbol{\epsilon}_2)\cdot(\boldsymbol{\epsilon}_3^\dagger\times\boldsymbol{\epsilon}_{1a})]T(\boldsymbol{\epsilon}_{4n}^\dagger,\boldsymbol{\epsilon}_{1b})\\
&\qquad+\frac{1}{54}\sum[(\boldsymbol{\epsilon}_{4m}^\dagger\times\boldsymbol{\epsilon}_2)\cdot\boldsymbol{\epsilon}_{1b}]T(\boldsymbol{\epsilon}_{4n}^\dagger,\boldsymbol{\epsilon}_3^\dagger\times\boldsymbol{\epsilon}_{1a})\\
&\qquad+\frac{1}{54}\sum(\boldsymbol{\epsilon}_{4n}^\dagger\cdot\boldsymbol{\epsilon}_{1b})T(\boldsymbol{\epsilon}_{4m}^\dagger\times\boldsymbol{\epsilon}_2,\boldsymbol{\epsilon}_3^\dagger\times\boldsymbol{\epsilon}_{1a})\\
&\qquad+\frac{1}{54}\sum[\boldsymbol{\epsilon}_{4n}^\dagger\cdot(\boldsymbol{\epsilon}_3^\dagger\times\boldsymbol{\epsilon}_{1a})]T(\boldsymbol{\epsilon}_{4m}^\dagger\times\boldsymbol{\epsilon}_2,\boldsymbol{\epsilon}_{1b}).
\end{aligned}
\tag{A1}
$$

Here, we define $\mathcal{S}=\sum_{m,n,a,b}C^{2,m+n}_{1m,1n}C^{2,a+b}_{1a,1b}$, and $T(\boldsymbol{x},\boldsymbol{y})=3(\hat{\boldsymbol{r}}\cdot\boldsymbol{x})(\hat{\boldsymbol{r}}\cdot\boldsymbol{y})-\boldsymbol{x}\cdot\boldsymbol{y}$ is the tensor force operator. For these operators $\mathcal{O}_k^{(\prime)}$, they should be sandwiched by the relevant spin-orbital wave functions $|^{2S+1}L_J\rangle$ for these investigated tetraquark systems, such as $\langle D\bar{D}^*(^3\mathbb{S}_1)|\mathcal{O}_1|D\bar{D}^*(^3\mathbb{S}_1)\rangle=1$. The obtained operator matrix elements $\mathcal{O}_k^{(\prime)}[J]$ are summarized in Tables XIII and XIV, which will be used in our calculations.

In addition, the function $Y(\Lambda_i,m_i,r)$ is defined as

$$
Y_i\equiv\begin{cases}|q_i|\le m,\frac{e^{-m_ir}-e^{-\Lambda_i^2r}}{4\pi r}-\frac{\Lambda_i^2-m_i^2}{8\pi\Lambda_i}e^{-\Lambda_ir};\\ |q_i|>m,\frac{\cos(m_i'r)-e^{-\Lambda_ir}}{4\pi r}-\frac{\Lambda_i^2+m_i'^2}{8\pi\Lambda_i}e^{-\Lambda_ir};\end{cases}
\tag{A2}
$$

where $m_i=\sqrt{m^2-q_i^2}$, $m_i'=\sqrt{q_i^2-m^2}$, and $\Lambda_i=\sqrt{\Lambda^2-q_i^2}$.

1. Hidden-charm molecular tetraquark systems without hidden-strange quantum number

For convenience, we define two functions $\mathcal{H}(I)Y\times(\Lambda,m_P,r)$ and $\mathcal{G}(I)Y(\Lambda,m_V,r)$ for these investigated hidden-charm tetraquark systems, i.e.,

$$
\mathcal{H}(0)Y(\Lambda,m_P,r)=\frac{3}{2}Y(\Lambda,m_\pi,r)+\frac{1}{6}Y(\Lambda,m_\eta,r),
\tag{A3}
$$

$$
\mathcal{H}(1)Y(\Lambda,m_P,r)=-\frac{1}{2}Y(\Lambda,m_\pi,r)+\frac{1}{6}Y(\Lambda,m_\eta,r),
\tag{A4}
$$

TABLE XIII. The relevant operator matrix elements $\mathcal{O}_k^{(\prime)}[J] = \langle f|\mathcal{O}_k^{(\prime)}|i\rangle$.

$\mathcal{O}_1[1] = \mathrm{diag}(1,1)$
$\mathcal{O}_2[1] = \mathrm{diag}(1,1)$
$\mathcal{O}_3[1] = \begin{pmatrix} 0 & -\sqrt{2} \\ -\sqrt{2} & 1 \end{pmatrix}$
$\mathcal{O}_6[1] = \begin{pmatrix} 0 & -\sqrt{2} & 0 \\ -\sqrt{2} & 1 & 0 \\ 0 & 0 & 1 \end{pmatrix}$

$\mathcal{O}_4[0] = \mathrm{diag}(1,1)$
$\mathcal{O}_5[0] = \mathrm{diag}(2,-1)$
$\mathcal{O}_6[0] = \begin{pmatrix} 0 & \sqrt{2} \\ \sqrt{2} & 2 \end{pmatrix}$
$\mathcal{O}_4[2] = \mathrm{diag}(1,1,1,1)$
$\mathcal{O}_5[2] = \mathrm{diag}(-1,2,1,-1)$
$\mathcal{O}_7[2] = \mathrm{diag}(1,1)$
$\mathcal{O}_8[2] = \mathrm{diag}(\frac{2}{27},\frac{2}{27})$

$\mathcal{O}_4[1] = \mathrm{diag}(1,1,1)$
$\mathcal{O}_5[1] = \mathrm{diag}(1,1,-1)$
$\mathcal{O}_6[2] = \begin{pmatrix} 0 & \frac{\sqrt{2}}{\sqrt{5}} & 0 & -\frac{\sqrt{14}}{\sqrt{5}} \\ \frac{\sqrt{2}}{\sqrt{5}} & 0 & 0 & -\frac{2}{\sqrt{7}} \\ 0 & 0 & -1 & 0 \\ -\frac{\sqrt{14}}{\sqrt{5}} & -\frac{2}{\sqrt{7}} & 0 & -\frac{3}{7} \end{pmatrix}$

$\mathcal{O}_9[2] = \begin{pmatrix} \frac{8}{135} & -\frac{4\sqrt{2}}{27\sqrt{35}} \\ -\frac{4\sqrt{2}}{27\sqrt{35}} & \frac{4}{27} \end{pmatrix}$

$\mathcal{O}_{10}[2] = \begin{pmatrix} 0 & -\frac{\sqrt{7}}{27\sqrt{10}} \\ -\frac{\sqrt{7}}{27\sqrt{10}} & -\frac{1}{126} \end{pmatrix}$

$\mathcal{O}_{11}[0] = \mathrm{diag}(\frac{2}{3},-\frac{1}{3})$
$\mathcal{O}_{11}[1] = \mathrm{diag}(-\frac{1}{3},-\frac{1}{3},-\frac{1}{3})$
$\mathcal{O}_{11}[2] = \mathrm{diag}(-\frac{1}{3},\frac{2}{3},-\frac{1}{3},-\frac{1}{3})$

$\mathcal{O}_{12}[0] = \begin{pmatrix} \frac{4}{3} & -\frac{2\sqrt{2}}{3} \\ -\frac{2\sqrt{2}}{3} & 4 \end{pmatrix}$

$\mathcal{O}_{13}[0] = \begin{pmatrix} 0 & \frac{\sqrt{2}}{15} \\ -\frac{8\sqrt{2}}{15} & -\frac{1}{15} \end{pmatrix}$

$\mathcal{O}_{12}[1] = \begin{pmatrix} -\frac{2}{3} & -\frac{2\sqrt{2}}{3} & 0 \\ -\frac{2\sqrt{2}}{3} & 0 & 0 \\ 0 & 0 & -\frac{4}{3} \end{pmatrix}$

$\mathcal{O}_{13}[1] = \begin{pmatrix} 0 & -\frac{1}{30\sqrt{2}} & \frac{\sqrt{3}}{10\sqrt{2}} \\ -\frac{1}{30\sqrt{2}} & \frac{4}{105} & \frac{3\sqrt{3}}{70} \\ \frac{\sqrt{3}}{10\sqrt{2}} & \frac{3\sqrt{3}}{70} & -\frac{1}{105} \end{pmatrix}$

$\mathcal{O}_{12}[2] = \begin{pmatrix} \frac{8}{15} & -\frac{2\sqrt{2}}{3\sqrt{5}} & 0 & -\frac{4\sqrt{2}}{3\sqrt{35}} \\ -\frac{2\sqrt{2}}{3\sqrt{5}} & \frac{4}{3} & 0 & \frac{4}{3\sqrt{7}} \\ 0 & 0 & -\frac{4}{3} & 0 \\ -\frac{4\sqrt{2}}{3\sqrt{35}} & \frac{4}{3\sqrt{7}} & 0 & \frac{4}{3} \end{pmatrix}$

$\mathcal{O}_{13}[2] = \begin{pmatrix} 0 & -\frac{1}{\sqrt{10}} & 0 & \frac{\sqrt{2}}{3\sqrt{35}} \\ 0 & 0 & 0 & -\frac{4}{21\sqrt{7}} \\ 0 & 0 & -\frac{1}{14} & \frac{1}{14\sqrt{7}} \\ \frac{\sqrt{2}}{3\sqrt{35}} & \frac{23}{21\sqrt{7}} & \frac{1}{14\sqrt{7}} & \frac{13}{294} \end{pmatrix}$

$\mathcal{O}_{14}^{(\prime)}[1] = \mathrm{diag}(1,1,1,1)$
$\mathcal{O}_{15}^{(\prime)}[1] = \mathrm{diag}(\frac{3}{2},\frac{3}{2},\frac{1}{2},-1)$
$\mathcal{O}_{17}^{(\prime)}[1] = \mathrm{diag}(\frac{1}{6},\frac{1}{6},\frac{1}{2},1)$
$\mathcal{O}_{19}^{(\prime)}[1] = \mathrm{diag}(\frac{1}{18},\frac{1}{18},\frac{5}{54},-\frac{1}{27})$

$\mathcal{O}_{16}[1] = \begin{pmatrix} 0 & \frac{3}{5\sqrt{2}} & \frac{\sqrt{6}}{\sqrt{5}} & \frac{\sqrt{21}}{5\sqrt{2}} \\ \frac{3}{5\sqrt{2}} & -\frac{3}{10} & \frac{\sqrt{3}}{\sqrt{5}} & -\frac{\sqrt{3}}{5\sqrt{7}} \\ \frac{\sqrt{6}}{\sqrt{5}} & \frac{\sqrt{3}}{\sqrt{5}} & \frac{1}{2} & \frac{2}{\sqrt{35}} \\ \frac{\sqrt{21}}{5\sqrt{2}} & -\frac{\sqrt{3}}{5\sqrt{7}} & \frac{2}{\sqrt{35}} & \frac{48}{35} \end{pmatrix}$

$\mathcal{O}'_{16}[1] = \begin{pmatrix} 0 & \frac{3}{5\sqrt{2}} & -\frac{\sqrt{6}}{\sqrt{5}} & \frac{\sqrt{21}}{5\sqrt{2}} \\ \frac{3}{5\sqrt{2}} & -\frac{3}{10} & -\frac{\sqrt{3}}{\sqrt{5}} & -\frac{\sqrt{3}}{5\sqrt{7}} \\ -\frac{\sqrt{6}}{\sqrt{5}} & -\frac{\sqrt{3}}{\sqrt{5}} & \frac{1}{2} & -\frac{2}{\sqrt{35}} \\ \frac{\sqrt{21}}{5\sqrt{2}} & -\frac{\sqrt{3}}{5\sqrt{7}} & -\frac{2}{\sqrt{35}} & \frac{48}{35} \end{pmatrix}$

$\mathcal{O}_{18}[1] = \begin{pmatrix} 0 & -\frac{23}{15\sqrt{2}} & -\frac{2\sqrt{2}}{\sqrt{15}} & -\frac{\sqrt{7}}{5\sqrt{6}} \\ -\frac{23}{15\sqrt{2}} & \frac{23}{30} & -\frac{2}{\sqrt{15}} & \frac{1}{5\sqrt{21}} \\ \frac{2\sqrt{2}}{\sqrt{15}} & \frac{2}{\sqrt{15}} & \frac{1}{2} & -\frac{2}{\sqrt{35}} \\ -\frac{\sqrt{7}}{5\sqrt{6}} & \frac{1}{5\sqrt{21}} & \frac{2}{\sqrt{35}} & \frac{24}{35} \end{pmatrix}$

$\mathcal{O}'_{18}[1] = \begin{pmatrix} 0 & -\frac{23}{15\sqrt{2}} & \frac{2\sqrt{2}}{\sqrt{15}} & -\frac{\sqrt{7}}{5\sqrt{6}} \\ -\frac{23}{15\sqrt{2}} & \frac{23}{30} & \frac{2}{\sqrt{15}} & \frac{1}{5\sqrt{21}} \\ -\frac{2\sqrt{2}}{\sqrt{15}} & -\frac{2}{\sqrt{15}} & \frac{1}{2} & \frac{2}{\sqrt{35}} \\ -\frac{\sqrt{7}}{5\sqrt{6}} & \frac{1}{5\sqrt{21}} & -\frac{2}{\sqrt{35}} & \frac{24}{35} \end{pmatrix}$

$\mathcal{O}_{20}[1] = \begin{pmatrix} \frac{2}{45} & -\frac{\sqrt{2}}{45} & 0 & \frac{\sqrt{2}}{15\sqrt{21}} \\ -\frac{\sqrt{2}}{45} & \frac{1}{15} & 0 & -\frac{8}{15\sqrt{21}} \\ 0 & 0 & -\frac{1}{9} & -\frac{2\sqrt{5}}{27\sqrt{7}} \\ \frac{\sqrt{2}}{15\sqrt{21}} & -\frac{8}{15\sqrt{21}} & \frac{2\sqrt{5}}{27\sqrt{7}} & \frac{92}{945} \end{pmatrix}$

$\mathcal{O}'_{20}[1] = \begin{pmatrix} \frac{2}{45} & -\frac{\sqrt{2}}{45} & 0 & \frac{\sqrt{2}}{15\sqrt{21}} \\ -\frac{\sqrt{2}}{45} & \frac{1}{15} & 0 & -\frac{8}{15\sqrt{21}} \\ 0 & 0 & -\frac{1}{9} & \frac{2\sqrt{5}}{27\sqrt{7}} \\ \frac{\sqrt{2}}{15\sqrt{21}} & -\frac{8}{15\sqrt{21}} & -\frac{2\sqrt{5}}{27\sqrt{7}} & \frac{92}{945} \end{pmatrix}$

$\mathcal{O}_{21}[1] = \begin{pmatrix} 0 & -\frac{7}{90\sqrt{2}} & 0 & \frac{\sqrt{7}}{30\sqrt{6}} \\ -\frac{7}{90\sqrt{2}} & \frac{7}{180} & 0 & -\frac{1}{30\sqrt{21}} \\ 0 & 0 & \frac{1}{108} & \frac{\sqrt{5}}{27\sqrt{7}} \\ \frac{\sqrt{7}}{30\sqrt{6}} & -\frac{1}{30\sqrt{21}} & -\frac{\sqrt{5}}{27\sqrt{7}} & \frac{4}{315} \end{pmatrix}$

$\mathcal{O}'_{21}[1] = \begin{pmatrix} 0 & -\frac{7}{90\sqrt{2}} & 0 & \frac{\sqrt{7}}{30\sqrt{6}} \\ -\frac{7}{90\sqrt{2}} & \frac{7}{180} & 0 & -\frac{1}{30\sqrt{21}} \\ 0 & 0 & \frac{1}{108} & -\frac{\sqrt{5}}{27\sqrt{7}} \\ \frac{\sqrt{7}}{30\sqrt{6}} & -\frac{1}{30\sqrt{21}} & \frac{\sqrt{5}}{27\sqrt{7}} & \frac{4}{315} \end{pmatrix}$

$$\mathcal{G}(0)Y(\Lambda, m_V, r) = \frac{3}{2}Y(\Lambda, m_\rho, r) + \frac{1}{2}Y(\Lambda, m_\omega, r), \quad \text{(A5)}$$

$$\mathcal{G}(1)Y(\Lambda, m_V, r) = -\frac{1}{2}Y(\Lambda, m_\rho, r) + \frac{1}{2}Y(\Lambda, m_\omega, r). \quad \text{(A6)}$$

Here, $\mathcal{H}(I)$ and $\mathcal{G}(I)$ are the isospin factors for these investigated hidden-charm tetraquark systems, and I denote the isospin quantum numbers.

Through the above preparation, we can write the effective potentials in the coordinate space for all of the investigated hidden-charm tetraquark systems, which include

(1) The $D\bar{D}$ system:

$$\mathcal{V} = -g_\sigma^2 Y_\sigma - \frac{1}{2}\beta^2 g_V^2 \mathcal{G}(I) Y_V. \quad \text{(A7)}$$

(2) The $D\bar{D}^*$ system:

$$\mathcal{V}_D = -g_\sigma^2 \mathcal{O}_1 Y_\sigma - \frac{1}{2}\beta^2 g_V^2 \mathcal{O}_1 \mathcal{G}(I) Y_V,$$
$$\mathcal{V}_C = -\frac{g^2}{3f_\pi^2}(\mathcal{O}_2\mathcal{Z} + \mathcal{O}_3\mathcal{T})\mathcal{H}(I)Y_{P0} + \frac{2}{3}\lambda^2 g_V^2 (2\mathcal{O}_2\mathcal{Z} - \mathcal{O}_3\mathcal{T})\mathcal{G}(I)Y_{V0}. \quad \text{(A8)}$$

(3) The $D^*\bar{D}^*$ system:

$$\mathcal{V} = -g_\sigma^2 \mathcal{O}_4 Y_\sigma + \frac{g^2}{3f_\pi^2}(\mathcal{O}_5\mathcal{Z} + \mathcal{O}_6\mathcal{T})\mathcal{H}(I)Y_P - \frac{1}{2}\beta^2 g_V^2 \mathcal{O}_4 \mathcal{G}(I) Y_V + \frac{2}{3}\lambda^2 g_V^2 (2\mathcal{O}_5\mathcal{Z} - \mathcal{O}_6\mathcal{T})\mathcal{G}(I)Y_V. \quad \text{(A9)}$$

TABLE XIV. The relevant operator matrix elements $\mathcal{O}_k^{(\prime)}[J]=\langle f|\mathcal{O}_k^{(\prime)}|i\rangle$.

$$\mathcal{O}_{14}^{(\prime)}[2]=\mathrm{diag}(1,1,1,1)$$
$$\mathcal{O}_{15}^{(\prime)}[2]=\mathrm{diag}(\tfrac{1}{2},\tfrac{3}{2},\tfrac{1}{2},-1)$$
$$\mathcal{O}_{17}^{(\prime)}[2]=\mathrm{diag}(\tfrac{1}{2},\tfrac{1}{6},\tfrac{1}{2},1)$$
$$\mathcal{O}_{19}^{(\prime)}[2]=\mathrm{diag}(\tfrac{5}{54},\tfrac{1}{18},\tfrac{5}{54},-\tfrac{1}{27})$$

$$\mathcal{O}_{16}[2]=\begin{pmatrix} 0 & -\frac{3\sqrt{2}}{5} & -\frac{\sqrt{7}}{\sqrt{10}} & \frac{\sqrt{7}}{5} \\ -\frac{3\sqrt{2}}{5} & \frac{3}{10} & \frac{3}{\sqrt{35}} & -\frac{3\sqrt{2}}{5\sqrt{7}} \\ -\frac{\sqrt{7}}{\sqrt{10}} & \frac{3}{\sqrt{35}} & -\frac{3}{14} & \frac{4\sqrt{2}}{7\sqrt{5}} \\ \frac{\sqrt{7}}{5} & -\frac{3\sqrt{2}}{5\sqrt{7}} & \frac{4\sqrt{2}}{7\sqrt{5}} & \frac{12}{35} \end{pmatrix}$$

$$\mathcal{O}'_{16}[2]=\begin{pmatrix} 0 & \frac{3\sqrt{2}}{5} & -\frac{\sqrt{7}}{\sqrt{10}} & -\frac{\sqrt{7}}{5} \\ \frac{3\sqrt{2}}{5} & \frac{3}{10} & -\frac{3}{\sqrt{35}} & -\frac{3\sqrt{2}}{5\sqrt{7}} \\ -\frac{\sqrt{7}}{\sqrt{10}} & -\frac{3}{\sqrt{35}} & -\frac{3}{14} & -\frac{4\sqrt{2}}{7\sqrt{5}} \\ -\frac{\sqrt{7}}{5} & -\frac{3\sqrt{2}}{5\sqrt{7}} & -\frac{4\sqrt{2}}{7\sqrt{5}} & \frac{12}{35} \end{pmatrix}$$

$$\mathcal{O}_{18}[2]=\begin{pmatrix} 0 & -\frac{2\sqrt{2}}{5} & -\frac{\sqrt{7}}{\sqrt{10}} & -\frac{\sqrt{7}}{5} \\ \frac{2\sqrt{2}}{5} & -\frac{23}{30} & -\frac{2}{\sqrt{35}} & \frac{\sqrt{2}}{5\sqrt{7}} \\ -\frac{\sqrt{7}}{\sqrt{10}} & \frac{2}{\sqrt{35}} & -\frac{3}{14} & -\frac{4\sqrt{2}}{7\sqrt{5}} \\ \frac{\sqrt{7}}{5} & \frac{\sqrt{2}}{5\sqrt{7}} & \frac{4\sqrt{2}}{7\sqrt{5}} & \frac{6}{35} \end{pmatrix}$$

$$\mathcal{O}'_{18}[2]=\begin{pmatrix} 0 & \frac{2\sqrt{2}}{5} & -\frac{\sqrt{7}}{\sqrt{10}} & \frac{\sqrt{7}}{5} \\ -\frac{2\sqrt{2}}{5} & -\frac{23}{30} & \frac{2}{\sqrt{35}} & \frac{\sqrt{2}}{5\sqrt{7}} \\ -\frac{\sqrt{7}}{\sqrt{10}} & -\frac{2}{\sqrt{35}} & -\frac{3}{14} & \frac{4\sqrt{2}}{7\sqrt{5}} \\ -\frac{\sqrt{7}}{5} & \frac{\sqrt{2}}{5\sqrt{7}} & -\frac{4\sqrt{2}}{7\sqrt{5}} & \frac{6}{35} \end{pmatrix}$$

$$\mathcal{O}_{20}[2]=\begin{pmatrix} \frac{2}{27} & 0 & -\frac{\sqrt{2}}{27\sqrt{35}} & \frac{2}{27\sqrt{7}} \\ 0 & \frac{1}{45} & 0 & \frac{\sqrt{2}}{15\sqrt{7}} \\ -\frac{\sqrt{2}}{27\sqrt{35}} & 0 & \frac{29}{189} & \frac{5\sqrt{10}}{189} \\ -\frac{2}{27\sqrt{7}} & \frac{\sqrt{2}}{15\sqrt{7}} & -\frac{5\sqrt{10}}{189} & -\frac{28}{135} \end{pmatrix}$$

$$\mathcal{O}'_{20}[2]=\begin{pmatrix} \frac{2}{27} & 0 & -\frac{\sqrt{2}}{27\sqrt{35}} & -\frac{2}{27\sqrt{7}} \\ 0 & \frac{1}{45} & 0 & \frac{\sqrt{2}}{15\sqrt{7}} \\ -\frac{\sqrt{2}}{27\sqrt{35}} & 0 & \frac{29}{189} & -\frac{5\sqrt{10}}{189} \\ \frac{2}{27\sqrt{7}} & \frac{\sqrt{2}}{15\sqrt{7}} & \frac{5\sqrt{10}}{189} & -\frac{28}{135} \end{pmatrix}$$

$$\mathcal{O}_{21}[2]=\begin{pmatrix} 0 & 0 & -\frac{\sqrt{7}}{54\sqrt{10}} & \frac{\sqrt{7}}{54} \\ 0 & -\frac{7}{180} & 0 & -\frac{1}{15\sqrt{14}} \\ -\frac{\sqrt{7}}{54\sqrt{10}} & 0 & -\frac{1}{252} & \frac{2\sqrt{10}}{189} \\ -\frac{\sqrt{7}}{54} & -\frac{1}{15\sqrt{14}} & -\frac{2\sqrt{10}}{189} & \frac{1}{135} \end{pmatrix}$$

$$\mathcal{O}'_{21}[2]=\begin{pmatrix} 0 & 0 & -\frac{\sqrt{7}}{54} & -\frac{\sqrt{7}}{54} \\ 0 & -\frac{7}{180} & 0 & -\frac{1}{15\sqrt{14}} \\ -\frac{\sqrt{7}}{54\sqrt{10}} & 0 & -\frac{1}{252} & -\frac{2\sqrt{10}}{189} \\ \frac{\sqrt{7}}{54} & -\frac{1}{15\sqrt{14}} & \frac{2\sqrt{10}}{189} & \frac{1}{135} \end{pmatrix}$$

$$\mathcal{O}_{14}^{(\prime)}[3]=\mathrm{diag}(1,1,1,1)$$
$$\mathcal{O}_{15}^{(\prime)}[3]=\mathrm{diag}(-1,\tfrac{3}{2},\tfrac{1}{2},-1)$$
$$\mathcal{O}_{17}^{(\prime)}[3]=\mathrm{diag}(1,\tfrac{1}{6},\tfrac{1}{2},1)$$
$$\mathcal{O}_{19}^{(\prime)}[3]=\mathrm{diag}(-\tfrac{1}{27},\tfrac{1}{18},\tfrac{5}{54},-\tfrac{1}{27})$$

$$\mathcal{O}_{16}[3]=\begin{pmatrix} 0 & \frac{3}{5\sqrt{2}} & -\frac{1}{\sqrt{5}} & -\frac{4\sqrt{3}}{5} \\ \frac{3}{5\sqrt{2}} & -\frac{3}{35} & -\frac{6\sqrt{2}}{7\sqrt{5}} & -\frac{6\sqrt{6}}{35} \\ -\frac{1}{\sqrt{5}} & -\frac{6\sqrt{2}}{7\sqrt{5}} & -\frac{4}{7} & \frac{\sqrt{3}}{7\sqrt{5}} \\ -\frac{4\sqrt{3}}{5} & -\frac{6\sqrt{6}}{35} & \frac{\sqrt{3}}{7\sqrt{5}} & -\frac{22}{35} \end{pmatrix}$$

$$\mathcal{O}'_{16}[3]=\begin{pmatrix} 0 & \frac{3}{5\sqrt{2}} & \frac{1}{\sqrt{5}} & -\frac{4\sqrt{3}}{5} \\ \frac{3}{5\sqrt{2}} & -\frac{3}{35} & \frac{6\sqrt{2}}{7\sqrt{5}} & -\frac{6\sqrt{6}}{35} \\ \frac{1}{\sqrt{5}} & \frac{6\sqrt{2}}{7\sqrt{5}} & -\frac{4}{7} & -\frac{\sqrt{3}}{7\sqrt{5}} \\ -\frac{4\sqrt{3}}{5} & -\frac{6\sqrt{6}}{35} & -\frac{\sqrt{3}}{7\sqrt{5}} & -\frac{22}{35} \end{pmatrix}$$

$$\mathcal{O}_{18}[3]=\begin{pmatrix} 0 & -\frac{1}{5\sqrt{2}} & -\frac{1}{\sqrt{5}} & -\frac{2\sqrt{3}}{5} \\ -\frac{1}{5\sqrt{2}} & \frac{23}{105} & \frac{4\sqrt{2}}{7\sqrt{5}} & \frac{2\sqrt{6}}{35} \\ \frac{1}{\sqrt{5}} & -\frac{4\sqrt{2}}{7\sqrt{5}} & -\frac{4}{7} & -\frac{\sqrt{3}}{7\sqrt{5}} \\ -\frac{2\sqrt{3}}{5} & \frac{2\sqrt{6}}{35} & \frac{\sqrt{3}}{7\sqrt{5}} & -\frac{11}{35} \end{pmatrix}$$

$$\mathcal{O}'_{18}[3]=\begin{pmatrix} 0 & -\frac{1}{5\sqrt{2}} & \frac{1}{\sqrt{5}} & -\frac{2\sqrt{3}}{5} \\ -\frac{1}{5\sqrt{2}} & \frac{23}{105} & -\frac{4\sqrt{2}}{7\sqrt{5}} & \frac{2\sqrt{6}}{35} \\ -\frac{1}{\sqrt{5}} & \frac{4\sqrt{2}}{7\sqrt{5}} & -\frac{4}{7} & \frac{\sqrt{3}}{7\sqrt{5}} \\ -\frac{2\sqrt{3}}{5} & \frac{2\sqrt{6}}{35} & -\frac{\sqrt{3}}{7\sqrt{5}} & -\frac{11}{35} \end{pmatrix}$$

$$\mathcal{O}_{20}[3]=\begin{pmatrix} -\frac{4}{135} & \frac{\sqrt{2}}{105} & \frac{2\sqrt{5}}{189} & -\frac{4}{315\sqrt{3}} \\ \frac{\sqrt{2}}{105} & \frac{16}{315} & 0 & -\frac{\sqrt{2}}{35\sqrt{3}} \\ -\frac{2\sqrt{5}}{189} & 0 & \frac{1}{21} & -\frac{\sqrt{5}}{63\sqrt{3}} \\ -\frac{4}{315\sqrt{3}} & -\frac{\sqrt{2}}{35\sqrt{3}} & \frac{\sqrt{5}}{63\sqrt{3}} & \frac{82}{945} \end{pmatrix}$$

$$\mathcal{O}'_{20}[3]=\begin{pmatrix} -\frac{4}{135} & \frac{\sqrt{2}}{105} & -\frac{2\sqrt{5}}{189} & -\frac{4}{315\sqrt{3}} \\ \frac{\sqrt{2}}{105} & \frac{16}{315} & 0 & -\frac{\sqrt{2}}{35\sqrt{3}} \\ \frac{2\sqrt{5}}{189} & 0 & \frac{1}{21} & \frac{\sqrt{5}}{63\sqrt{3}} \\ -\frac{4}{315\sqrt{3}} & -\frac{\sqrt{2}}{35\sqrt{3}} & -\frac{\sqrt{5}}{63\sqrt{3}} & \frac{82}{945} \end{pmatrix}$$

$$\mathcal{O}_{21}[3]=\begin{pmatrix} 0 & \frac{1}{30\sqrt{2}} & \frac{\sqrt{5}}{54} & -\frac{1}{45\sqrt{3}} \\ \frac{1}{30\sqrt{2}} & \frac{1}{90} & 0 & -\frac{\sqrt{2}}{35\sqrt{3}} \\ -\frac{\sqrt{5}}{54} & 0 & -\frac{2}{189} & \frac{\sqrt{5}}{126\sqrt{3}} \\ -\frac{1}{45\sqrt{3}} & -\frac{\sqrt{2}}{35\sqrt{3}} & -\frac{\sqrt{5}}{126\sqrt{3}} & -\frac{11}{1890} \end{pmatrix}$$

$$\mathcal{O}'_{21}[3]=\begin{pmatrix} 0 & \frac{1}{30\sqrt{2}} & -\frac{\sqrt{5}}{54} & -\frac{1}{45\sqrt{3}} \\ \frac{1}{30\sqrt{2}} & \frac{1}{90} & 0 & -\frac{\sqrt{2}}{35\sqrt{3}} \\ \frac{\sqrt{5}}{54} & 0 & -\frac{2}{189} & -\frac{\sqrt{5}}{126\sqrt{3}} \\ -\frac{1}{45\sqrt{3}} & -\frac{\sqrt{2}}{35\sqrt{3}} & \frac{\sqrt{5}}{126\sqrt{3}} & -\frac{11}{1890} \end{pmatrix}$$

(4) The $D\bar{D}_1$ system:

$$\mathcal{V}_D = g_\sigma g''_\sigma \mathcal{O}_1 Y_\sigma + \frac{1}{2}\beta\beta'' g_V^2 \mathcal{O}_1 \mathcal{G}(I) Y_V,$$
$$\mathcal{V}_C = \frac{2h'^2_\sigma}{9f_\pi^2}(\mathcal{O}_2\mathcal{Z}+\mathcal{O}_3\mathcal{T})Y_{\sigma 1} + \frac{\zeta_1^2 g_V^2}{3}\mathcal{O}_2\mathcal{G}(I)Y_{V1}. \tag{A10}$$

(5) The $D\bar{D}_2^*$ system:

$$\mathcal{V}_D = g_\sigma g''_\sigma \mathcal{O}_7 Y_\sigma + \frac{1}{2}\beta\beta'' g_V^2 \mathcal{O}_7 \mathcal{G}(I) Y_V,$$
$$\mathcal{V}_C = \frac{h'^2}{f_\pi^2}[\mathcal{O}_8\mathcal{Z}\mathcal{Z}+\mathcal{O}_9\mathcal{T}\mathcal{T}+\mathcal{O}_{10}\{\mathcal{T},\mathcal{Z}\}]\mathcal{H}(I)Y_{P2}. \tag{A11}$$

(6) The $D^*\bar{D}_1$ system:

$$\begin{aligned}\mathcal{V}_D &= g_\sigma g''_\sigma \mathcal{O}_4 Y_\sigma + \frac{5gk}{18f_\pi^2}(\mathcal{O}_5\mathcal{Z}+\mathcal{O}_6\mathcal{T})\mathcal{H}(I)Y_P \\ &\quad + \frac{1}{2}\beta\beta'' g_V^2 \mathcal{O}_4 \mathcal{G}(I) Y_V \\ &\quad - \frac{5}{9}\lambda\lambda'' g_V^2 (2\mathcal{O}_5\mathcal{Z}-\mathcal{O}_6\mathcal{T})\mathcal{G}(I)Y_V, \\ \mathcal{V}_C &= \frac{h'^2_\sigma}{18\pi_\pi^2}(\mathcal{O}_5\mathcal{Z}+\mathcal{O}_6\mathcal{T})Y_{\sigma 3} + \frac{\zeta_1^2 g_V^2}{12}\mathcal{O}_5\mathcal{G}(I)Y_{V3} \\ &\quad + \frac{h'^2}{6f_\pi^2}[\mathcal{O}_{11}\mathcal{Z}\mathcal{Z}+\mathcal{O}_{12}\mathcal{T}\mathcal{T} \\ &\quad + \mathcal{O}_{13}\{\mathcal{T},\mathcal{Z}\}]\mathcal{H}(I)Y_{P3}.\end{aligned} \tag{A12}$$

(7) The $D^*\bar{D}_2^*$ system:

$$\begin{aligned}\mathcal{V}_D=&g_\sigma g_\sigma''\frac{\mathcal{O}_{14}+\mathcal{O}'_{14}}{2}Y_\sigma+\frac{1}{2}\beta\beta''g_V^2\frac{\mathcal{O}_{14}+\mathcal{O}'_{14}}{2}\mathcal{G}(I)Y_V\\&+\frac{gk}{3f_\pi^2}\left(\frac{\mathcal{O}_{15}+\mathcal{O}'_{15}}{2}\mathcal{Z}+\frac{\mathcal{O}_{16}+\mathcal{O}'_{16}}{2}\mathcal{T}\right)\mathcal{H}(I)Y_P\\&-\frac{2}{3}\lambda\lambda''g_V^2\left(2\frac{\mathcal{O}_{15}+\mathcal{O}'_{15}}{2}\mathcal{Z}-\frac{\mathcal{O}_{16}+\mathcal{O}'_{16}}{2}\mathcal{T}\right)\\&\times\mathcal{G}(I)Y_V,\\\mathcal{V}_C=&\frac{h_\sigma'^2}{3f_\pi^2}\left(\frac{\mathcal{O}_{17}+\mathcal{O}'_{17}}{2}\mathcal{Z}+\frac{\mathcal{O}_{18}+\mathcal{O}'_{18}}{2}\mathcal{T}\right)Y_{\sigma4}\\&+\frac{h'^2}{f_\pi^2}\left[\frac{\mathcal{O}_{19}+\mathcal{O}'_{19}}{2}\mathcal{Z}\mathcal{Z}+\frac{\mathcal{O}_{20}+\mathcal{O}'_{20}}{2}\mathcal{T}\mathcal{T}\right.\\&\left.+\frac{\mathcal{O}_{21}+\mathcal{O}'_{21}}{2}\{\mathcal{T},\mathcal{Z}\}\right]\mathcal{H}(I)Y_{P4}\\&+\frac{\zeta_1^2g_V^2}{2}\frac{\mathcal{O}_{17}+\mathcal{O}'_{17}}{2}\mathcal{G}(I)Y_{V4}.\end{aligned}\tag{A13}$$

In the above expressions, the operators are defined as $\mathcal{Z}=\frac{1}{r^2}\frac{\partial}{\partial r}r^2\frac{\partial}{\partial r}$, $\mathcal{T}=r\frac{\partial}{\partial r}\frac{1}{r}\frac{\partial}{\partial r}$, and $\{\mathcal{T},\mathcal{Z}\}=\mathcal{T}\mathcal{Z}+\mathcal{Z}\mathcal{T}$. Additionally, the variables q_i are written as $q_0=m_{D^*}-m_D$, $q_1=m_{D_1}-m_D$, $q_2=m_{D_2^*}-m_D$, $q_3=m_{D_1}-m_{D^*}$, and $q_4=m_{D_2^*}-m_{D^*}$.

2. Hidden-charm tetraquark systems with hidden-strange quantum number

For these discussed hidden-charm tetraquark systems with hidden-strange quantum number, we consider the effective potentials from the η and ϕ exchanges [67]. In the following, we collect the expressions of the effective potentials for these discussed systems.

(i) The $D_s\bar{D}_s$ system:

$$\mathcal{V}=-\frac{1}{2}\beta^2g_V^2Y_\phi.\tag{A14}$$

(ii) The $D_s\bar{D}_s^*$ system:

$$\begin{aligned}\mathcal{V}_D=&-\frac{1}{2}\beta^2g_V^2\mathcal{O}_1Y_\phi,\\\mathcal{V}_C=&-\frac{2g^2}{9f_\pi^2}(\mathcal{O}_2\mathcal{Z}+\mathcal{O}_3\mathcal{T})Y_{\eta5}\\&+\frac{2}{3}\lambda^2g_V^2(2\mathcal{O}_2\mathcal{Z}-\mathcal{O}_3\mathcal{T})Y_{\phi5}.\end{aligned}\tag{A15}$$

(iii) The $D_s^*\bar{D}_s^*$ system:

$$\begin{aligned}\mathcal{V}=&\frac{2g^2}{9f_\pi^2}(\mathcal{O}_5\mathcal{Z}+\mathcal{O}_6\mathcal{T})Y_\eta-\frac{1}{2}\beta^2g_V^2\mathcal{O}_4Y_\phi\\&+\frac{2}{3}\lambda^2g_V^2(2\mathcal{O}_5\mathcal{Z}-\mathcal{O}_6\mathcal{T})Y_\phi.\end{aligned}\tag{A16}$$

(iv) The $D_s\bar{D}_{s0}^*$ system:

$$\begin{aligned}\mathcal{V}_D=&\frac{1}{2}\beta\beta'g_V^2Y_\phi,\\\mathcal{V}_C=&-\frac{2h^2q_6^2}{3f_\pi^2}Y_{\eta6}.\end{aligned}\tag{A17}$$

(v) The $D_s\bar{D}'_{s1}$ system:

$$\begin{aligned}\mathcal{V}_D=&\frac{1}{2}\beta\beta'g_V^2\mathcal{O}_1Y_\phi,\\\mathcal{V}_C=&\frac{1}{2}(\zeta^2g_V^2-4\mu^2g_V^2q_7^2)\mathcal{O}_2Y_{\phi7}\\&-\frac{2}{3}\mu^2g_V^2(\mathcal{O}_2\mathcal{Z}+\mathcal{O}_3\mathcal{T})Y_{\phi7}.\end{aligned}\tag{A18}$$

(vi) The $D_s^*\bar{D}_{s0}^*$ system:

$$\begin{aligned}\mathcal{V}_D=&\frac{1}{2}\beta\beta'g_V^2\mathcal{O}_1Y_\phi,\\\mathcal{V}_C=&-\frac{1}{2}(\zeta^2g_V^2-4\mu^2g_V^2q_8^2)\mathcal{O}_2Y_{\phi8}\\&+\frac{2}{3}\mu^2g_V^2(\mathcal{O}_2\mathcal{Z}+\mathcal{O}_3\mathcal{T})Y_{\phi8}.\end{aligned}\tag{A19}$$

(vii) The $D_s^*\bar{D}'_{s1}$ system:

$$\begin{aligned}\mathcal{V}_D=&\frac{2g\tilde{k}}{9f_\pi^2}(\mathcal{O}_5\mathcal{Z}+\mathcal{O}_6\mathcal{T})Y_\eta+\frac{1}{2}\beta\beta'g_V^2\mathcal{O}_4Y_\phi\\&-\frac{2}{3}\lambda\lambda'g_V^2(2\mathcal{O}_5\mathcal{Z}-\mathcal{O}_6\mathcal{T})Y_\phi,\\\mathcal{V}_C=&-\frac{2h^2q_9^2}{3f_\pi^2}\mathcal{O}_4Y_{\eta9}-\frac{1}{2}(\zeta^2g_V^2-4\mu^2g_V^2q_9^2)\mathcal{O}_6Y_{\phi9}\\&+\frac{2}{3}\mu^2g_V^2(\mathcal{O}_5\mathcal{Z}+\mathcal{O}_6\mathcal{T})Y_{\phi9}.\end{aligned}\tag{A20}$$

Here, the variables q_i are defined as $q_5=m_{D_s^*}-m_{D_s}$, $q_6=m_{D_{s0}^*}-m_{D_s}$, $q_7=m_{D'_{s1}}-m_{D_s}$, $q_8=m_{D_{s0}^*}-m_{D_s^*}$, and $q_9=m_{D'_{s1}}-m_{D_s^*}$. When performing the numerical calculations, the operators $\mathcal{O}_k$ will be replaced by the corresponding numerical matrixes, which are summarized in Table XIII.

[1] R. Aaij *et al.* (LHCb Collaboration), Observation of $J/\psi p$ Resonances Consistent with Pentaquark States in $\Lambda_b^0 \to J/\psi K^- p$ Decays, Phys. Rev. Lett. **115**, 072001 (2015).

[2] R. Aaij *et al.* (LHCb Collaboration), Observation of a Narrow Pentaquark State, $P_c(4312)^+$, and of Two-Peak Structure of the $P_c(4450)^+$, Phys. Rev. Lett. **122**, 222001 (2019).

[3] X. Q. Li and X. Liu, A possible global group structure for exotic states, Eur. Phys. J. C **74**, 3198 (2014).

[4] J. J. Wu, R. Molina, E. Oset, and B. S. Zou, Prediction of Narrow N^* and Λ^* Resonances with Hidden Charm Above 4 GeV, Phys. Rev. Lett. **105**, 232001 (2010).

[5] M. Karliner and J. L. Rosner, New Exotic Meson and Baryon Resonances from Doubly-Heavy Hadronic Molecules, Phys. Rev. Lett. **115**, 122001 (2015).

[6] W. L. Wang, F. Huang, Z. Y. Zhang, and B. S. Zou, $\Sigma_c \bar{D}$ and $\Lambda_c \bar{D}$ states in a chiral quark model, Phys. Rev. C **84**, 015203 (2011).

[7] Z. C. Yang, Z. F. Sun, J. He, X. Liu, and S. L. Zhu, The possible hidden-charm molecular baryons composed of anticharmed meson and charmed baryon, Chin. Phys. C **36**, 6 (2012).

[8] J. J. Wu, T. S. H. Lee, and B. S. Zou, Nucleon resonances with hidden charm in coupled-channel models, Phys. Rev. C **85**, 044002 (2012).

[9] R. Chen, X. Liu, X. Q. Li, and S. L. Zhu, Identifying Exotic Hidden-Charm Pentaquarks, Phys. Rev. Lett. **115**, 132002 (2015).

[10] S. K. Choi *et al.* (Belle Collaboration), Observation of a Narrow Charmonium-Like State in Exclusive $B^\pm \to K^\pm \pi^+ \pi^- J/\psi$ Decays, Phys. Rev. Lett. **91**, 262001 (2003).

[11] C. Y. Wong, Molecular states of heavy quark mesons, Phys. Rev. C **69**, 055202 (2004).

[12] E. S. Swanson, Short range structure in the $X(3872)$, Phys. Lett. B **588**, 189 (2004).

[13] M. Suzuki, The $X(3872)$ boson: Molecule or charmonium, Phys. Rev. D **72**, 114013 (2005).

[14] Y. R. Liu, X. Liu, W. Z. Deng, and S. L. Zhu, Is $X(3872)$ really a molecular state?, Eur. Phys. J. C **56**, 63 (2008).

[15] C. E. Thomas and F. E. Close, Is $X(3872)$ a molecule?, Phys. Rev. D **78**, 034007 (2008).

[16] X. Liu, Z. G. Luo, Y. R. Liu, and S. L. Zhu, $X(3872)$ and other possible heavy molecular states, Eur. Phys. J. C **61**, 411 (2009).

[17] I. W. Lee, A. Faessler, T. Gutsche, and V. E. Lyubovitskij, $X(3872)$ as a molecular DD^* state in a potential model, Phys. Rev. D **80**, 094005 (2009).

[18] H. X. Chen, W. Chen, X. Liu, and S. L. Zhu, The hidden-charm pentaquark and tetraquark states, Phys. Rep. **639**, 1 (2016).

[19] X. Liu, An overview of XYZ new particles, Chin. Sci. Bull. **59**, 3815 (2014).

[20] A. Hosaka, T. Iijima, K. Miyabayashi, Y. Sakai, and S. Yasui, Exotic hadrons with heavy flavors: X, Y, Z, and related states, Prog. Theor. Exp. Phys. **2016**, 062C01 (2016).

[21] Y. R. Liu, H. X. Chen, W. Chen, X. Liu, and S. L. Zhu, Pentaquark and tetraquark states, Prog. Part. Nucl. Phys. **107**, 237 (2019).

[22] N. Brambilla, S. Eidelman, C. Hanhart, A. Nefediev, C. P. Shen, C. E. Thomas, A. Vairo, and C. Z. Yuan, The XYZ states: Experimental and theoretical status and perspectives, Phys. Rep. **873**, 1 (2020).

[23] S. L. Olsen, T. Skwarnicki, and D. Zieminska, Nonstandard heavy mesons and baryons: Experimental evidence, Rev. Mod. Phys. **90**, 015003 (2018).

[24] F. K. Guo, C. Hanhart, U. G. Meißner, Q. Wang, Q. Zhao, and B. S. Zou, Hadronic molecules, Rev. Mod. Phys. **90**, 015004 (2018).

[25] K. Abe *et al.* (Belle Collaboration), Observation of a Near-Threshold $\omega J/\psi$ Mass Enhancement in Exclusive $B \to K\omega J/\psi$ Decays, Phys. Rev. Lett. **94**, 182002 (2005).

[26] T. Aaltonen *et al.* (CDF Collaboration), Evidence for a Narrow Near-Threshold Structure in the $J/\psi\phi$ Mass Spectrum in $B^+ \to J/\psi\phi K^+$ Decays, Phys. Rev. Lett. **102**, 242002 (2009).

[27] X. Liu and S. L. Zhu, $Y(4143)$ is probably a molecular partner of $Y(3930)$, Phys. Rev. D **80**, 017502 (2009).

[28] R. Aaij *et al.* (LHCb Collaboration), Observation of $J/\psi\phi$ Structures Consistent with Exotic States from Amplitude Analysis of $B^+ \to J/\psi\phi K^+$ Decays, Phys. Rev. Lett. **118**, 022003 (2017).

[29] R. Aaij *et al.* (LHCb Collaboration), Amplitude analysis of $B^+ \to J/\psi\phi K^+$ decays, Phys. Rev. D **95**, 012002 (2017).

[30] S. K. Choi *et al.* (Belle Collaboration), Observation of a Resonancelike Structure in the $\pi^\pm \psi'$ Mass Distribution in Exclusive $B \to K\pi^\pm \psi'$ Decays, Phys. Rev. Lett. **100**, 142001 (2008).

[31] X. Liu, Y. R. Liu, W. Z. Deng, and S. L. Zhu, Is $Z^+(4430)$ a loosely bound molecular state?, Phys. Rev. D **77**, 034003 (2008).

[32] X. Liu, Y. R. Liu, W. Z. Deng, and S. L. Zhu, $Z^+(4430)$ as a $D_1' D^* (D_1 D^*)$ molecular state, Phys. Rev. D **77**, 094015 (2008).

[33] K. Chilikin *et al.* (Belle Collaboration), Experimental constraints on the spin and parity of the $Z(4430)^+$, Phys. Rev. D **88**, 074026 (2013).

[34] R. Aaij *et al.* (LHCb Collaboration), Observation of the Resonant Character of the $Z(4430)^-$ State, Phys. Rev. Lett. **112**, 222002 (2014).

[35] E. Kou *et al.* (BelleII Collaboration), The Belle II physics book, Prog. Theor. Exp. Phys. **2019**, 123C01 (2019); **2020**, 029201(E) (2020).

[36] R. Aaij *et al.* (LHCb Collaboration), Physics case for an LHCb Upgrade II—Opportunities in flavour physics, and beyond, in the HL-LHC era, arXiv:1808.08865.

[37] M. B. Wise, Chiral perturbation theory for hadrons containing a heavy quark, Phys. Rev. D **45**, R2188 (1992).

[38] P. A. Zyla *et al.* (Particle Data Group), Review of particle physics, Prog. Theor. Exp. Phys. **2020**, 083C01 (2020).

[39] C. Hanhart, Y. S. Kalashnikova, and A. V. Nefediev, Lineshapes for composite particles with unstable constituents, Phys. Rev. D **81**, 094028 (2010).

[40] A. A. Filin, A. Romanov, V. Baru, C. Hanhart, Y. S. Kalashnikova, A. E. Kudryavtsev, U.-G. Meissner, and A. V. Nefediev, Comment on "Possibility of Deeply Bound Hadronic Molecules from Single Pion Exchange", Phys. Rev. Lett. **105**, 019101 (2010).

[41] B. Aubert *et al.* (*BABAR* Collaboration), Observation of Y (3940) $\to J/\psi\omega$ in $B \to J/\psi\omega K$ at *BABAR*, Phys. Rev. Lett. **101**, 082001 (2008).

[42] P. del Amo Sanchez *et al.* (*BABAR* Collaboration), Evidence for the decay $X(3872) \to J/\psi\omega$, Phys. Rev. D **82**, 011101 (2010).

[43] B. Aubert *et al.* (*BABAR* Collaboration), Observation of the Decay $B \to J/\psi\eta K$ and Search for $X(3872) \to J/\psi\eta$, Phys. Rev. Lett. **93**, 041801 (2004).

[44] S. Chatrchyan *et al.* (CMS Collaboration), Observation of a peaking structure in the $J/\psi\phi$ mass spectrum from $B^{\pm} \to J/\psi\phi K^{\pm}$ decays, Phys. Lett. B **734**, 261 (2014).

[45] R. Aaij *et al.* (LHCb Collaboration), Search for the $X(4140)$ state in $B^+ \to J/\psi\phi K^+$ decays, Phys. Rev. D **85**, 091103 (2012).

[46] V. M. Abazov *et al.* (D0 Collaboration), Search for the $X(4140)$ state in $B^+ \to J/\psi\phi K^+$ decays with the D0 Detector, Phys. Rev. D **89**, 012004 (2014).

[47] J. P. Lees *et al.* (*BABAR* Collaboration), Study of $B^{\pm,0} \to J/\psi K^+K^-K^{\pm,0}$ and search for $B^0 \to J/\psi\phi$ at *BABAR*, Phys. Rev. D **91**, 012003 (2015).

[48] T. Aaltonen *et al.* (CDF Collaboration), Observation of the $Y(4140)$ structure in the $J/\psi\phi$ mass spectrum in $B^{\pm} \to J/\psi\phi K^{\pm}$ decays, Mod. Phys. Lett. A **32**, 1750139 (2017).

[49] R. Aaij *et al.* (LHCb Collaboration), Observation of New Resonances Decaying to $J/\psi K^+$ and $J/\psi\phi$, Phys. Rev. Lett. **127**, 082001 (2021).

[50] R. Aaij *et al.* (LHCb Collaboration), Evidence for an $\eta_c(1S)\pi^-$ resonance in $B^0 \to \eta_c(1S)K^+\pi^-$ decays, Eur. Phys. J. C **78**, 1019 (2018).

[51] K. Chilikin *et al.* (Belle Collaboration), Observation of a new charged charmoniumlike state in $\bar{B}^0 \to J/\psi K^-\pi^+$ decays, Phys. Rev. D **90**, 112009 (2014).

[52] V. M. Abazov *et al.* (D0 Collaboration), Evidence for $Z_c^{\pm}(3900)$ in semi-inclusive decays of b-flavored hadrons, Phys. Rev. D **98**, 052010 (2018).

[53] R. Aaij *et al.* (LHCb Collaboration), Model-Independent Observation of Exotic Contributions to $B^0 \to J/\psi K^+\pi^-$ Decays, Phys. Rev. Lett. **122**, 152002 (2019).

[54] R. Mizuk *et al.* (Belle Collaboration), Dalitz analysis of $B \to K\pi^+\psi'$ decays and the $Z(4430)^+$, Phys. Rev. D **80**, 031104 (2009).

[55] R. Mizuk *et al.* (Belle Collaboration), Observation of two resonance-like structures in the $\pi^+\chi_{c1}$ mass distribution in exclusive $\bar{B}^0 \to K^-\pi^+\chi_{c1}$ decays, Phys. Rev. D **78**, 072004 (2008).

[56] J. P. Lees *et al.* (*BABAR* Collaboration), Search for the $Z_1(4050)^+$ and $Z_2(4250)^+$ states in $\bar{B}^0 \to \chi_{c1}K^-\pi^+$ and $B^+ \to \chi_{c1}K_S^0\pi^+$, Phys. Rev. D **85**, 052003 (2012).

[57] V. Bhardwaj *et al.* (Belle Collaboration), Inclusive and exclusive measurements of B decays to χ_{c1} and χ_{c2} at Belle, Phys. Rev. D **93**, 052016 (2016).

[58] V. Bhardwaj *et al.* (Belle Collaboration), Search for $X(3872)$ and $X(3915)$ decay into $\chi_{c1}\pi^0$ in B decays at Belle, Phys. Rev. D **99**, 111101 (2019).

[59] F. Close and C. Downum, On the Possibility of Deeply Bound Hadronic Molecules from Single Pion Exchange, Phys. Rev. Lett. **102**, 242003 (2009).

[60] M. Ablikim *et al.* (BESIII Collaboration), Observation of a Charged Charmoniumlike Structure in $e^+e^- \to \pi^+\pi^- J/\psi$ at $\sqrt{s} = 4.26$ GeV, Phys. Rev. Lett. **110**, 252001 (2013).

[61] Z. Q. Liu *et al.* (Belle Collaboration), Study of $e^+e^- \to \pi^+\pi^- J/\psi$ and Observation of a Charged Charmoniumlike State at Belle, Phys. Rev. Lett. **110**, 252002 (2013); **111**, 019901(E) (2013).

[62] H. Yukawa, On the interaction of elementary particles I, Proc. Phys. Math. Soc. Jap. **17**, 48 (1935).

[63] F. L. Wang, X. D. Yang, R. Chen, and X. Liu, Hidden-charm pentaquarks with triple strangeness due to the $\Omega_c^{(*)}\bar{D}_s^{(*)}$ interactions, Phys. Rev. D **103**, 054025 (2021).

[64] X. D. Yang, F. L. Wang, Z. W. Liu, and X. Liu, Newly observed $X(4630)$: A new charmonium-like molecule, Eur. Phys. J. C **81**, 807 (2021).

[65] F. L. Wang, R. Chen, Z. W. Liu, and X. Liu, Probing new types of P_c states inspired by the interaction between $S-$wave charmed baryon and anti-charmed meson in a $\bar{T}$ doublet, Phys. Rev. C **101**, 025201 (2020).

[66] F. L. Wang, R. Chen, Z. W. Liu, and X. Liu, Possible triple-charm molecular pentaquarks from $\Xi_{cc}D_1/\Xi_{cc}D_2^*$ interactions, Phys. Rev. D **99**, 054021 (2019).

[67] F. L. Wang and X. Liu, Exotic double-charm molecular states with hidden or open strangeness and around 4.5–4.7 GeV, Phys. Rev. D **102**, 094006 (2020).

[68] F. L. Wang, R. Chen, and X. Liu, Prediction of hidden-charm pentaquarks with double strangeness, Phys. Rev. D **103**, 034014 (2021).

[69] R. Chen, F. L. Wang, A. Hosaka, and X. Liu, Exotic triple-charm deuteronlike hexaquarks, Phys. Rev. D **97**, 114011 (2018).

[70] G. Breit, The effect of retardation on the interaction of two electrons, Phys. Rev. **34**, 553 (1929).

[71] G. Breit, The fine structure of HE as a test of the spin interactions of two electrons, Phys. Rev. **36**, 383 (1930).

[72] N. A. Tornqvist, From the deuteron to deusons, an analysis of deuteronlike meson-meson bound states, Z. Phys. C **61**, 525 (1994).

[73] N. A. Tornqvist, On deusons or deuteron-like meson-meson bound states, Nuovo Cimento Soc. Ital. Fis. **107A**, 2471 (1994).

[74] G. J. Ding, Are $Y(4260)$ and Z_2^+ are D_1D or D_0D^* hadronic molecules?, Phys. Rev. D **79**, 014001 (2009).

[75] R. Casalbuoni, A. Deandrea, N. Di Bartolomeo, R. Gatto, F. Feruglio, and G. Nardulli, Light vector resonances in the effective chiral Lagrangian for heavy mesons, Phys. Lett. B **292**, 371 (1992).

[76] R. Casalbuoni, A. Deandrea, N. Di Bartolomeo, R. Gatto, F. Feruglio, and G. Nardulli, Phenomenology of heavy meson chiral Lagrangians, Phys. Rep. **281**, 145 (1997).

[77] T. M. Yan, H. Y. Cheng, C. Y. Cheung, G. L. Lin, Y. C. Lin, and H. L. Yu, Heavy quark symmetry and chiral dynamics, Phys. Rev. D **46**, 1148 (1992); **55**, 5851(E) (1997).

[78] M. Bando, T. Kugo, and K. Yamawaki, Nonlinear realization and hidden local symmetries, Phys. Rep. **164**, 217 (1988).

[79] M. Harada and K. Yamawaki, Hidden local symmetry at loop: A new perspective of composite gauge boson and chiral phase transition, Phys. Rep. **381**, 1 (2003).

[80] B. Hu, X. L. Chen, Z. G. Luo, P. Z. Huang, S. L. Zhu, P. F. Yu, and X. Liu, Possible heavy molecular states composed of a pair of excited charm-strange mesons, Chin. Phys. C **35**, 113 (2011).

[81] L. L. Shen, X. L. Chen, Z. G. Luo, P. Z. Huang, S. L. Zhu, P. F. Yu, and X. Liu, The molecular systems composed of the charmed mesons in the $H\bar{S}$ + H.c. doublet, Eur. Phys. J. C **70**, 183 (2010).

[82] H. Y. Cheng and K. C. Yang, Charmless hadronic B decays into a tensor meson, Phys. Rev. D **83**, 034001 (2011).

[83] Y. R. Liu, Heavy quark spin selection rules in meson-antimeson states, Phys. Rev. D **88**, 074008 (2013).

[84] Z. F. Sun, X. Liu, M. Nielsen, and S. L. Zhu, Hadronic molecules with both open charm and bottom, Phys. Rev. D **85**, 094008 (2012).

[85] M. T. Li, W. L. Wang, Y. B. Dong, and Z. Y. Zhang, A study of one $S-$ and one P-wave heavy meson interaction in a chiral quark model, Commun. Theor. Phys. **63**, 63 (2015).

[86] M. T. Li, W. L. Wang, Y. B. Dong, and Z. Y. Zhang, A study of P-wave heavy meson interactions in a chiral quark model, arXiv:1303.4140.

[87] X. K. Dong, F. K. Guo, and B. S. Zou, A survey of heavy-antiheavy hadronic molecules, Prog. Phys. **41**, 65 (2021).

[88] R. Chen, X. Liu, Y. R. Liu, and S. L. Zhu, Predictions of the hidden-charm molecular states with four-quark component, Eur. Phys. J. C **76**, 319 (2016).

[89] A. F. Falk and M. E. Luke, Strong decays of excited heavy mesons in chiral perturbation theory, Phys. Lett. B **292**, 119 (1992).

[90] C. Isola, M. Ladisa, G. Nardulli, and P. Santorelli, Charming penguins in $B \to K^*\pi, K(\rho, \omega, \phi)$ decays, Phys. Rev. D **68**, 114001 (2003).

[91] M. Cleven and Q. Zhao, Cross section line shape of $e^+e^- \to \chi_{c0}\omega$ around the $Y(4260)$ mass region, Phys. Lett. B **768**, 52 (2017).

[92] J. He, Y. Liu, J. T. Zhu, and D. Y. Chen, $Y(4626)$ as a molecular state from interaction $D_s^*\bar{D}_{s1}(2536) - D_s\bar{D}_{s1}(2536)$, Eur. Phys. J. C **80**, 246 (2020).

[93] Z. Y. Wang, J. J. Qi, J. Xu, and X. H. Guo, Studying the D_1D molecule in the Bethe-Salpeter equation approach, Phys. Rev. D **102**, 036008 (2020).

[94] D. O. Riska and G. E. Brown, Nucleon resonance transition couplings to vector mesons, Nucl. Phys. **A679**, 577 (2001).

[95] W. A. Bardeen, E. J. Eichten, and C. T. Hill, Chiral multiplets of heavy—light mesons, Phys. Rev. D **68**, 054024 (2003).

[96] H. Y. Cheng, C. K. Chua, and A. Soni, Final state interactions in hadronic B decays, Phys. Rev. D **71**, 014030 (2005).

[97] X. Liu, Z. G. Luo, and S. L. Zhu, Novel charmonium-like structures in the $J/\psi\phi$ and $J/\psi\omega$ invariant mass spectra, Phys. Lett. B **699**, 341 (2011); **707**, 577(E) (2012).

[98] J. He and P. L. Lü, Understanding $Y(4274)$ and $X(4320)$ in the $J/\psi\phi$ invariant mass spectrum, Nucl. Phys. **A919**, 1 (2013).

[99] J. He, Understanding spin parity of $P_c(4450)$ and $Y(4274)$ in a hadronic molecular state picture, Phys. Rev. D **95**, 074004 (2017).

[100] J. He, D. Y. Chen, and X. Liu, New structure around 3250 MeV in the baryonic B decay and the $D_0^*(2400)N$ molecular hadron, Eur. Phys. J. C **72**, 2121 (2012).

[101] X. K. Dong, Y. H. Lin, and B. S. Zou, Prediction of an exotic state around 4240 MeV with $J^{PC} = 1^{-+}$ as C-parity partner of $Y(4260)$ in molecular picture, Phys. Rev. D **101**, 076003 (2020).

[102] R. Chen, A. Hosaka, and X. Liu, Searching for possible Ω_c-like molecular states from meson-baryon interaction, Phys. Rev. D **97**, 036016 (2018).

[103] L. Zhao, L. Ma, and S. L. Zhu, The recoil correction and spin-orbit force for the possible $B^*\bar{B}^*$ and $D^*\bar{D}^*$ states, Nucl. Phys. **A942**, 18 (2015).

[104] Y. R. Liu and Z. Y. Zhang, The bound state problem of S-wave heavy quark meson-aitimeson systems, Phys. Rev. C **80**, 015208 (2009).

[105] Y. Liu and I. Zahed, Heavy exotic molecules with charm and bottom, Phys. Lett. B **762**, 362 (2016).

[106] L. R. Dai, G. Y. Wang, X. Chen, E. Wang, E. Oset, and D. M. Li, The $B^+ \to J/\psi\omega K^+$ reaction and $D^*\bar{D}^*$ molecular states, Eur. Phys. J. A **55**, 36 (2019).

[107] Z. F. Sun, J. He, X. Liu, Z. G. Luo, and S. L. Zhu, $Z_b(10610)^{\pm}$ and $Z_b(10650)^{\pm}$ as the $B^*\bar{B}$ and $B^*\bar{B}^*$ molecular states, Phys. Rev. D **84**, 054002 (2011).

[108] M. Z. Liu, D. J. Jia, and D. Y. Chen, Possible hadronic molecular states composed of $S-$wave heavy-light mesons, Chin. Phys. C **41**, 053105 (2017).

[109] Z. F. Sun, Z. G. Luo, J. He, X. Liu, and S. L. Zhu, A note on the $B^*\bar{B}$, $B^*\bar{B}^*$, $D^*\bar{D}$, $D^*\bar{D}^*$, molecular states, Chin. Phys. C **36**, 194 (2012).

[110] Z. M. Ding, H. Y. Jiang, and J. He, Molecular states from $D^{(*)}\bar{D}^{(*)}/B^{(*)}\bar{B}^{(*)}$ and $D^{(*)}D^{(*)}/\bar{B}^{(*)}\bar{B}^{(*)}$ interactions, Eur. Phys. J. C **80**, 1179 (2020).

[111] Y. C. Yang, Z. Y. Tan, J. Ping, and H. S. Zong, Possible $D^{(*)}\bar{D}^{(*)}$ and $B^{(*)}\bar{B}^{(*)}$ molecular states in the extended constituent quark models, Eur. Phys. J. C **77**, 575 (2017).

[112] Y. J. Zhang, H. C. Chiang, P. N. Shen, and B. S. Zou, Possible S-wave bound-states of two pseudoscalar mesons, Phys. Rev. D **74**, 014013 (2006).

[113] A. De Rujula, H. Georgi, and S. L. Glashow, Molecular Charmonium: A New Spectroscopy?, Phys. Rev. Lett. **38**, 317 (1977).

[114] A. Ozpineci, C. W. Xiao, and E. Oset, Hidden beauty molecules within the local hidden gauge approach and heavy quark spin symmetry, Phys. Rev. D **88**, 034018 (2013).

[115] M. Ablikim *et al.* (BESIII Collaboration), Observation of $e^+e^- \to \eta J/\psi$ at center-of-mass energy $\sqrt{s} = 4.009$ GeV, Phys. Rev. D **86**, 071101 (2012).

[116] T. Iwashita *et al.* (Belle Collaboration), Measurement of branching fractions for $B \to J/\psi\eta K$ decays and search for a narrow resonance in the $J/\psi\eta$ final state, Prog. Theor. Exp. Phys. **2014**, 043C01 (2014).

[117] F. Close, C. Downum, and C. E. Thomas, Novel charmonium and bottomonium spectroscopies due to deeply bound hadronic molecules from single pion exchange, Phys. Rev. D **81**, 074033 (2010).

[118] J. He and D. Y. Chen, Interpretation of $Y(4390)$ as an isoscalar partner of $Z(4430)$ from $D^*(2010)\bar{D}_1(2420)$ interaction, Eur. Phys. J. C **77**, 398 (2017).

[119] W. Zhu, Y. R. Liu, and T. Yao, Is $J^{PC} = 3^{-+}$ molecule possible?, Chin. Phys. C **39**, 023101 (2015).

[120] L. Zhao, L. Ma, and S. L. Zhu, Spin-orbit force, recoil corrections, and possible $B\bar{B}^*$ and $D\bar{D}^*$ molecular states, Phys. Rev. D **89**, 094026 (2014).

[121] N. Li and S. L. Zhu, Isospin breaking, coupled-channel effects and diagnosis of $X(3872)$, Phys. Rev. D **86**, 074022 (2012).

[122] M. B. Voloshin, Interference and binding effects in decays of possible molecular component of $X(3872)$, Phys. Lett. B **579**, 316 (2004).

[123] F. E. Close and P. R. Page, The $D^{*0}\bar{D}^0$ threshold resonance, Phys. Lett. B **578**, 119 (2004).

[124] N. A. Tornqvist, Isospin breaking of the narrow charmonium state of Belle at 3872 MeV as a deuson, Phys. Lett. B **590**, 209 (2004).

[125] J. He, Study of the $B\bar{B}^*/D\bar{D}^*$ bound states in a Bethe-Salpeter approach, Phys. Rev. D **90**, 076008 (2014).

[126] Z. Y. Wang, J. J. Qi, X. H. Guo, and C. Wang, $X(3872)$ as a molecular $D\bar{D}^*$ state in the Bethe-Salpeter equation approach, Phys. Rev. D **97**, 016015 (2018).

[127] B. X. Sun, D. M. Wan, and S. Y. Zhao, The $D\bar{D}^*$ interaction with isospin zero in an extended hidden gauge symmetry approach, Chin. Phys. C **42**, 053105 (2018).

[128] G. J. Ding, J. F. Liu, and M. L. Yan, Dynamics of hadronic molecule in one-boson exchange approach and possible heavy flavor molecules, Phys. Rev. D **79**, 054005 (2009).

[129] R. Chen, A. Hosaka, and X. Liu, Heavy molecules and one-σ/ω-exchange model, Phys. Rev. D **96**, 116012 (2017).

[130] M. Ablikim *et al.* (BESIII Collaboration), Precise Measurement of the $e^+e^- \to \pi^+\pi^- J/\psi$ Cross Section at Center-of-Mass Energies from 3.77 to 4.60 GeV, Phys. Rev. Lett. **118**, 092001 (2017).

[131] B. Aubert *et al.* (*BABAR* Collaboration), Observation of a Broad Structure in the $\pi^+\pi^- J/\psi$ Mass Spectrum Around 4.26-GeV/c^2, Phys. Rev. Lett. **95**, 142001 (2005).

[132] G. J. Ding, Possible molecular states of $D_s^*\bar{D}_s^*$ system and $Y(4140)$, Eur. Phys. J. C **64**, 297-308 (2009).

[133] L. Meng, B. Wang, and S. L. Zhu, Predicting the $\bar{D}_s^{(*)}D_s^{(*)}$ bound states as the partners of $X(3872)$, Sci. Bull. **66**, 1288 (2021).

[134] J. Z. Wang, D. Y. Chen, X. Liu, and T. Matsuki, Constructing J/ψ family with updated data of charmoniumlike Y states, Phys. Rev. D **99**, 114003 (2019).

[135] J. Z. Wang, R. Q. Qian, X. Liu, and T. Matsuki, Are the Y states around 4.6 GeV from e^+e^- annihilation higher charmonia?, Phys. Rev. D **101**, 034001 (2020).

[136] Y. R. Liu and Z. Y. Zhang, A chiral quark model study of $Z^+(4430)$ in the molecular picture, arXiv:0908.1734.

[137] T. Uchino, W. H. Liang, and E. Oset, Baryon states with hidden charm in the extended local hidden gauge approach, Eur. Phys. J. A **52**, 43 (2016).

[138] L. Meng, B. Wang, G. J. Wang, and S. L. Zhu, Implications of the $Z_{cs}(3985)$ and $Z_{cs}(4000)$ as two different states, Sci. Bull. **66**, 2065 (2021).

[139] B. Wang, L. Meng, and S. L. Zhu, Decoding the nature of $Z_{cs}(3985)$ and establishing the spectrum of charged heavy quarkoniumlike states in chiral effective field theory, Phys. Rev. D **103**, L021501 (2021).

[140] L. Meng, B. Wang, and S. L. Zhu, $Z_{cs}(3985)^-$ as the U-spin partner of $Z_c(3900)^-$ and implication of other states in the $\mathrm{SU}(3)_F$ symmetry and heavy quark symmetry, Phys. Rev. D **102**, 111502 (2020).

[141] B. Wang, L. Meng, and S. L. Zhu, Deciphering the charged heavy quarkoniumlike states in chiral effective field theory, Phys. Rev. D **102**, 114019 (2020).

[142] Y. Ikeda, Sinya Aoki, Takumi Doi, Shinya Gongyo, Tetsuo Hatsuda, Takashi Inoue, Takumi Iritani, Noriyoshi Ishii, Keiko Murano, and Kenji Sasaki (HAL QCD Collaboration), Fate of the Tetraquark Candidate $Z_c(3900)$ from Lattice QCD, Phys. Rev. Lett. **117**, 242001 (2016).

[143] W. A. Yamada, O. Morimatsu, T. Sato, and K. Yazaki, Near-threshold spectrum from uniformized Mittag-Leffler expansion -pole structure of $Z(3900)$-, arXiv:2108.11605.

[144] X. K. Dong, F. K. Guo, and B. S. Zou, Explaining the Many Threshold Structures in the Heavy-Quark Hadron Spectrum, Phys. Rev. Lett. **126**, 152001 (2021).

[145] P. G. Ortega, J. Segovia, D. R. Entem, and F. Fernández, The Z_c structures in a coupled-channels model, Eur. Phys. J. C **79**, 78 (2019).

[146] J. He and D. Y. Chen, $Z_c(3900)/Z_c(3885)$ as a virtual state from $\pi J/\psi - \bar{D}^* D$ interaction, Eur. Phys. J. C **78**, 94 (2018).

[147] D. Y. Chen, X. Liu, and T. Matsuki, Reproducing the $Z_c(3900)$ structure through the initial-single-pion-emission mechanism, Phys. Rev. D **88**, 036008 (2013).

[148] J. Z. Wang, D. Y. Chen, X. Liu, and T. Matsuki, Mapping a new cluster of charmonium-like structures at e^+e^- collisions, Phys. Lett. B **817**, 136345 (2021).

[149] J. Z. Wang, D. Y. Chen, X. Liu, and T. Matsuki, Universal non-resonant explanation to charmonium-like structures $Z_c(3885)$ and $Z_c(4025)$, Eur. Phys. J. C **80**, 1040 (2020).

[150] J. Z. Wang, Q. S. Zhou, X. Liu, and T. Matsuki, Toward charged $Z_{cs}(3985)$ structure under a reflection mechanism, Eur. Phys. J. C **81**, 51 (2021).

[151] D. Y. Chen, J. He, and X. Liu, Nonresonant explanation for the $Y(4260)$ structure observed in the $e^+e^- \to J/\psi\pi^+\pi^-$ process, Phys. Rev. D **83**, 054021 (2011).

[152] D. Y. Chen, J. He, and X. Liu, A novel explanation of charmoniumlike structure in $e^+e^- \to \psi(2S)\pi^+\pi^-$, Phys. Rev. D **83**, 074012 (2011).

[153] D. Y. Chen, X. Liu, X. Q. Li, and H. W. Ke, Unified Fano-like interference picture for charmoniumlike states $Y(4008)$, $Y(4260)$ and $Y(4360)$, Phys. Rev. D **93**, 014011 (2016).

[154] D. Y. Chen, X. Liu, and T. Matsuki, Interference effect as resonance killer of newly observed charmonium-like states $Y(4320)$ and $Y(4390)$, Eur. Phys. J. C **78**, 136 (2018).

[155] D. Y. Chen and X. Liu, Predicted charged charmoniumlike structures in the hidden-charm dipion decay of higher charmonia, Phys. Rev. D **84**, 034032 (2011).

[156] D. Y. Chen and X. Liu, $Z_b(10610)$ and $Z_b(10650)$ structures produced by the initial single pion emission in the $\Upsilon(5S)$ decays, Phys. Rev. D **84**, 094003 (2011).

[157] D. Y. Chen, X. Liu, and T. Matsuki, Interpretation of $Z_b(10610)$ and $Z_b(10650)$ in the ISPE mechanism and the charmonium counterpart, Chin. Phys. C **38**, 053102 (2014).

[158] X. Liu, D. Y. Chen, and T. Matsuki, The initial single chiral particle emission mechanism and the predictions of charged charmonium-like structures, Acta Phys. Pol. B Proc. Suppl. **8**, 153 (2015).

[159] D. Y. Chen, X. Liu, and T. Matsuki, Charged charmonium-like structures and the initial single chiral particle emission mechanism, AIP Conf. Proc. **1701**, 050010 (2016).

[160] Q. Huang, D. Y. Chen, X. Liu, and T. Matsuki, Charged charmonium-like structures in the $e^+e^- \to \psi(3686)\pi^+\pi^-$ process based on the ISPE mechanism, Eur. Phys. J. C **79**, 613 (2019).

[161] F. K. Guo, X. H. Liu, and S. Sakai, Threshold cusps and triangle singularities in hadronic reactions, Prog. Part. Nucl. Phys. **112**, 103757 (2020).